Platelet alpha(IIb)beta(3) Integrin and Myosin II ATPase Guide Fibrin Network Structure and Enhance Clot Stiffness During Clot Formation

---

A Dissertation

Presented to

the faculty of the School of Engineering and Applied Science

University of Virginia

---

in partial fulfillment
of the requirements for the degree

Doctor of Philosophy

by

Nicole Frances Brackett

May 2018

APPROVAL SHEET

This Dissertation
is submitted in partial fulfillment of the requirements
for the degree of
Doctor of Philosophy

Author Signature: 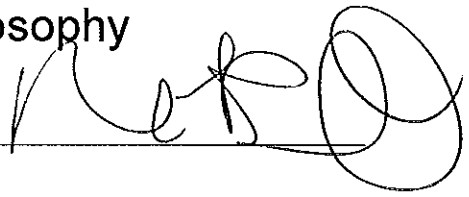

This Dissertation has been read and approved by the examining committee:

Advisor: Michael Lawrence, Ph.D.

Committee Member: Jeffrey Saucerman, Ph.D.

Committee Member: William Guilford, Ph.D.

Committee Member: Brian Helmke, Ph.D

Committee Member: Kevin Janes, Ph.D.

Committee Member: Dorothy Schafer, Ph.D.

Accepted for the School of Engineering and Applied Science:

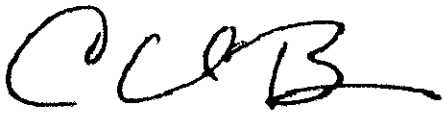

Craig H. Benson, School of Engineering and Applied Science

May 2018

Acknowledgements

I would like to thank my advisor, Dr. Michael Lawrence, for his mentorship and encouragement during my time as both an undergraduate and graduate student. I would also like to thank my committee members Dr. Jeff Saucerman, Dr. Dorothy Schafer, Dr. Will Guilford, Dr. Brian Helmke, and Dr. Kevin Janes for their support and valuable insight.

Thank you to the members of the Lawrence lab, Jose Tlaxca, Annika Shuali, Yuhling Wang, Caroline Wang, and Matt Perez. I'm grateful for all of the help you provided in the lab, and I'm especially grateful for the friendships we've built.

Thank you to Brittany Earnest, Sunil Unnikrishnan, and Phillip Yen for your support and encouragement. Thank you Olga Askinazi for your help with confocal microscopy, and thank you Francesco Viola and Elisa Ferrante for your guidance with sonorheometry.

Finally, I would like to thank my family for their love and support. To my husband Jake, thank you for your unconditional love and encouragement. I couldn't have done it without you. And thank you to my cat Taco for always sticking by my side, especially while I was writing my thesis.

Table of Contents

Abstract

At the site of vascular injury, coagulation is critical for the restoration of hemostasis. Despite the life-preserving function of coagulation, clotting abnormalities are associated with numerous vascular disorders including myocardial infarction, stroke, and hemophilia. Platelets, the primary cellular component of blood clots, drive clot progression through interactions with the clot fibrin network by platelet $\alpha_{IIb}\beta_3$ integrin-mediated adhesion to fibrin and cytoskeleton-mediated tensioning of the fibrin network.

Previous research has identified clot stiffness as a valuable metric for quantifying hypercoagulability or hypocoagulability affiliated with vascular disease. Similarly, previous studies have used features of abnormal clot structure to identify patients at risk of thrombotic events and to evaluate the efficacy of anti-thrombotic drugs. Given the prominent function of the platelet $\alpha_{IIb}\beta_3$ integrin and the platelet cytoskeleton in coagulation, and given the value of clot structure and stiffness as metrics of vascular disease, this study aimed to quantify the contribution of the platelet $\alpha_{IIb}\beta_3$ integrin and platelet cytoskeletal myosin II ATPase to fibrin network structure and clot stiffness during clot formation. We hypothesized that the platelet $\alpha_{IIb}\beta_3$ integrin and platelet myosin II ATPase enhance clot stiffness and regulate fibrin network structure. Additionally, we hypothesized that a network model of stiffness would find that platelet-mediated changes to fibrin network structure could be used to predict changes in clot stiffness.

To test our hypothesis, the contribution of the platelet $\alpha_{IIb}\beta_3$ integrin and platelet myosin II ATPase to whole blood and plasma clot stiffness was evaluated using sonorheometry and electromagnetic force techniques. The results found that inhibition of the platelet $\alpha_{IIb}\beta_3$ integrin or platelet myosin II ATPase significantly attenuated clot stiffness, indicating that platelet $\alpha_{IIb}\beta_3$ integrin-mediated binding to the fibrin network and myosin II ATPase-mediated tensioning of the fibrin network are critical components of clot stiffening during coagulation.

Next, to evaluate if changes in clot stiffness could be linked to platelet-mediated changes in clot structure, we used confocal microscopy and image analysis to quantify the contribution of the platelet $\alpha_{IIb}\beta_3$ integrin and platelet myosin II ATPase to fibrin network structure. The results found that inhibition of the platelet $\alpha_{IIb}\beta_3$ integrin or platelet myosin II ATPase produced clots with longer fibrin fibers, fewer fiber junctions, increased clot porosity, and reduced clot heterogeneity, suggesting that platelet $\alpha_{IIb}\beta_3$ integrin-mediated binding to the clot fibrin network and myosin II ATPase-mediated tensioning of the network are critical modulators of fibrin network structure during coagulation. Finally, the application of a simple network model found that platelet $\alpha_{IIb}\beta_3$ integrin- and platelet myosin II ATPase-mediated changes in fibrin network structure are useful predictors of relative changes in clot stiffness.

Quantifiable features of fibrin network structure and clot mechanical stability are a valuable means to guide the detection of vascular disease. In this study, we demonstrated that platelet myosin II ATPase is a critical modulator of clot stiffening during coagulation. In addition, we quantified the contribution of the platelet $\alpha_{IIb}\beta_3$ integrin and platelet myosin II ATPase to specific structural features of the clot fibrin network, and suggest that the platelet-mediated changes in clot structure could predict changes in clot stiffness. Finally, the study highlighted the utility of existing technologies for measuring clot structure and strength (confocal microscopy and sonorheometry), and presented a novel technique that offers the potential for simultaneous assessment of clot structure and stiffness (electromagnetic force).

List of Figures and Tables

List of Abbreviations

$\alpha_{IIb}\beta_3$	glycoprotein IIbIIIa
ARF	acoustic radiation force
$CaCl_2$	calcium chloride
D	displacement
E_0	network elastic modulus
F	force
G_o	shear modulus
k_B	Boltzmann's constant
κ_o	single filament bending modulus
l_c	distance between crosslinks
μ	viscosity
NA	numerical aperture
ν	terminal velocity
p	Poisson's ratio
PPP	platelet poor plasma
PRP	platelet rich plasma
R	radius
ROTEM	thromboelastometry
S	stiffness
SEM	standard error of the mean
T	temperature
TEG	thromboelastography
TF	tissue factor
tPA	tissue plasminogen activator
WGA	wheat germ agglutinin
ξ	network pore size

Chapter 1: Introduction

1.1: Coagulation

Coagulation is the process by which blood is converted from a viscous fluid into a viscoelastic gel, resulting in the formation of a blood clot (1). Blood coagulation serves as a means of host defense, maintaining the integrity of the closed circulatory system and initiating wound healing at the site of vascular injury (2). Coagulation is a highly conserved system, and is comprised primarily of a cellular platelet component and a fibrin mesh component. Hemostasis, or the regulation of blood clotting processes, is a delicate balance between inadequate coagulation found in hemorrhage and excessive coagulation characteristic of thrombosis. Despite the life-preserving function that coagulation serves in maintaining hemostasis, clotting abnormalities are associated with a number of vascular disorders including myocardial infarction, stroke, hemophilia, and diabetes (3). This introduction aims to summarize the primary components and underlying mechanisms of coagulation, and highlights the methods used to assess coagulation function.

1.1.1: Components of Coagulation

The primary components of coagulation are platelets and the fibrin network (**Figure 1-1**). At the site of vascular injury, platelets attenuate blood loss by aggregating to form a platelet plug, and the fibrin fiber mesh forms concurrently to strengthen the platelet plug. Fibrin polymerization is driven by thrombin-mediated conversion of fibrinogen to fibrin, which consists of the cleaving of fibrinopeptides from the surface of fibrinogen to form protofibrils, and subsequent lateral aggregation to form fibrin fibers (**Figure 1-1**) (4–7). The platelets bind to and interact with the fibrin network through the platelet $\alpha_{IIb}\beta_3$ integrin, discussed in further detail below (**Section 1.2.3**).

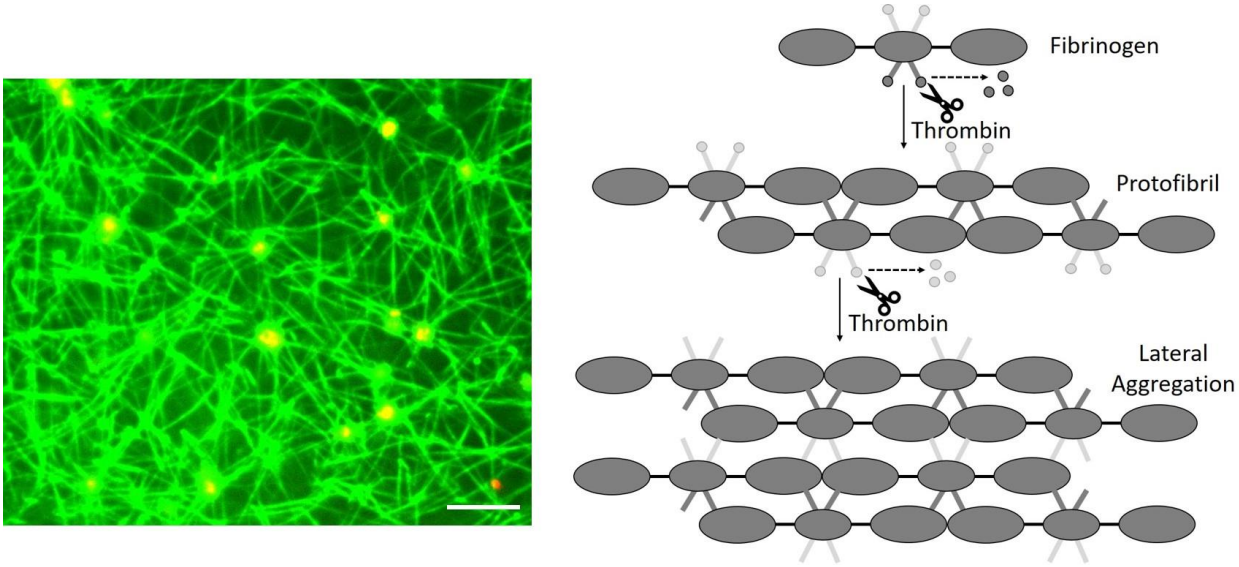

Figure 1-1: Components of coagulation: Platelets and fibrin. Left: Blood clots are comprised of a cellular platelet component (red) and fibrin mesh component (green). Areas of overlap between platelets and fibrin fibers are shown in yellow. Scale bar = 10µm. Right: Fibrin is produced through thrombin-mediated cleaving of fibrinopeptides from the surface of fibrinogen to form protofibrils, and subsequent lateral aggregation of protofibrils to form fibrin (Figure adapted from Wolberg 2007).

1.1.2: Mechanism of Coagulation

Coagulation is initiated almost instantaneously at the site of vascular injury, and can follow two distinct activation pathways to ultimately lead to fibrin formation. The coagulation cascade can follow the intrinsic (contact activation) pathway or the extrinsic (tissue factor activation) pathway (**Figure 1-2**) (2,8,9). The two pathways consist of a series of serine protease-mediated enzymatic reactions that ultimately lead to the production of fibrin.

In the extrinsic pathway, blood vessel damage causes cellular-bound tissue factor (TF) to be exposed to circulating factor VII (FVII), and the subsequent binding of FVII to TF initiates the coagulation cascade (8,10). The FVII-TF complex converts circulating factor X (FX) to the active enzyme FXa, which binds with the cofactor activated factor V (FVa) to form the prothrombinase complex and to subsequently activate prothrombin to thrombin (8,10). Thrombin then activates

additional components of the coagulation cascade and produces fibrin, as previously discussed (**Section 1.1.1**).

In the intrinsic coagulation pathway, factor XII (FXII) is activated through contact with a charged surface, leading to the activation of factor XI (FXIa) and factor IX (FIXa). FIXa then binds with its cofactor activated factor XIII (FXIIIa) to form the tenase complex, which activates FX and subsequently leads to the activation of thrombin (11). In the stiffness and structure studies presented in Chapters 2-4, the intrinsic coagulation pathway was used to initiate clotting in whole blood and plasma samples by exposing the blood to kaolin clay or glass coverslips.

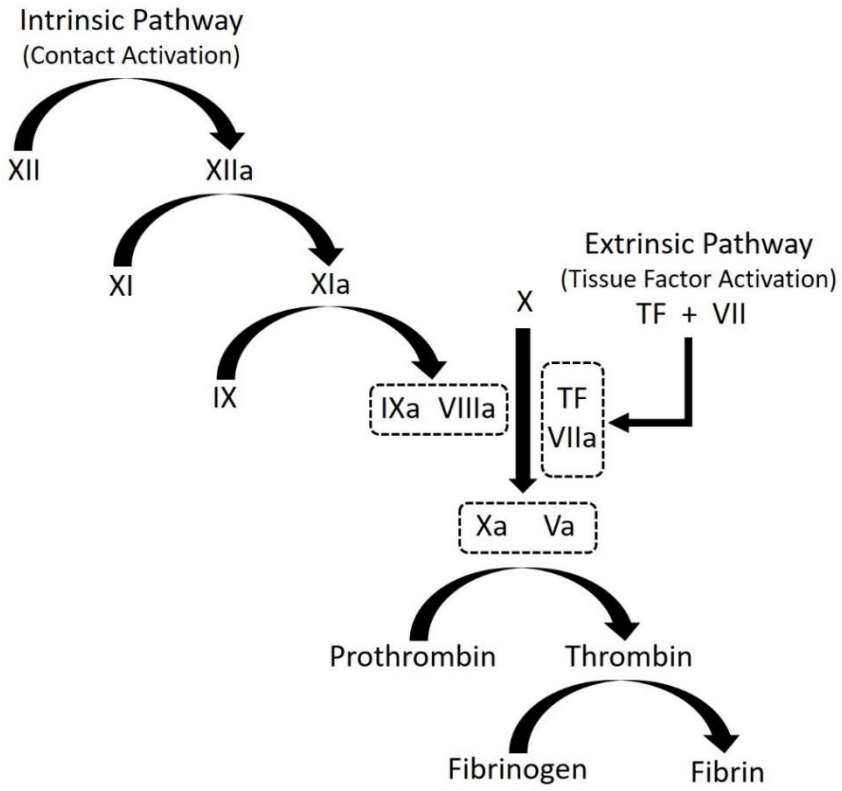

Figure 1-2: Coagulation cascade. A series of enzymatic reactions results in the production of fibrin following activation via the intrinsic or extrinsic pathway. Arrows denote activation and dashed lines indicate cofactor complexes.

1.1.3: Assays to Measure Coagulation Function

Endpoint biochemical assays such as activated thromboplastin time (APTT) and prothrombin time (PT) are used to evaluate coagulation in patients exhibiting bleeding symptoms (8). The APTT assay measures the rate of blood clotting due to activation of the intrinsic coagulation pathway via exposure to kaolin, and is the clinical test of choice in the management of heparin therapy (12). By contrast, the PT assay measures the rate of coagulation due to activation of the extrinsic pathway through exposure to tissue factor, and is the preferred clinical test in the management of warfarin therapy (12). Although the biochemical assays provide valuable insight regarding specific aspects of coagulation, they do not provide a comprehensive assessment of hemostasis and they are limited by the absence of functional platelets.

Additional assays that are used to evaluate coagulation function include thrombin generation tests and mechanical/viscoelastic analyzers. Thrombin generation assays measure the clotting capability of blood plasma and are used to assess patient risk for thrombosis or hemorrhage due to increased or deficient thrombin generation, respectively (13). Similar to the APTT and PT tests, thrombin generation assays provide important clinical insight particularly regarding patient risk for defective coagulation, however thrombin generation tests are limited to plasma rather than whole blood, and ultimately do not provide a complete representation of hemostasis. By contrast, viscoelastic methods such as thromboelastography, thromboelastometry, and sonorheometry can be used to monitor global hemostasis and assess platelet function in clotting by quantifying whole blood clot stiffness during coagulation (13,14). The viscoelastic assays and the value of clot stiffness as a tool for evaluating coagulation are discussed in further detail, below (**Section 1.3**).

1.2: Platelets in Coagulation

Platelets are small, anucleate cells that are derived from megakaryocytes in the bone marrow (15,16). Platelets and their role in hemostasis and thrombosis were first identified in 1881, and numerous platelet-specific coagulation disorders were identified from 1883-1950, which subsequently led to the development of platelet function assays from 1910-present (17). The platelet portion of this introduction aims to summarize the function, underlying mechanism, and relevant disorders of platelets in coagulation, and highlights the tools used to assess platelet function and the existing treatments for platelet disorders.

1.2.1: Function of Platelets in Coagulation

The primary function of platelets is to maintain hemostasis, which is achieved through enzymatic and adhesive processes. At the site of vascular injury, platelets initiate coagulation through the formation of a platelet plug. Adhesive molecules on the platelet surface facilitate adhesion of the platelets to the damaged vessel, and the release of pro-coagulant factors leads to the recruitment of nearby platelets and subsequent platelet aggregation (18). The fibrin network then develops within the platelet plug, and adhesive molecules on the platelet surface allow the platelets to adhere to and exert tension on the clot fibrin network. Finally, platelets tune the coagulation cascade by generating thrombin following activation of membrane-bound clotting factors, and by secreting granules that lead to the release of pro-coagulant and anti-coagulant molecules (18). The specific mechanisms underlying platelet function in coagulation are discussed in further detail below (**Section 1.2.2**).

1.2.2: Mechanism of Platelet Function in Coagulation

Platelet function in coagulation and the restoration of hemostasis is modulated through enzymatic and adhesive processes. On the enzymatic side, tenase and prothrombinase complexes bound to the platelet membrane catalyze the production of thrombin, which subsequently polymerizes fibrin (**Figure 1-3**) (18). In addition, platelet granule secretion of small molecules such as ADP and hemostatic factors such as fibrinogen, von Willebrand factor, and FV modulate the rate and degree of clot formation (19). On the adhesive side of platelet function in coagulation, exposed collagen and von Willebrand factor on the damaged endothelium anchor platelets to the site of vascular damage through platelet surface receptors GPVI and GPIb-IX-V, respectively (20,21). Additionally, the $\alpha_{IIb}\beta_3$ integrin on the platelet membrane facilitates the adhesion of platelets to the clot fibrin network (20), and the platelet contractile apparatus consisting of actin, myosin II ATPase, and additional small molecules facilitates platelet-mediated tensioning of the clot fibrin network (**Figure 1-3**) (22). A detailed discussion of the function of the platelet $\alpha_{IIb}\beta_3$ integrin and platelet myosin II ATPase in coagulation is provided below (**Sections 1.2.3 & 1.2.4**).

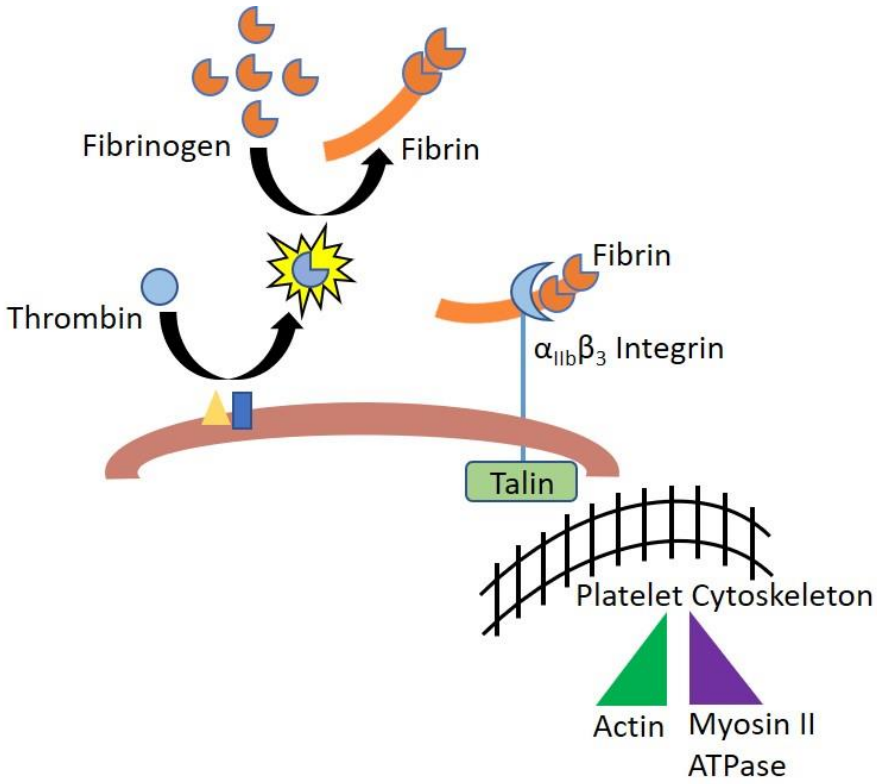

Figure 1-3: Platelet function in coagulation. Platelets modulate coagulation through enzymatic and adhesive processes. Enzymatic: platelets catalyze the production of thrombin. Adhesive: the platelet $\alpha_{IIb}\beta_3$ integrin and cytoskeletal regulators allow the platelet to bind and exert tension on the clot fibrin network, respectively.

1.2.3: Function of the Platelet $\alpha_{IIb}\beta_3$ Integrin in Coagulation

There are approximately 40-50x10^3 $\alpha_{IIb}\beta_3$ integrins per platelet (23). The platelet $\alpha_{IIb}\beta_3$ integrin modulates coagulation by binding to fibrin, thus serving as the physical link between the platelet cellular component and the fibrin mesh component of coagulation. During coagulation, the $\alpha_{IIb}\beta_3$ integrin can be activated by inside-out or outside-in signal transduction (24). The primary means of $\alpha_{IIb}\beta_3$ integrin activation, outside-in signal transduction, is mediated by fibrin binding, which subsequently results in platelet adhesion and the initiation of intracellular signaling events (**Figure 1-4**) (25). The series of intracellular signaling processes following platelet $\alpha_{IIb}\beta_3$ integrin activation leads to platelet spreading, granule secretion, platelet aggregation, and platelet

contractility. Given the prominent function of the platelet $\alpha_{IIb}\beta_3$ integrin in modulating coagulation, the $\alpha_{IIb}\beta_3$ integrin serves as a useful target of anti-platelet drugs in cases of vascular disease. The clinical indications for anti-$\alpha_{IIb}\beta_3$ drugs include acute coronary syndrome, myocardial infarction, and coronary angioplasty and stenting (26). In this study, the platelet $\alpha_{IIb}\beta_3$ integrin inhibitor abciximab (Reopro®) was used to prevent platelet binding to the clot fibrin network. The abciximab antibody binds non-selectively to the activated platelet $\alpha_{IIb}\beta_3$ integrin, resulting in integrin conformational changes that subsequently prevent fibrin binding (26,27).

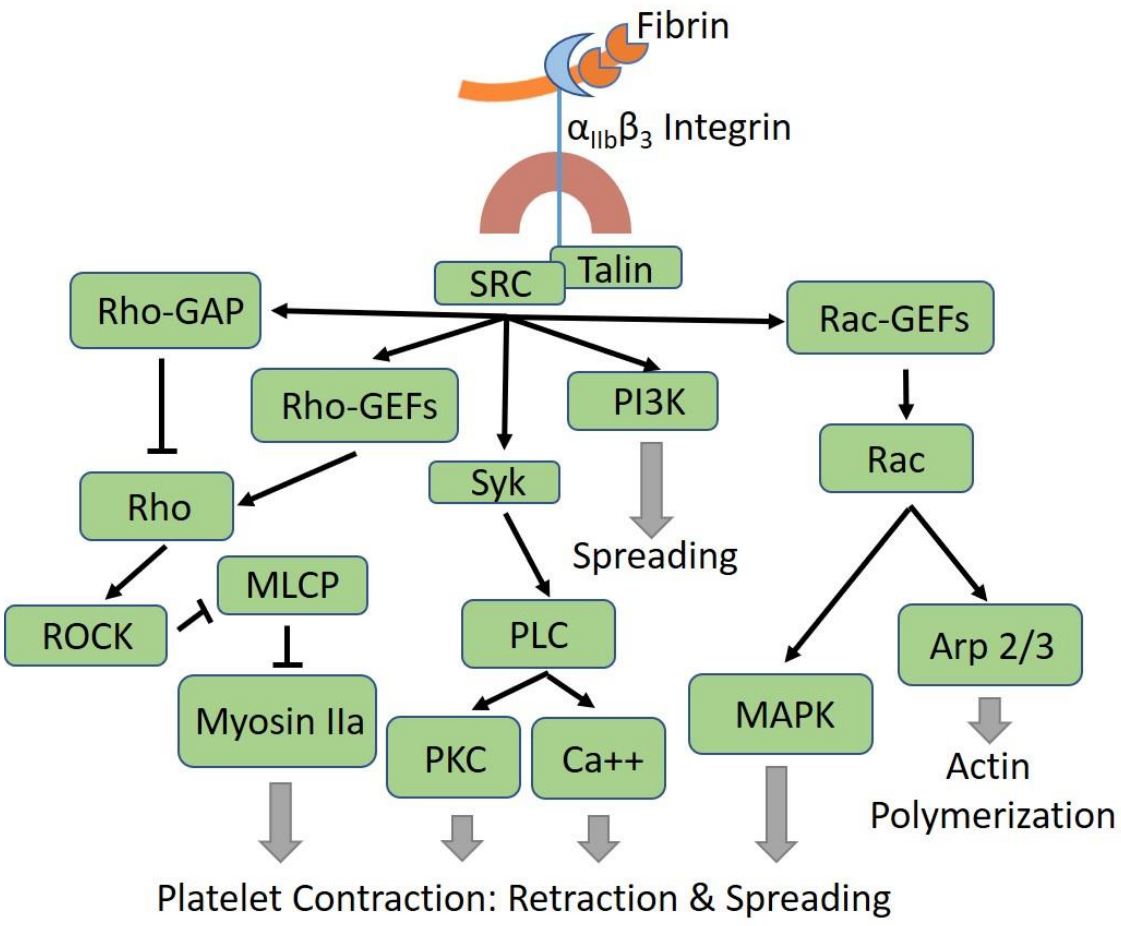

Figure 1-4: Platelet $\alpha_{IIb}\beta_3$ integrin signaling pathway. Activation of the platelet $\alpha_{IIb}\beta_3$ integrin by fibrin-dependent outside-in signal transduction produces a series of intracellular signaling events that lead to platelet spreading and contractility. Pathway adapted from Shen et al. 2012.

1.2.4: Function of Platelet Myosin II ATPase in Coagulation

Following platelet $\alpha_{IIb}\beta_3$ integrin activation, intracellular signaling events result in cytoskeleton-dependent platelet contractility. One of the components of the platelet cytoskeleton, myosin II ATPase, is physically linked to the $\alpha_{IIb}\beta_3$ integrin by talin following fibrin-mediated activation of the integrin (28). While the function of platelet myosin II ATPase in the late clot contraction phase of coagulation has been characterized (29), there have been limited studies of the role of platelet myosin II ATPase in the early clot formation phase of coagulation (30). In this study, the myosin II ATPase inhibitor blebbistatin was used to evaluate the contribution of platelet myosin II ATPase to clot stiffness and fibrin network structure during clot formation (**Figure 1-5**). Blebbistatin is a non-competitive inhibitor that blocks myosin II ATPase in a products complex with low actin affinity (22).

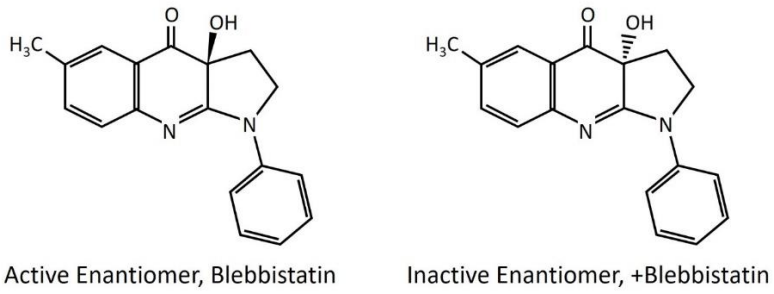

Figure 1-5: Chemical structure of blebbistatin enantiomers. The chemical structure of the active enantiomer blebbistatin (left) and the inactive enantiomer +blebbistatin (right). The inactive enantiomer +blebbistatin serves as a negative control for the active blebbistatin.

1.2.5: Platelet Disorders

Platelet disorders can be generally categorized as the following: deficient platelet concentration, excessive platelet concentration, or platelet dysfunction. Thrombocytopenia, characterized by deficient platelet concentrations, accompanies a number of hereditary syndromes such as Bernard-Soulier syndrome, May-Hegglin anomaly, Alport syndrome, and Wiskott-Aldrich

syndrome (17,31). In contrast to thrombocytopenia, thrombocythemia (thrombocytosis) is characterized by excessive platelet concentrations, and may be observed in cases of inflammation, arthritis, nephritis, bacterial disease, and others. One platelet disorder that results from platelet dysfunction is Glanzmann's thrombasthenia, which is a hereditary disorder characterized by platelet $\alpha_{IIb}\beta_3$ integrin deficiency (17,32). The primary symptom of Glanzmann's thrombasthenia is bleeding, which can vary from minimal bruising to severe hemorrhage. Genetic abnormalities in myosin II ATPase (MYH9 disorders) can be found in cases of the May-Hegglin anomaly and Epstein, Sebastian, and Fechtner syndromes (30). MYH9 disorders are characterized by minor bleeding due to the platelet inability to undergo shape change following activation.

1.2.6: Current Treatments for Platelet Disorders

In mild cases of thrombocytopenia, dietary supplements or corticosteroids may be prescribed to stimulate platelet production, while severe cases of thrombocytopenia may require blood transfusions or plasma replacement therapy (33). For thrombocythemia, anti-platelet drugs including platelet $\alpha_{IIb}\beta_3$ integrin inhibitors may be prescribed to reduce the patient's risk of thrombosis (34,35). In the case of Glanzmann's thrombasthenia, anti-fibrinolytic therapy or recombinant FVIIa may be prescribed to prevent hemorrhage (32). Finally, for MYH9 disorders, treatment resembles that of thrombocytopenia, and may range from the use of corticosteroids to blood transfusions depending on the severity of bleeding (30).

1.2.7: Assays to Measure Platelet Function in Coagulation

In the clinical setting, platelet function assays are used to identify patients with bleeding disorders, monitor patient response to antiplatelet therapy, and evaluate perioperative hemostasis

(36). One class of platelet-specific coagulation assays measures the rate and degree of platelet aggregation to assess platelet function. These tests include plasma-based light transmission platelet aggregometry, whole blood-based impedance aggregometry, luminescent plasma- or whole blood-based lumiaggregometry, and the turbidimetric whole blood-based VerifyNow system (36). Platelet aggregation assays are useful tools for detecting platelet-specific deficiencies, but they are rather limited in scope and they neglect the contribution of the fibrin meshwork to coagulation.

Another class of platelet function assays measures platelet adhesion under shear flow. These tests include the Platelet Function Analyzer, the IMPACT Cone and Plate(Let) Analyzer, and the global thrombosis test (36). An advantage of the shear flow-based platelet function assays is their consideration of the contribution of blood flow to platelet activity and coagulation, however the tests are similarly limited to platelet-specific measurements of platelet adhesion or platelet aggregation. Finally, viscoelastic assays, including thromboelastography, thromboelastometry, and sonorheometry, measure blood clot stiffness during coagulation to evaluate platelet function (13,14,36). The viscoelastic assays are discussed in further detail, below (**Section 1.3.2**).

1.3: Evaluating Coagulation with Clot Stiffness and Clot Structure

1.3.1: Clot Stiffness as a Metric of Hemostasis

At its core, hemostasis is a predominantly mechanical process, as the main goal of hemostasis is to produce a mechanically stable blood clot to mitigate blood loss. Hemostasis is a fine balance between inadequate or excessive clotting, and abnormal coagulation is associated with a number of vascular disorders (3,37). Clot stiffness has been identified as a valuable metric for quantifying hypercoagulability and hypocoagulability affiliated with vascular disease.

Previous studies found that increased clot stiffness and ultimately increased coagulability is indicated in patients exhibiting acute ischemic stroke, coronary artery disease, or type II diabetes mellitus (38–40). Alternatively, studies of hemophilia suggest that the disorder is predominantly characterized by reduced clot stiffness and hypocoagulability (37). In addition to characterizing the mechanical properties of hemostasis for a variety of pathologies, clot stiffness may also serve as a useful tool for identifying patients at risk of bleeding and thrombotic disorders, and subsequently informing appropriate medical treatment.

1.3.2: Tools to Quantify Blood Clot Stiffness

Various technologies and devices have been developed to evaluate hemostasis by quantifying blood clot stiffness. Two of the primary technologies used for measuring clot stiffness are thromboelastography (TEG) (Haemonetics, Braintree, MA, USA) and rotational thromboelastometry (ROTEM) (Instrumentation Laboratory, Columbia, MD, USA). The TEG and ROTEM technologies utilize a pin and cup geometry, where a whole blood sample is loaded into a cylindrical cuvette and a small pin is inserted in the blood sample. The cup (TEG) or the pin (ROTEM) is rotated as the clot forms over time, and the motion of the cup or pin is ultimately coupled to blood clot stiffness (37). Although the TEG and ROTEM provide valuable clinical insight, the devices are limited by complexities in operation and difficult interpretation of results. Additionally, the TEG and ROTEM apply relatively large shear strains to the blood sample, which may interfere with clot formation (41,42).

Recently, a number of studies used ultrasound-based technologies to quantify blood clot stiffness. One study coupled ultrasound acoustic radiation force (ARF) with optical imaging to measure plasma clot stiffness (43). Similarly, a study coupled ultrasound ARF with an optical

coherence tomography detection system to measure whole blood clot stiffness for a variety of hemostatic conditions (44). A novel device, the Quantra Hemostasis Analyzer (Quantra) (Hemosonics LLC, Charlottesville, VA, USA), uses the ultrasound-based technology sonic estimation of elasticity via resonance (SEER) sonorheometry to measure whole blood clot stiffness during coagulation (14,45). Some advantages of the ultrasound-based technologies include enhanced measurement sensitivity, and low shear strains applied to the blood sample compared to TEG and ROTEM (14,45–47). Due to these advantages as well as relative ease of operation and interpretation of results, the Quantra device was used in this study to evaluate the contribution of the platelet $\alpha_{IIb}\beta_3$ integrin and platelet myosin II ATPase to clot stiffness.

1.3.3: Clot Structure as a Metric of Hemostasis

Abnormal clot structure has been associated with numerous vascular disorders including myocardial infarction, stroke, coronary artery disease (CAD), venous thromboembolism (VTE), and diabetes (3). In a study of VTE, abnormal clot microstructure served as a biomarker to distinguish VTE patients from non-VTE patients (48). Similarly, a study of CAD patients investigated the effect of anti-thrombotic drugs on clot porosity (49). Given the prevalence of fibrin network structural abnormalities in cases of vascular disease, features of clot structure may represent a novel means to identify and subsequently treat individuals at risk of thrombotic events.

Recently, a number of studies have sought to correlate clot structure parameters with clot mechanical stability. Chernysh et al. measured clot structural and mechanical properties to elucidate the relative time sequence of events during clot formation (50). Kim et al. used confocal microscopy and rheometry to correlate clot structure and platelet contractile force during coagulation (51). Similarly, Alber et al. developed a computational model to estimate elastic

properties of fibrin networks from confocal images of fibrin clots (52). Additionally, a number of studies have used the susceptibility of fibrin clot structure to dissolution via fibrinolysis to estimate clot mechanical stability (3,5,49,53). Overall, research suggests that quantifiable abnormalities in clot structure and mechanical stability could guide the detection of vascular disease, and may aid in the development and assessment of novel anticoagulant therapies.

1.4: Outline of the Study

The overall objective of the study was to evaluate the contribution of the platelet $\alpha_{IIb}\beta_3$ integrin and platelet myosin II ATPase to clot stiffness and fibrin network structure during coagulation. Chapter 2 uses sonorheometry to measure the effect of platelet $\alpha_{IIb}\beta_3$ integrin inhibition or platelet myosin II ATPase inhibition on whole blood and plasma clot stiffness. Similarly, chapter 3 applies a novel, electromagnetic force-based stiffness measurement technique to evaluate the contribution of the platelet $\alpha_{IIb}\beta_3$ integrin and platelet myosin II ATPase to plasma clot stiffness. The electromagnetic force study was intended to serve as a bridge between whole blood clot stiffness measured using sonorheometry and fibrin network structural features assessed in plasma clots. Additionally, the plasma sonorheometry study was completed to evaluate if discrepancies between the sonorheometry and electromagnetic force stiffness results were due to assay-specific differences or biological differences. In Chapter 4, confocal microscopy and image analysis are used to evaluate the contribution of the platelet $\alpha_{IIb}\beta_3$ integrin and platelet myosin II ATPase to fibrin network structure of plasma clots. Finally, Chapter 5 provides a discussion of the results, and highlights the novelty of the findings and the achievements of the study in the broader context of coagulation research.

Chapter 2: Evaluating the Contribution of the Platelet $\alpha_{IIb}\beta_3$ Integrin or Platelet Myosin II ATPase to Clot Stiffness by Sonorheometry

2.1: Introduction

2.1.1: The Quantra Device and Sonorheometry

The Quantra is a novel, automated instrument designed for rapid, near-patient monitoring of hemostasis (**Figure 2-1**) (14). The Quantra device consists of an embedded processor, a touchscreen user interface, ultrasound transducers, optical sensors, and a peristaltic pump (45). A multi-well test cartridge allows four independent measurements to be run in parallel, and consists of a series of chambers for blood sample warming, volume control, reagents, and stiffness measurement using SEER sonorheometry (**Figure 2-1**) (14,45). At the onset of a test, the peristaltic pump pulls the blood into the warming chamber, and then into the volume control chamber to ensure consistent blood volumes between the four channels. Next, the blood is pulled into the reagent chamber, and the blood is pumped repeatedly through serpentine channels in the cartridge to ensure adequate reagent mixing. Finally, the blood is pulled into the measurement chamber where clot stiffness is evaluated using SEER sonorheometry.

SEER sonorheometry is a proprietary technology that uses ultrasound to quantify shear modulus (stiffness) of a clot during coagulation (45). Briefly, a focused ultrasound pulse is transmitted into the blood sample to apply ARF, which displaces the force transducers (red blood cells in whole blood) in the sample. These localized displacements produce shear waves that travel perpendicular to the direction of the focused ultrasound pulse. Low intensity tracking ultrasound pulses are then transmitted, and the returning echoes from the tracking pulses serve as an estimate of the localized displacements (**Figure 2-2**). The shape of the resulting time versus displacement curve is proportional to the shear modulus of the sample.

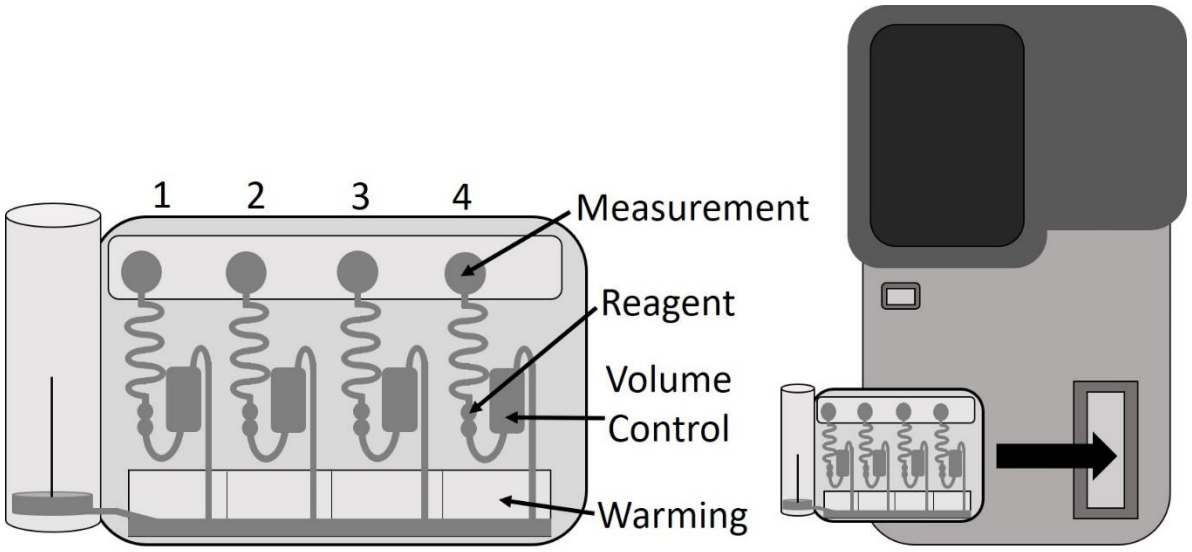

Figure 2-1: The Quantra device and the Quantra multi-well cartridge. The Quantra Hemostasis Analyzer (right) uses SEER sonorheometry for automated, rapid monitoring of hemostasis. The Quantra multi-well cartridge (left) has four test channels to allow four independent measurements to be run in parallel, and four chambers (warming, volume control, reagent, and measurement chambers) per channel.

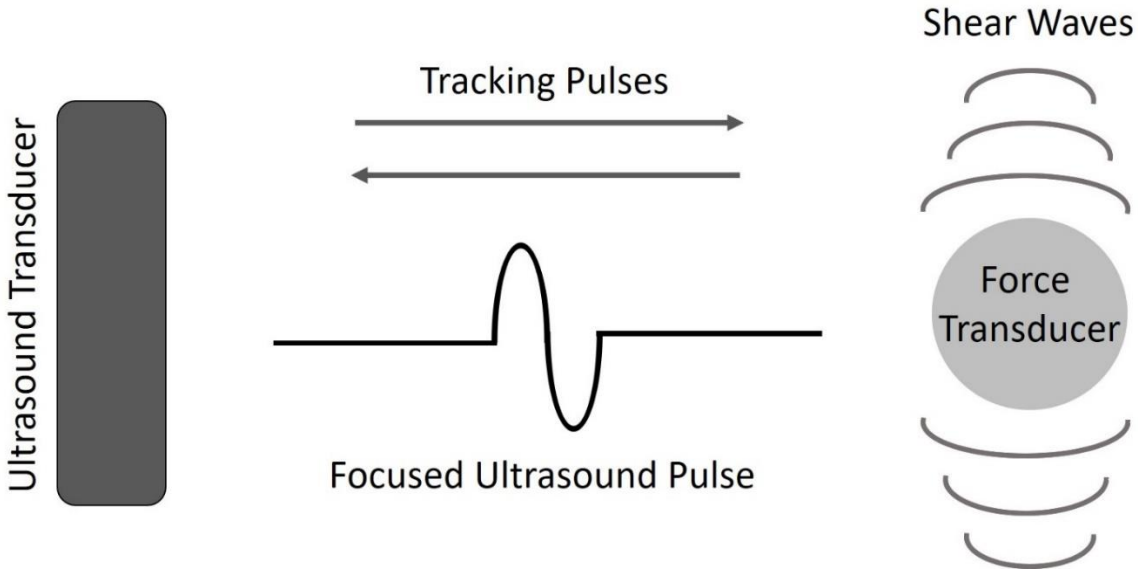

Figure 2-2: SEER sonorheometry. The ultrasound transducer transmits a focused ultrasound pulse, causing localized displacements of force transducers and subsequent production of shear waves. Tracking pulses are transmitted, and their subsequent echoes serve as an estimate of the localized displacements. Figure adapted from Ferrante et al. 2016.

2.1.2: The Platelet $\alpha_{IIb}\beta_3$ Integrin and Platelet Myosin II ATPase in Clot Stiffness

Previous studies using TEG, ROTEM, and sonorheometry technologies evaluated the platelet contribution to whole blood clot stiffness by inhibiting platelet $\alpha_{IIb}\beta_3$ integrin-mediated adhesion to the clot fibrin network via the antagonist abciximab (14,54). Ferrante et al. found that platelet $\alpha_{IIb}\beta_3$ integrin inhibition by abciximab reduced whole blood clot stiffness by more than 5-fold compared to control, emphasizing the significant contribution of platelet integrins to clot stiffness and mechanical stability (14). The following sonorheometry study aimed to recapitulate the abciximab results in whole blood, and to compare the attenuating effect of platelet $\alpha_{IIb}\beta_3$ integrin inhibition on clot stiffness in whole blood versus plasma clots.

In addition to platelet integrin-dependent adhesion to the clot fibrin network, platelets also tune coagulation through cytoskeleton-dependent contraction (51,55). Previous studies found that inhibition of platelet cytoskeletal actin by cytochalasins significantly reduced blood clot stiffness (56,57), suggesting that the integrity of the platelet actin cytoskeleton is critical in coagulation. Myosin II ATPase, another platelet cytoskeletal component, is also essential in platelet contraction (28,58). Platelet myosin II ATPase is linked to the platelet $\alpha_{IIb}\beta_3$ integrin by the cytoskeletal protein talin (51,59), suggesting that myosin II ATPase may be a key downstream component of platelet $\alpha_{IIb}\beta_3$ integrin-mediated regulation of clot stiffness during coagulation. A recent study found that inhibition of platelet myosin II ATPase by blebbistatin reduced platelet contractile stress in local regions of platelets in plasma clots (51). The following sonorheometry study aimed to determine if inhibition of platelet myosin II ATPase significantly reduces bulk clot stiffness. Given the previous observation that inhibition of platelet myosin II ATPase significantly reduces local platelet contractile stress (51), we predicted that inhibiting myosin II ATPase-mediated platelet tensioning of the clot fibrin network would attenuate global clot stiffness.

2.1.3: Sonorheometry Study Goals

The goal of the sonorheometry experiments was to build on existing knowledge regarding the contribution of the platelet $\alpha_{IIb}\beta_3$ integrin or platelet myosin II ATPase to blood clot stiffness. The sonorheometry study aimed to compare the effect of abciximab-mediated platelet $\alpha_{IIb}\beta_3$ integrin inhibition on clot stiffness in whole blood versus plasma samples. Since our study included an electromagnetic force measurement of the effect of platelet $\alpha_{IIb}\beta_3$ integrin inhibition on plasma clot stiffness, the sonorheometry plasma results were intended to evaluate if discrepancies between the whole blood sonorheometry data and the plasma electromagnetic force data were due to assay-specific differences (i.e. sonorheometry versus electromagnetic force) or biological differences (i.e. whole blood versus plasma).

The sonorheometry study also aimed to evaluate the effect of blebbistatin-mediated platelet myosin II ATPase inhibition on whole blood and plasma clot stiffness. A previous study found that inhibition of platelet myosin II ATPase attenuated local platelet contractile stress (51). We hypothesized that platelet myosin II ATPase inhibition by blebbistatin would significantly reduce global clot stiffness during coagulation, possibly due to impaired platelet contractility. Additionally, the sonorheometry study in plasma was used to evaluate if discrepancies between the myosin II ATPase stiffness results of the whole blood sonorheometry and plasma electromagnetic force studies were due to assay-specific or biological differences. Overall, our sonorheometry study aimed to add to the field by measuring the contribution of platelet myosin II ATPase to whole blood and plasma clot stiffness during coagulation.

2.2: Methods

2.2.1: Ethics Statement

The objective of the sonorheometry portion of the study was to evaluate the mechanical properties of human blood in response to various biochemical stimuli. As a result, the study required the use of primary human cells. Blood was collected from healthy, consenting adults by venipuncture in accordance with a protocol (IRB-HSR 12600) approved by the University of Virginia Institutional Review Board. All contaminated materials, biohazardous waste, and reagents were handled and disposed of properly, in accordance with the University of Virginia and OSHA regulations.

2.2.2: Blood Collection and Plasma Separation

Blood was drawn by venipuncture from healthy volunteers into 3.2% sodium citrate (0.109M) 2.7mL Vacutainer® tubes (Becton Dickinson, Franklin Lakes, NJ, USA). Whole blood samples were placed on a rocker prior to experimentation to maintain adequate blood mixing. Blood samples were used for experimentation within 6 hours post blood draw. To obtain platelet-rich plasma (PRP), the citrated whole blood was centrifuged at 100 x g at 25°C for 20 minutes, and the PRP supernatant of the centrifuged sample was collected by pipette. To obtain platelet-poor plasma (PPP), the blood was centrifuged two additional times at 3000 x g at 25°C for 15 minutes, and the PPP supernatant was subsequently collected by pipette.

2.2.3: Reagents

The inhibitor abciximab (Reopro®) was used to block platelet $\alpha_{IIb}\beta_3$ integrin-mediated adhesion to the clot fibrin network (Eli Lilly, Indianapolis, IN, USA). Whole blood or PRP samples

were incubated with 20µg/mL abciximab to ensure saturation of the $\alpha_{IIb}\beta_3$ integrin (14,26,57). A non-blocking, anti-human CD61 antibody served as a negative control for abciximab-mediated platelet $\alpha_{IIb}\beta_3$ integrin inhibition (BioLegend, San Diego, CA, USA). The inhibitor blebbistatin was used to block platelet myosin II ATPase (Selleckchem, Houston, TX, USA). Whole blood or PRP samples were incubated with 25µM blebbistatin to achieve adequate inhibition of platelet myosin II ATPase (22). The inactive enantiomer +blebbistatin served as a negative control for blebbistatin-mediated platelet myosin II ATPase inhibition (Sigma, St. Louis, MO, USA). $CaCl_2$ was used to re-calcify the citrated whole blood and plasma samples (Sigma, St. Louis, MO, USA; 12mM final concentration), and kaolin was used to initiate clotting through the contact/intrinsic activation pathway (JT Baker, VWR, Radnor, PA, USA; 100µg/mL final concentration).

2.2.4: Whole Blood Clot Stiffness Measured by Sonorheometry

The Quantra device was used to measure changes in whole blood clot stiffness during coagulation. Inhibitors abciximab (20µg/mL) or blebbistatin (25µM) were incubated in the blood to inhibit platelet $\alpha_{IIb}\beta_3$ integrin-mediated adhesion to the fibrin network or platelet myosin II ATPase-mediated contraction of the network, respectively. Control whole blood samples were incubated with saline. The Quantra multi-well cartridge was loaded with $CaCl_2$ and kaolin to initiate clotting in the sample (**Figure 2-3**). The multi-well cartridge was loaded into the Quantra, and the whole blood sample was attached to the cartridge. All subsequent steps including sample mixing and stiffness measurement via sonorheometry were automated by the Quantra. The Quantra device used SEER sonorheometry to measure the shear modulus (stiffness) of the blood every 3 seconds during coagulation, and data was output in MATLAB as shear modulus versus time from 0-30 minutes post clot initiation.

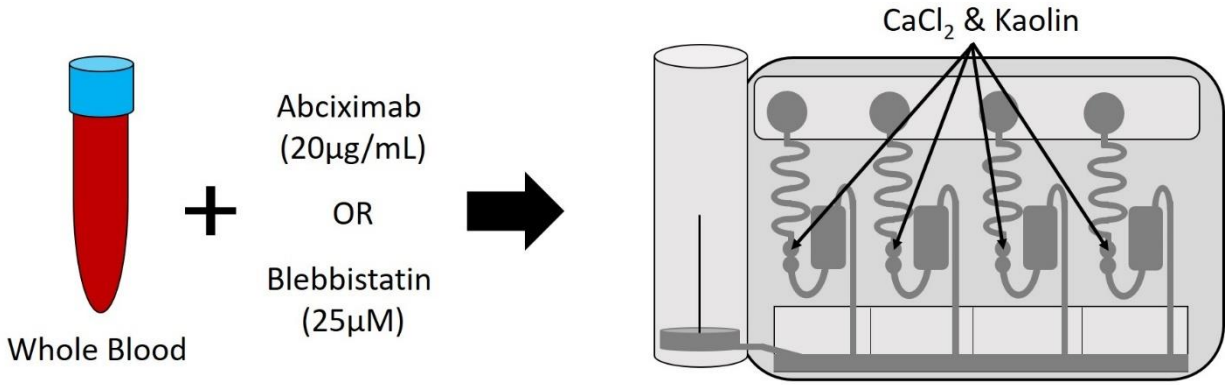

Figure 2-3: Whole blood clot stiffness assessment using sonorheometry. Citrated whole blood was incubated with 20µg/mL abciximab or 25µM blebbistatin to inhibit $\alpha_{IIb}\beta_3$ integrin-mediated platelet binding to the fibrin network or myosin II ATPase-mediated platelet tensioning of the fibrin network, respectively. The Quantra multi-well cartridge was loaded with $CaCl_2$ to re-calcify the citrated whole blood sample, and kaolin to initiate clotting through the contact/intrinsic activation pathway.

2.2.5: Plasma Clot Stiffness Measured by Sonorheometry

Sonorheometry was used to evaluate changes in plasma clot stiffness following inhibition of $\alpha_{IIb}\beta_3$ integrin-mediated platelet binding to the fibrin network or inhibition of myosin II ATPase-mediated platelet tensioning of the fibrin network. The plasma sonorheometry data was intended to serve as a bridge between the whole blood sonorheometry stiffness data and the plasma stiffness data obtained by electromagnetic force (see Chapter 3). Additionally, the plasma sonorheometry data was used to evaluate if discrepancies between the whole blood sonorheometry data and the plasma electromagnetic force data were due to assay-specific differences (i.e. sonorheometry versus electromagnetic force) or biological differences (i.e. whole blood versus plasma). Whole blood was centrifuged at 100 x g for 20 minutes to obtain PRP, and two additional times at 3000 x g for 15 minutes to obtain PPP. The Quantra device was used to measure changes in clot stiffness of PRP or PPP during coagulation. Inhibitors abciximab (20µg/mL) or blebbistatin (25µM) were

incubated in PRP samples to inhibit platelet $\alpha_{IIb}\beta_3$ integrin-mediated adhesion to the fibrin network or platelet myosin II ATPase-mediated contraction of the network, respectively. Control PRP samples were incubated with saline. The Quantra multi-well cartridge was loaded with $CaCl_2$, kaolin, and 6µm polystyrene beads (Polysciences, Warrington, PA, USA; 5 x 10^6 beads/mL final concentration) (**Figure 2-4**). The polystyrene beads served as force transducers in the plasma samples for the ultrasound pulses output by the Quantra device, similar to the role of red blood cells as force transducers in the whole blood samples. The multi-well cartridge was loaded into the Quantra, and the plasma sample was attached to the cartridge. The Quantra device used SEER sonorheometry to measure the shear modulus (stiffness) of the plasma every 3 seconds during coagulation, and data was output in MATLAB as shear modulus versus time from 0-30 minutes post clot initiation.

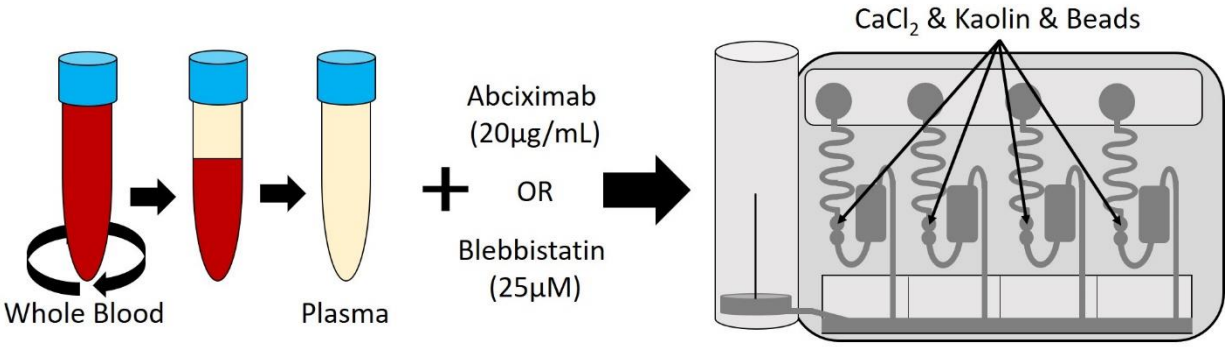

Figure 2-4: Plasma clot stiffness assessment using sonorheometry. Citrated whole blood was centrifuged to obtain plasma. The plasma was incubated with 20µg/mL abciximab or 25µM blebbistatin to inhibit $\alpha_{IIb}\beta_3$ integrin-mediated platelet binding to the fibrin network or myosin II ATPase-mediated platelet tensioning of the fibrin network, respectively. The Quantra multi-well cartridge was loaded with $CaCl_2$ to re-calcify the citrated plasma sample, and kaolin to initiate clotting through the contact/intrinsic activation pathway. Additionally, the cartridge was loaded with polystyrene beads that served as force transducers for the ultrasound pulses output by the Quantra device to assess plasma clot stiffness.

2.2.6: Statistical Analysis

A power analysis was completed to calculate the appropriate sample size for the sonorheometry experiments given a 5% level of significance and 80% power. A two-way ANOVA and paired student t-tests were used to calculate statistical significance (defined as $p < 0.05$).

2.3: Results

2.3.1: Platelet $\alpha_{IIb}\beta_3$ Integrin and Myosin II ATPase Enhance Whole Blood Clot Stiffness

Sonorheometry was used to evaluate the contribution of platelet $\alpha_{IIb}\beta_3$ integrin-mediated binding to the fibrin network and platelet myosin II ATPase-mediated tensioning of the fibrin network to whole blood clot stiffness. Control whole blood samples began clotting within 3 minutes and reached a maximum clot stiffness of 2078 ± 64 Pa by t = 30 minutes (**Figure 2-5**). Inhibition of the platelet $\alpha_{IIb}\beta_3$ integrin by abciximab significantly ($p < 0.05$ for $t > 4.5$ minutes) attenuated whole blood clot stiffness, which supports the finding of previous studies that the platelet $\alpha_{IIb}\beta_3$ integrin is an essential component in the regulation of clot mechanical integrity (14,54). By 30 minutes post clot initiation, abciximab-treated whole blood samples reached a maximum clot stiffness of 348 ± 21 Pa, indicating that inhibition of platelet $\alpha_{IIb}\beta_3$ integrin function reduced whole blood clot stiffness by 83% **(Figure 2-5**).

Similarly, the whole blood sonorheometry results found that inhibition of platelet myosin II ATPase by blebbistatin significantly ($p < 0.05$ for $t > 5.5$ minutes) reduced whole blood clot stiffness, suggesting that platelet myosin II ATPase is an integral component of clot stiffening. By t = 30 minutes, blebbistatin-treated whole blood samples reached a maximum clot stiffness of 956 ± 132 Pa, indicating that inhibition of platelet myosin II ATPase reduced whole blood clot stiffness by 54%. Overall, the whole blood sonorheometry results suggest that $\alpha_{IIb}\beta_3$ integrin-mediated

platelet binding to the fibrin network and myosin II ATPase-mediated platelet tensioning of the fibrin network are significant components of whole blood clot stiffening during coagulation.

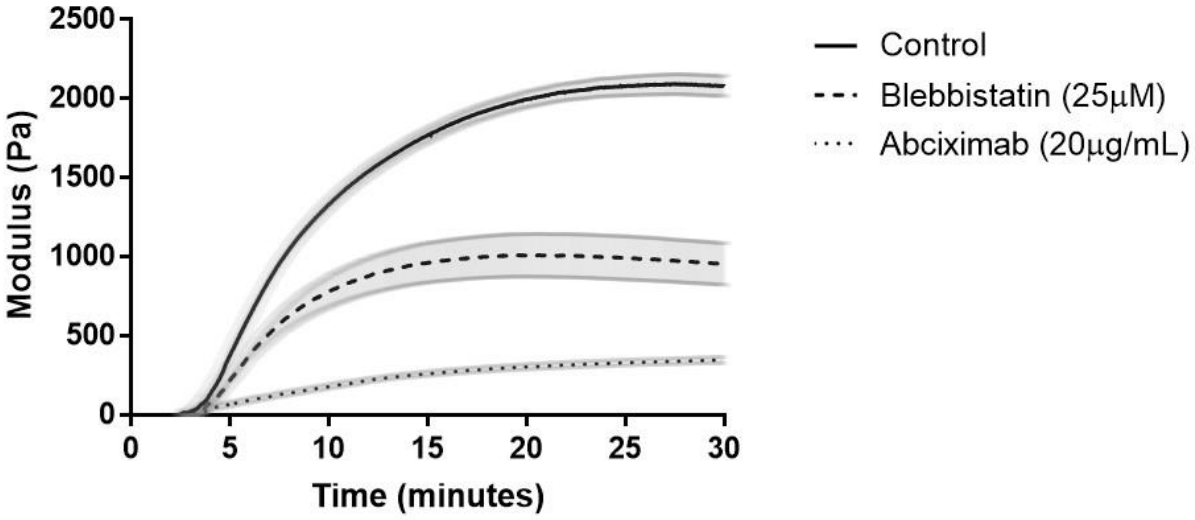

Figure 2-5: Whole blood clot stiffness measured by sonorheometry. Shear modulus (stiffness) of control, abciximab-treated, and blebbistatin-treated whole blood clots was measured by sonorheometry every 3 seconds from 0-30 minutes post clot initiation. Abciximab (20μg/mL) and blebbistatin (25μM) treatment significantly reduced whole blood clot stiffness compared to control ($p < 0.05$ using two-way ANOVA). Data are plotted as mean ± standard error of the mean; n = 5 subjects, 2-4 replicates per subject.

2.3.2 Abciximab- and Blebbistatin-Mediated Reduced Clot Stiffness is Drug Specific

To evaluate the specificity of abciximab-mediated reduced blood clot stiffness observed in **2.3.1**, a non-blocking CD61 antibody (i.e. a non-blocking β_3 integrin antibody) served as a negative control. Whole blood samples were incubated with 20μg/mL CD61 antibody, and clot stiffness was measured by sonorheometry from 0 to 30 minutes post clot initiation using the Quantra device. CD61 antibody-treated whole blood clot stiffness was not significantly different from control clot stiffness for n=3 subjects (**Figure 2-6**), suggesting that the abciximab-mediated reduced whole blood clot stiffness observed in **2.3.1** was specific to the abciximab drug.

Similarly, to evaluate the specificity of blebbistatin-mediated reduced blood clot stiffness observed in **2.3.1**, the inactive enantiomer +blebbistatin served as a negative control (**Figure 1-5, Section 1.2.4**). Whole blood samples were incubated with 25μM +blebbistatin, and clot stiffness was measured by sonorheometry from 0 to 30 minutes post clot initiation using the Quantra device. Inactive enantiomer +blebbistatin-treated whole blood clot stiffness was not significantly different from control clot stiffness for n = 3 subjects (**Figure 2-6**), suggesting that the blebbistatin-mediated reduced whole blood clot stiffness observed in **2.3.1** was specific to blebbistatin.

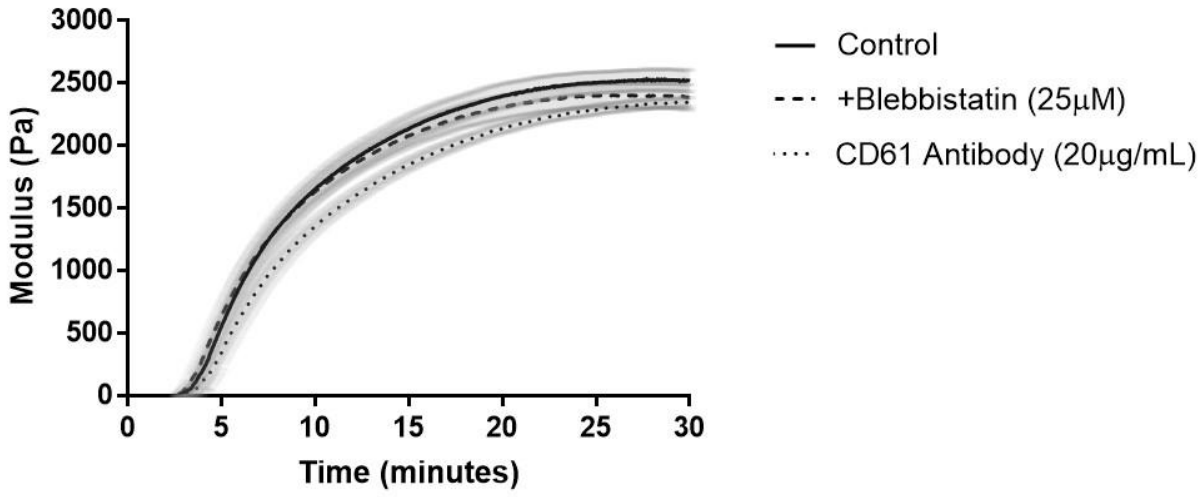

Figure 2-6: Platelet $\alpha_{IIb}\beta_3$ integrin and myosin II ATPase negative control study. Shear modulus (stiffness) of control, CD61 antibody-treated, and +blebbistatin-treated whole blood clots was measured by sonorheometry every 3 seconds from 0-30 minutes post clot initiation. The negative controls CD61 antibody (20μg/mL) and inactive enantiomer +blebbistatin (25μM) did not significantly affect whole blood clot stiffness compared to control ($p > 0.05$). Data are plotted as mean ± standard error of the mean; n = 3 subjects, 2-4 replicates per subject.

2.3.3: Plasma Clot Stiffness is Consistent for a Range of Polystyrene Bead Concentrations

To quantify plasma clot stiffness by sonorheometry using the Quantra device, 6μm polystyrene beads were added to the plasma sample to serve as force transducers for the ultrasound pulses output by the Quantra. A bead titration study was conducted to evaluate the effect of bead

concentration on plasma clot stiffness. The study results found that mean plasma clot stiffness was comparable ($R > 0.94$) for polystyrene bead concentrations of 5×10^5 beads/mL, 1×10^6 beads/mL, or 5×10^6 beads/mL in PRP samples (**Figure 2-7**). The higher concentration of 5×10^6 beads/mL was chosen for the subsequent sonorheometry plasma clot stiffness study because the 5×10^6 beads/mL titration results were slightly less variable than those for the lower bead concentrations of 5×10^5 beads/mL or 1×10^6 beads/mL. The decrease in plasma clot stiffness variability with increased bead concentration suggests that the greater concentration of force transducers captures a more homogenous estimate of plasma clot stiffness. Compared to the whole blood clots measured by sonorheometry, the plasma samples with 5×10^6 beads/mL contain nearly 1000 times fewer force transducers (assuming roughly 5×10^6 red blood cells/µL in whole blood (23)).

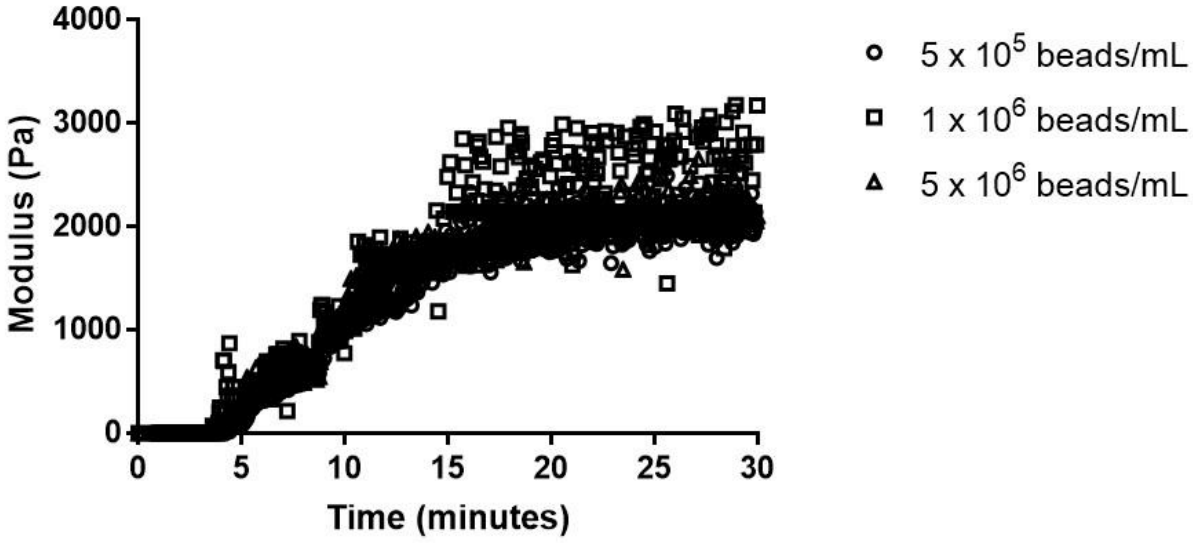

Figure 2-7: Polystyrene bead titration in plasma clots. Shear modulus (stiffness) of PRP clots with 6µm polystyrene bead concentrations of 5×10^5 beads/mL, 1×10^6 beads/mL, and 5×10^6 beads/mL was measured by sonorheometry every 3 seconds from 0-30 minutes post clot initiation. Mean plasma clot stiffness was not dependent on bead concentration ($R > 0.94$), however, increased bead concentration reduced clot stiffness variability. Data are plotted as mean; n = 2 subjects, 2-4 replicates per subject.

2.3.4: Platelet $\alpha_{IIb}\beta_3$ Integrin and Myosin II ATPase Enhance Plasma Clot Stiffness

To directly compare clot stiffness measured by sonorheometry with plasma clot structural features evaluated by confocal microscopy, the sonorheometry stiffness measurement was repeated for plasma clots. Additionally, the plasma sonorheometry data was used to evaluate if discrepancies between whole blood clot stiffness measured by sonorheometry and plasma clot stiffness assessed by electromagnetic force could be attributed to assay-specific differences or biological differences.

Control PRP samples began clotting by 4 minutes post clot initiation and reached a maximum stiffness of 3455 ± 518 Pa by t = 30 minutes (**Figure 2-8**). Similar to the whole blood results, the plasma sonorheometry study found that inhibition of the platelet $\alpha_{IIb}\beta_3$ integrin by abciximab significantly ($p < 0.05$) attenuated PRP clot stiffness. By 30 minutes post clot initiation, abciximab-treated PRP clots reached a maximum clot stiffness of 1192 ± 202 Pa, indicating that inhibition of platelet $\alpha_{IIb}\beta_3$ integrin function reduced PRP clot stiffness by 65%.

Similarly, the plasma sonorheometry results found that inhibition of platelet myosin II ATPase by blebbistatin significantly ($p < 0.05$) reduced PRP clot stiffness (**Figure 2-8**), which agrees with the findings of the whole blood sonorheometry study and suggests that platelet myosin II ATPase is an integral component of clot stiffening. By t = 30 minutes, blebbistatin-treated PRP clots reached a maximum clot stiffness of 1918 ± 79 Pa, indicating that inhibition of platelet myosin II ATPase reduced PRP clot stiffness by 44% compared to control. Additionally, removal of a majority of the platelets (PPP) significantly ($p < 0.05$) reduced clot stiffness compared to control PRP (**Figure 2-8**), where PPP clot stiffness (667 ± 159 Pa) was 80% softer than control PRP clot stiffness by t=30 minutes. Overall, the plasma sonorheometry results support the whole blood sonorheometry results, and suggest that $\alpha_{IIb}\beta_3$ integrin-mediated platelet binding to the fibrin

network and myosin II ATPase-mediated platelet tensioning of the fibrin network are critical modulators of clot stiffness.

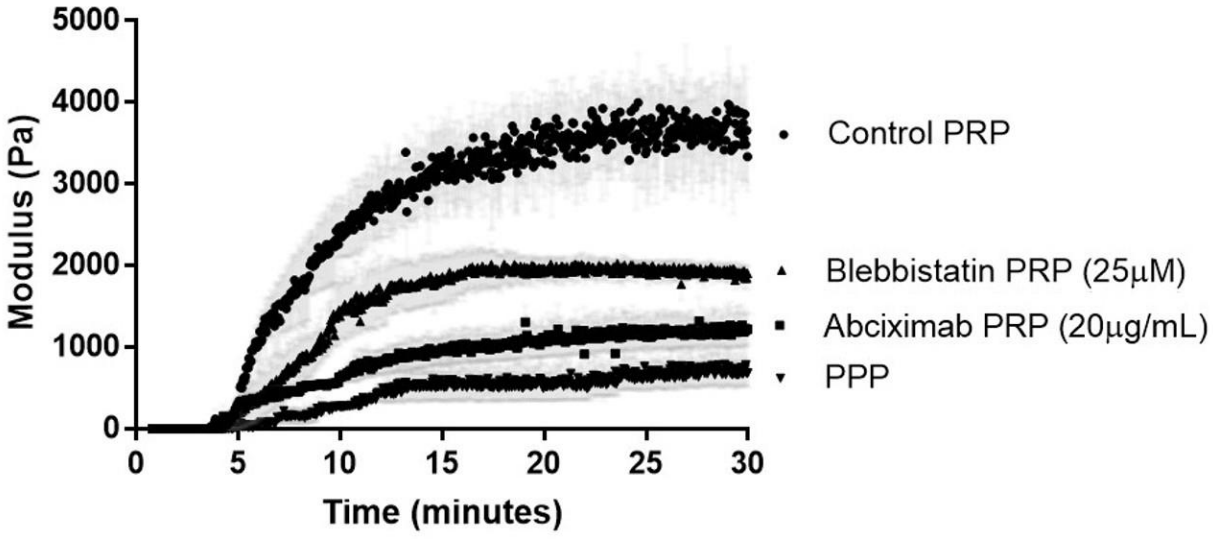

Figure 2-8: Plasma clot stiffness measured by sonorheometry. Shear modulus (stiffness) of control PRP, abciximab-treated PRP, blebbistatin-treated PRP and PPP clots was measured by sonorheometry every 3 seconds from 0-30 minutes post clot initiation. Abciximab (20μg/mL) and blebbistatin (25μM) treatment significantly reduced PRP clot stiffness compared to control ($p < 0.05$ using two-way ANOVA). PPP clots were significantly less stiff than control PRP clots ($p < 0.05$ using two-way ANOVA). Data are plotted as mean ± standard error of the mean; n = 3 subjects, 2-4 replicates per subject.

2.4: Discussion

The sonorheometry study was conducted to evaluate the contribution of the platelet $\alpha_{IIb}\beta_3$ integrin and platelet myosin II ATPase to clot stiffness. The study aimed to build on existing knowledge, and provide further detail regarding the effect of abciximab-mediated inhibition of the platelet $\alpha_{IIb}\beta_3$ integrin and blebbistatin-mediated inhibition of platelet myosin II ATPase on the stiffness of whole blood and plasma clots. The following discussion offers interpretation of the sonorheometry study results, and highlights the novelty of the findings. Finally, the limitations of the study and relevant future experiments are discussed.

2.4.1: Whole Blood Clot Stiffness Measured by Sonorheometry

The whole blood sonorheometry results indicate that $\alpha_{IIb}\beta_3$ integrin-mediated platelet binding to the fibrin network and myosin II ATPase-mediated platelet tensioning of the fibrin network are significant components of whole blood clot stiffening during coagulation. Previous studies using TEG and SEER sonorheometry found that abciximab-mediated inhibition of platelet $\alpha_{IIb}\beta_3$ integrin function reduced whole blood clot stiffness by approximately 70% and 80%, respectively, compared to control (14,57). By comparison, our sonorheometry study results indicated that abciximab treatment reduced whole blood clot stiffness by 83%, which agrees well with the previous studies (**Table 2-1**).

Similarly, our sonorheometry study found that blebbistatin-mediated inhibition of platelet myosin II ATPase function attenuated whole blood clot stiffness by 54% (**Table 2-1**). To our knowledge, there has been no previous study of the contribution of platelet myosin II ATPase to global clot stiffness (i.e. clot shear modulus) during clot formation. A recent study found that inhibition of platelet myosin II ATPase by blebbistatin reduced local platelet contractile stress during coagulation (51). Our whole blood sonorheometry study elucidated the novel finding that inhibition of platelet myosin II ATPase significantly reduced global clot stiffness, which may be due in part to blebbistatin-mediated inhibition of local platelet contractility.

Overall, our whole blood sonorheometry study recapitulated existing findings from previous studies regarding the effect of abciximab-mediated inhibition of the platelet $\alpha_{IIb}\beta_3$ integrin on whole blood clot stiffness, but offered new insight on the effect of blebbistatin-mediated platelet myosin II ATPase inhibition on whole blood clot stiffness. The results confirm that the platelet $\alpha_{IIb}\beta_3$ integrin is a vital regulator of clot mechanical integrity, and suggest that myosin II ATPase is also a significant component of whole blood clot stiffening during coagulation.

Table 2-1: Whole blood clot stiffness summary

	Current Study	Previous Studies*
Abciximab in Whole Blood	Clot Stiffness 83%	Clot Stiffness 70-80%
Blebbistatin in Whole Blood	Clot Stiffness 54%	—

(*Previous Studies: Lang et al. 2004 (TEG); Ferrante et al. 2016 (Sonorheometry))

2.4.2: Plasma Clot Stiffness Measured by Sonorheometry

The plasma sonorheometry results similarly indicate that the platelet $\alpha_{IIb}\beta_3$ integrin and platelet myosin II ATPase are critical regulators of clot stiffness during coagulation. Previous studies using TEG found that abciximab-mediated inhibition of platelet $\alpha_{IIb}\beta_3$ integrin function reduced PRP clot stiffness by approximately 55% compared to control (57). Our plasma sonorheometry study found that abciximab treatment attenuated PRP clot stiffness by 65%, which agrees well with the previous study using the TEG (**Table 2-2**). Interestingly, our whole blood and plasma stiffness studies both found that inhibition of the platelet $\alpha_{IIb}\beta_3$ integrin by abciximab attenuated clot stiffness more effectively (approximately 10-15%) when measured by sonorheometry versus thromboelastography. We hypothesize that this slight discrepancy between the two stiffness assessment techniques may be due to the enhanced measurement sensitivity of sonorheometry, or an underestimation of stiffness by the TEG due to the application of large shear strains to the sample that may interfere with clot formation (41,42,45,47).

Our plasma sonorheometry study found that blebbistatin-mediated inhibition of platelet myosin II ATPase function reduced PRP clot stiffness by 44% (**Table 2-2**). As mentioned above, to our knowledge there have been no previous studies of the contribution of platelet myosin II

ATPase to global clot stiffness. Our finding that inhibition of platelet myosin II ATPase significantly attenuates global clot stiffness may be due to blebbistatin-mediated inhibition of local platelet contractile stress, as previously observed (51). Overall, our plasma sonorheometry results generally agree with those of our sonorheometry stiffness study in whole blood, and suggest that the platelet $\alpha_{IIb}\beta_3$ integrin and platelet myosin II ATPase enhance clot stiffness during coagulation.

Table 2-2: Plasma clot stiffness summary

	Current Study	Previous Study*
Abciximab in PRP	Clot Stiffness 65%	Clot Stiffness 55%
Blebbistatin in PRP	Clot Stiffness 44%	—

(*Previous Study: Lang et al. 2004 (TEG))

2.4.3: Whole Blood vs. Plasma Clot Stiffness Measured by Sonorheometry

The whole blood and plasma sonorheometry results indicate that $\alpha_{IIb}\beta_3$ integrin-mediated platelet binding to the fibrin network and myosin II ATPase-mediated platelet tensioning of the fibrin network are critical components of clot stiffening during coagulation. Interestingly, both the whole blood and plasma sonorheometry studies found that abciximab treatment attenuated clot stiffness more effectively than blebbistatin treatment (**Table 2-3**). We predict this discrepancy is likely due to the more complete inhibition of platelet-fibrin binding by abciximab versus inhibition of platelet-fibrin tensioning by blebbistatin. Abciximab-mediated inhibition of platelet $\alpha_{IIb}\beta_3$ integrin function effectively inhibits the ability of platelets to bind to the clot fibrin network, while blebbistatin-mediated inhibition of platelet myosin II ATPase inhibits platelet-dependent

tensioning of the fibrin network, but does not inhibit platelet-fibrin binding. Therefore, the observation that abciximab attenuates clot stiffness more effectively than blebbistatin was not completely surprising.

In a preliminary sonorheometry study we found that the increased concentration of 100μM blebbistatin reduced whole blood clot stiffness by approximately 70%. Our preliminary data suggests that a more complete inhibition of platelet myosin II ATPase with increased concentrations of blebbistatin may attenuate clot stiffness to a nearly comparable degree as abciximab-mediated inhibition of platelet $\alpha_{IIb}\beta_3$ integrin function. However, given the IC50 value of 5μM for blebbistatin, we chose to use a modest concentration of blebbistatin (25μM) in our study to avoid the cytotoxic and phototoxic effects of blebbistatin observed at high concentrations (60,61).

Another potential explanation for the reduced efficacy of blebbistatin (particularly in the whole blood sonorheometry study), is the likely interaction between blebbistatin and the red blood cells. Myosin II ATPase is present in red blood cells and regulates cell membrane curvature and deformability (62). The reduced efficacy of whole blood clot stiffness attenuation by blebbistatin may have resulted, in part, from the effective dilution of blebbistatin due to the red blood cells.

Although the whole blood and plasma sonorheometry studies found that abciximab treatment more effectively attenuated clot stiffness compared to blebbistatin, the PPP clot stiffness results of the plasma sonorheometry study indicate that neither inhibition of the platelet $\alpha_{IIb}\beta_3$ integrin nor inhibition of platelet myosin II ATPase fully eliminated the platelet contribution to clot stiffness. The PPP clot stiffness results suggest that additional platelet functions such as platelet-mediated generation of thrombin or platelet granule release may contribute to global clot stiffness.

Finally, when comparing the whole blood and plasma clot stiffness results, we observed a prominent decrease in stiffness magnitude for whole blood clots (**Table 2-4**). This discrepancy between whole blood and plasma clot stiffness was similarly observed in a previous study using the TEG (57). We hypothesize that the decreased stiffness in whole blood versus plasma clots is due to a buffering effect of the red blood cells, with the red blood cells in whole blood clots serving as physical barriers that limit the clot fibrin network density and therefore limit clot stiffness.

Table 2-3: Whole blood and plasma clot stiffness summary

	Current Study	Previous Studies*
Abciximab in Whole Blood	Clot Stiffness 83%	Clot Stiffness 70-80%
Abciximab in PRP	Clot Stiffness 65%	Clot Stiffness 55%
Blebbistatin in Whole Blood	Clot Stiffness 54%	—
Blebbistatin in PRP	Clot Stiffness 44%	—

(*Previous Studies: Lang et al. 2004 (TEG); Ferrante et al. 2016 (Sonorheometry))

Table 2-4: Summary of whole blood and plasma clot stiffness magnitude, t = 30 minutes

	Whole Blood	Plasma
Control	2078 ± 64 Pa	3455 ± 518 Pa
Abciximab	348 ± 21 Pa	1192 ± 202 Pa
Blebbistatin	956 ± 132 Pa	1918 ± 79 Pa
PPP	---	667 ± 159 Pa

2.4.4: Sonorheometry Study Limitations and Future Directions

The advantages of the Quantra device for measuring clot stiffness include relative ease of operation and interpretation of results, and low shear strains applied to the sample, compared to existing point of care tests (14,45,63,64). One limitation of the Quantra device that was discovered during this study is the inability to readily adapt the Quantra to measure clot stiffness in plasma samples versus whole blood. The Quantra and the underlying SEER sonorheometry technology were intended to evaluate clot stiffness in whole blood in order to measure the combined effects of all components of hemostasis (46). One of the key features of the Quantra device is the system of optical sensors that helps regulate blood sample filling of the Quantra multi-well test cartridge. The optical sensors rely on the light-absorbing capability of hematocrit to function properly. Consequently, tuning the Quantra device to measure plasma clot stiffness required bypassing the optical sensors to ensure proper filling of the multi-well cartridge.

In the future, it would be valuable to expand the polystyrene bead titration analysis to optimize the bead concentration in the PRP samples and to subsequently optimize the PRP clot stiffness results. As previously mentioned, the preliminary bead titration analysis suggested that increased bead concentration reduced variability in the PRP clot stiffness data, potentially due to a more homogenous estimate of plasma clot stiffness with the increased concentration of force transducers. A more thorough study of optimal bead concentration could significantly improve the plasma clot stiffness data output by the Quantra.

Finally, it would be interesting to see if the simultaneous inhibition of the platelet $\alpha_{IIb}\beta_3$ integrin and myosin II ATPase has an additive attenuating effect on clot stiffness. We predict that a combined treatment of abciximab and blebbistatin will produce clot stiffness results identical to abciximab treatment alone, due to the complete inhibition of platelet-fibrin binding by abciximab.

Chapter 3: Evaluating the Contribution of the Platelet $\alpha_{IIb}\beta_3$ Integrin or Platelet Myosin II ATPase to Plasma Clot Stiffness by Electromagnetic Force

3.1: Introduction

3.1.1: Measuring Blood Clots with Magnet-Based Technologies

A number of technologies have incorporated magnets and magnetic microparticles to quantify various aspects of coagulation. A recent study investigated the application of functionalized magnetic nanoparticles as a non-invasive, rapid tool for the detection of blood clots (65). The study used magnetic particle spectroscopy to detect blood clots targeted by magnetic nanoparticles conjugated with antithrombin aptamers. Other studies used magnetic nanoparticles as magnetically-targetable thrombolytic agents (66,67). Voros et al. used TPA-conjugated superparamagnetic nanoparticles to dissolve clots by TPA-mediated chemical lysis of the clot fibrin network, and by mechanical clot lysis due to localized hyperthermia following stimulation of the magnetic nanoparticles with alternating magnetic fields (66).

In addition to clot detection and clot dissolution by magnet-based technologies, studies have also incorporated magnets and magnetic particles to evaluate blood clot structure and stiffness. Oldenburg et al. used magnetomotive optical coherence tomography (MMOCT) to detect and measure the molecular structure of blood clots (68). Briefly, rehydrated lyophilized platelets loaded with superparamagnetic nanoparticles served as targeted imaging agents for the detection and subsequent imaging of blood clots by MMOCT. Judith et al. used magnetically actuated surface-attached posts to measure whole blood clot stiffness (69). An electromagnetic force was applied to the surface-attached posts, and the motion of the posts due to the force was imaged and quantified to evaluate clot stiffness of whole blood from 0-60 minutes post clot initiation.

Magnet-based assays have shown potential in the detection, evaluation, and dissolution of blood clots in coagulation research. The studies highlighted above suggest that some advantages of magnet-based technologies include the potential for non-invasive thrombus detection (65), targeted anti-thrombotic therapy (66,67), and simultaneous assessment of clot structure and stiffness (68,69).

3.1.2: Electromagnetic Force Study Goals

The goal of the electromagnetic force experiments was to build on existing knowledge regarding the contribution of the platelet $\alpha_{IIb}\beta_3$ integrin or platelet myosin II ATPase to blood clot stiffness. Additionally, the electromagnetic force study was intended to serve as a bridge between the whole blood stiffness data obtained by sonorheometry (Chapter 2) and the plasma clot structure data obtained by confocal microscopy (Chapter 4).

Similar to the sonorheometry study, the electromagnetic force study also aimed to evaluate the effect of blebbistatin-mediated platelet myosin II ATPase inhibition on plasma clot stiffness. We hypothesized that platelet myosin II ATPase inhibition by blebbistatin would significantly reduce global stiffness of plasma clots during coagulation, possibly due to attenuated local platelet contractile stress (51).

In contrast to existing point of care clot stiffness measurement tools such as the TEG, ROTEM, or Quantra, one advantage of the electromagnetic force assay is the potential for simultaneous assessment of clot structure and stiffness (**Figure 3-1**). Although the electromagnetic force study is limited to the application of plasma clots versus whole blood, the assay serves as a novel means for quantifying plasma clot stiffness, and offers the potential for the simultaneous measurement of plasma clot structural changes during coagulation by microscopy.

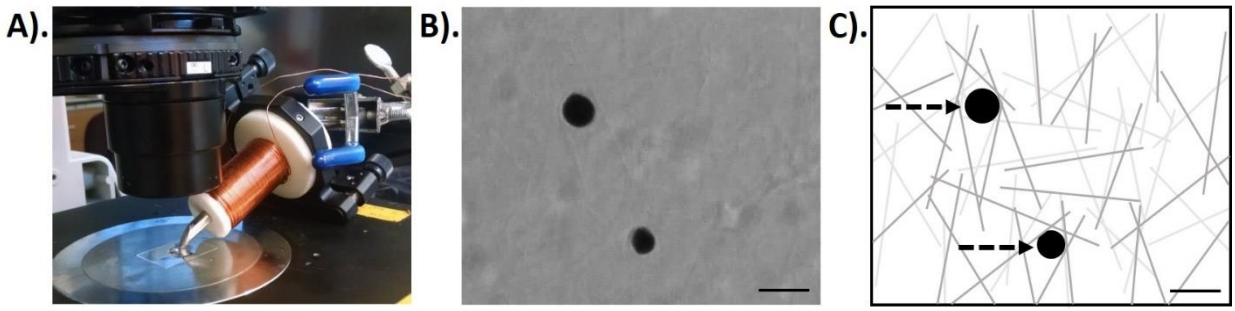

Figure 3-1: Electromagnetic force study goals. The electromagnetic force assay is a novel means for quantifying plasma clot stiffness (A). It offers the potential for simultaneous measurement of plasma clot structural features by microscopy (B) and assessment of clot stiffness by quantifying the displacement of magnetic beads due to applied electromagnetic force (C). Scale bar = 10μm

3.2: Methods

3.2.1: Ethics Statement

The objective of the electromagnetic force portion of the study was to evaluate the mechanical properties of human blood in response to various biochemical stimuli. As a result, the study required the use of primary human cells. Blood was collected from healthy, consenting adults by venipuncture in accordance with a protocol (IRB-HSR 12600) approved by the University of Virginia Institutional Review Board. All contaminated materials, biohazardous waste, and reagents were handled and disposed of properly, in accordance with the University of Virginia and OSHA regulations.

3.2.2: Blood Collection and Plasma Separation

Blood was drawn by venipuncture from healthy volunteers into 3.2% sodium citrate (0.109M) 2.7mL Vacutainer® tubes. Whole blood samples were placed on a rocker prior to experimentation to maintain adequate blood mixing. Blood samples were used for experimentation within 6 hours post blood draw. To obtain PRP, the citrated whole blood was centrifuged at 100 x

g at 25°C for 20 minutes, and the PRP supernatant of the centrifuged sample was collected by pipette. To obtain PPP, the blood was centrifuged two additional times at 3000 x g at 25°C for 15 minutes, and the PPP supernatant was subsequently collected by pipette.

3.2.3: Reagents

The inhibitor abciximab (Reopro®) was used to block platelet $\alpha_{IIb}\beta_3$ integrin-mediated adhesion to the clot fibrin network. PRP samples were incubated with 20µg/mL abciximab to ensure saturation of the $\alpha_{IIb}\beta_3$ integrin (14,26,57). The inhibitor blebbistatin was used to block platelet myosin II ATPase. PRP samples were incubated with 25µM blebbistatin to achieve adequate inhibition of myosin II ATPase (22). $CaCl_2$ was used to re-calcify the citrated plasma samples (12mM final concentration), and contact between the plasma sample and the glass coverslip initiated clotting within the plasma through the intrinsic activation pathway (**Figure 1-2, Section 1.1.2**).

3.2.4: Magnetic Beads

Ferrimagnetic iron oxide beads were a generous gift from the Fredberg Lab (Harvard University, Boston, MA, USA). The beads had an average diameter of 4.8µm, and a mean density of 5g/cm^3. The magnetic beads were pipetted incrementally into the clotting plasma samples to achieve a final concentration of approximately 1x10^6 beads/mL. Incremental pipetting during coagulation ensured that a fraction of the beads remained suspended within the plasma clot, while a significant portion of the beads sunk through the plasma to the glass coverslip due to the high density of the beads relative to the plasma samples. Only the beads that remained suspended within the plasma clot above the coverslip surface were included in the bead tracking analysis and subsequent clot stiffness calculation.

3.2.5: Plasma Clot Stiffness Measured by Electromagnetic Force

Electromagnetic force was used to evaluate the contribution of $\alpha_{IIb}\beta_3$ integrin dependent platelet-fibrin binding and myosin II ATPase dependent platelet-fibrin tensioning to plasma clot stiffness. The plasma stiffness data obtained by electromagnetic force was intended to link the whole blood sonorheometry stiffness data and the microscopy structure data in plasma. The electromagnet was hooked up to a power supply (BK Precision 1697, B&K Precision, Yorba Linda, CA, USA) and mounted on the stage of a microscope (Nikon Eclipse TE300, Nikon, Melville, NY, USA; 60X oil, 1.4NA). Plasma samples were loaded with $CaCl_2$ and inhibitors, and pipetted onto a glass coverslip on the microscope stage. The ferrimagnetic beads were pipetted incrementally into the clotting plasma sample from 5-9 minutes post clot initiation until a final concentration of approximately $1x10^6$ beads/mL was achieved. The tip of the electromagnet was submerged in the plasma sample, and the power supply was used (voltage=40V; current=5A) to apply electromagnetic force on the beads every 5 minutes from 10-30 minutes post clot initiation. The motion of the ferrimagnetic beads due to the electromagnetic force was imaged and recorded using a video camera (Canon Vixia HF S21, Canon, Melville, NY, USA) mounted to the microscope, and bead displacement was used to quantify the stiffness of the plasma clots, as described below (**Section 3.2.7**). (**Figure 3-2**)

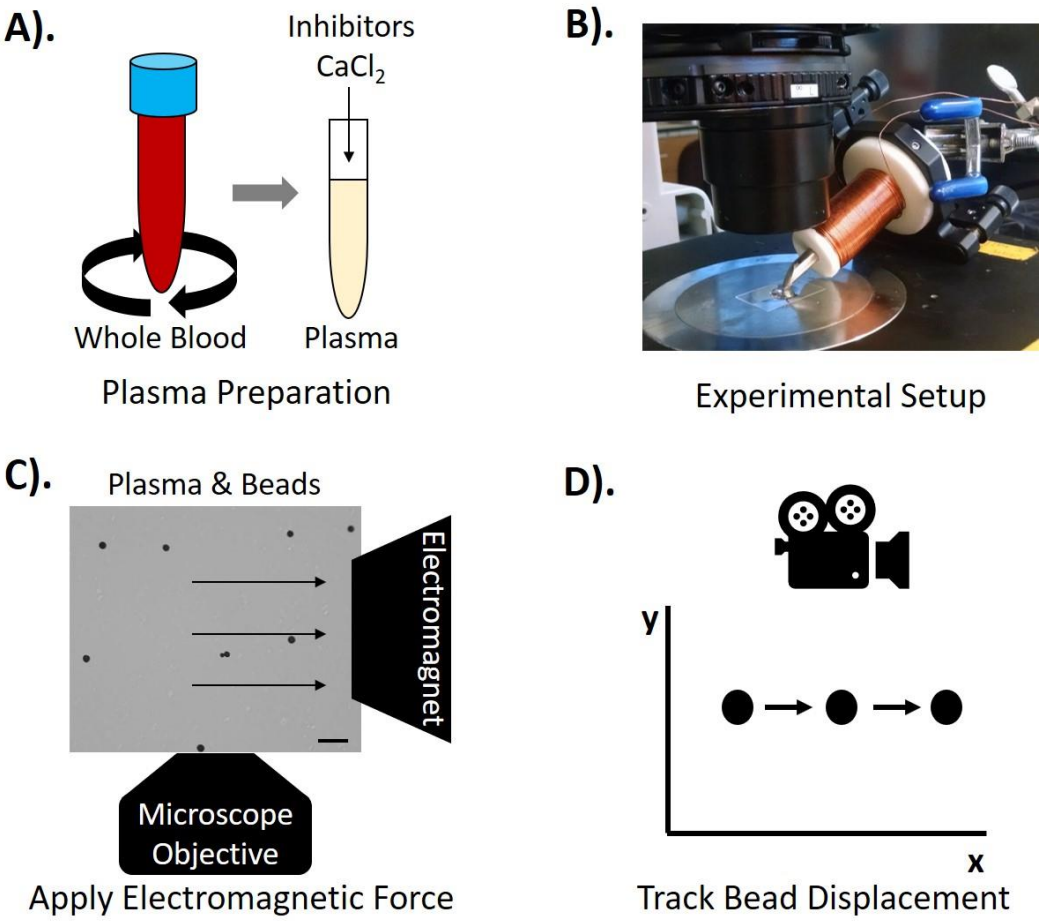

Figure 3-2: Plasma clot stiffness assessment using electromagnetic force. A). Citrated whole blood was centrifuged to obtain plasma. The plasma was incubated with inhibitors (20µg/mL abciximab or 25µM blebbistatin) and $CaCl_2$ (12mM). B). The plasma sample was pipetted onto a glass slide on the microscope stage, magnetic beads were incrementally pipetted into the sample, and the magnet tip was submerged in the sample. C). Electromagnetic force was applied on the beads every 5 minutes from 10-30 minutes post clot initiation (scale bar =10µm). D). The motion of the ferrimagnetic beads due to the electromagnetic force was imaged and recorded using a video camera mounted to the microscope, and bead displacement was measured to quantify the stiffness of the plasma clots.

3.2.6: Force Calculation

In order to calculate the stiffness of the plasma samples, the force applied to the ferrimagnetic beads by the electromagnet was evaluated. The electromagnetic force was estimated by tracking the motion of the ferrimagnetic beads and subsequently calculating the bead terminal

velocities through fluids with known viscosities. Three fluids with known viscosities were used to determine the electromagnetic force applied to the beads: two NIST traceable viscosity standards (S3 and S6; Cole Parmer, Vernon Hills, IL, USA) and blood plasma. Approximately $1x10^6$ beads/mL ferrimagnetic beads were pipetted into S3, S6, or blood plasma on a coverslip, and the magnet tip was submerged in the sample. The power supply was used to apply electromagnetic force on the beads (voltage=40V; current=5A), and the bead motion due to the applied force was imaged and recorded by video camera. The force applied to the beads was calculated using Stokes' law:

$$F = 6\,\pi\,\mu\,R\,\nu \qquad \text{(Equation 1)}$$

Where F is the force applied to the beads, μ is the fluid viscosity, R is the bead radius, and ν is the bead terminal velocity. The S3 and S6 standards have known viscosities of 4.063cP and 8.743cP at 25°C, respectively, while blood plasma has a mean viscosity of 1.6cP at room temperature (23,43). Plasma clot stiffness was subsequently calculated from the force applied to the beads as described below (**Section 3.2.7**).

3.2.7: Bead Tracking and Clot Stiffness Calculation

The motion of the ferrimagnetic beads due to the applied electromagnetic force was imaged and recorded by video camera, and subsequently tracked using automated and manual techniques in FIJI to calculate mean bead displacement (70). Plasma clot stiffness was calculated given:

$$S = F/D \qquad \text{(Equation 2)}$$

Where S is plasma clot stiffness, F is the force applied to the beads as described above (**Section 3.2.6**), and D is the mean bead displacement.

3.2.8: Statistical Analysis

A power analysis was completed to calculate the appropriate sample size for the electromagnetic force experiments given a 5% level of significance and 80% power. A two-way ANOVA and paired t-tests were used to calculate statistical significance (defined as $p < 0.05$).

3.3: Results

3.3.1: Electromagnetic Force Calculation Using Stokes' Law

The force applied to the ferrimagnetic beads by the electromagnet was evaluated to subsequently quantify plasma clot stiffness. The electromagnetic force was estimated by tracking the motion of the ferrimagnetic beads and calculating the bead terminal velocities through three fluids with known viscosities: two NIST traceable viscosity standards S3 and S6, and blood plasma. Force was subsequently calculated from the fluid viscosities and corresponding bead terminal velocities using Stokes' law (given that citrated blood plasma is a Newtonian fluid from strain rates of 0 s^{-1} to several thousand s^{-1} (71)). Due to the relatively low viscosity of citrated blood plasma and thus the corresponding relatively high bead terminal velocities in PRP, the S3 and S6 NIST viscosity standards were used as controls to validate the electromagnetic force measurement in blood plasma.

Mean bead terminal velocities due to electromagnetic force application in S3, S6, and blood plasma were measured to be 2560.0 ± 152.0μm/s, 1279.7 ± 49.1μm/s, and 6781.8 ± 453.9μm/s respectively (**Table 3-1**). Bead velocity was assessed by video microscopy using a 10X microscope air objective, and a video camera with a frame rate of 30 frames/s. The mean bead terminal velocity in blood plasma of 6781.8 ± 453.9μm/s divided by the camera frame rate of 30 frames/s, equates to a bead velocity of approximately 220μm/frame. In a 1920μm X 1080μm

image, a bead traveling at approximately 220μm/frame can be tracked over the course of 5-9 frames. Therefore, video microscopy at 10X magnification using a standard frame rate (30 frames/s) video camera can be used to assess bead terminal velocity due to electromagnetic force application in S3, S6, and blood plasma.

The measured bead terminal velocities and the mean fluid viscosities for S3, S6, and blood plasma were used to calculate the force applied to the beads using Stokes' law (**Equation 1, Section 3.2.6**). The electromagnetic force applied to the beads in S3, S6, and blood plasma were calculated to be 468.6 ± 27.9pN, 511.0 ± 19.4pN, and 493.2 ± 29.3pN respectively (**Table 3-1**). There was no statistically significant difference in applied force between the three fluids (p=0.56 using single factor ANOVA; n=15-20 beads per sample), which suggests that the electromagnetic force measured in blood plasma is an appropriate estimate of the force applied by the electromagnet on the ferrimagnetic beads.

Table 3-1: Electromagnetic force calculation summary

	S3 Viscosity Standard	S6 Viscosity Standard	Blood Plasma
Viscosity (cP)	4.063 cP	8.743 cP	1.6 cP*
Bead Velocity (μm/s)	2560.0 ± 152.0 μm/s	1279.7 ± 49.1 μm/s	6781.8 ± 453.9 μm/s
Force (pN)	468.6 ± 27.9 pN	511.0 ± 19.4 pN	493.2 ± 29.3 pN

(*Mean viscosity of blood plasma at room temperature (Shinton 2007))

3.3.2: Platelet $\alpha_{IIb}\beta_3$ Integrin and Myosin II ATPase Enhance Plasma Clot Stiffness

Electromagnetic force was used to measure the contribution of the platelet $\alpha_{IIb}\beta_3$ integrin and platelet myosin II ATPase to plasma clot stiffness. The plasma clot stiffness data obtained by

electromagnetic force was intended to serve as a bridge between the whole blood sonorheometry stiffness data and the plasma clot structural features evaluated by confocal microscopy. One advantage of the electromagnetic force measurement of clot stiffness versus the sonorheometry stiffness study was the use of nearly identical experimental conditions between the electromagnetic force and confocal microscopy studies.

Control PRP, abciximab-treated PRP, blebbistatin-treated PRP, and PPP clot stiffness was measured by electromagnetic force from 10-30 minutes post clot initiation. Control PRP samples clotted steadily from 10 to 30 minutes post clot initiation, and reached a maximum clot stiffness of 1680 ± 58 pN/μm by t = 30 minutes (**Figure 3-3**). Inhibition of the platelet $\alpha_{IIb}\beta_3$ integrin by abciximab significantly ($p < 0.05$) reduced PRP clot stiffness (**Figure 3-3**), which agrees with the results of the sonorheometry study, and supports the previous finding that the platelet $\alpha_{IIb}\beta_3$ integrin is an essential component in the regulation of clot mechanical integrity (57). By 30 minutes post clot initiation, abciximab-treated PRP samples reached a maximum clot stiffness of 789 ± 38 pN/μm, indicating that inhibition of platelet $\alpha_{IIb}\beta_3$ integrin function reduced PRP clot stiffness by 53%.

Similarly, the plasma electromagnetic force results found that inhibition of platelet myosin II ATPase by blebbistatin significantly ($p < 0.05$) reduced PRP clot stiffness (**Figure 3-3**), which agrees with the findings of the sonorheometry study and suggests that platelet myosin II ATPase is a critical modulator of clot stiffness. At 30 minutes post clot initiation, blebbistatin-treated PRP samples reached a maximum clot stiffness of 990 ± 36 pN/μm, indicating that inhibition of platelet myosin II ATPase attenuated PRP clot stiffness by 41%. Finally, the removal of a majority of the platelets (PPP) significantly ($p < 0.05$) reduced clot stiffness compared to control PRP (**Figure 3-3**), where PPP clot stiffness (744 ± 27 pN/μm) was 56% softer than control PRP clot stiffness by t

= 30 minutes. Overall, the plasma electromagnetic force results support the sonorheometry stiffness results, and suggest that $\alpha_{IIb}\beta_3$ integrin-mediated platelet binding to the fibrin network and myosin II ATPase-mediated platelet tensioning of the fibrin network are significant components of plasma clot stiffening.

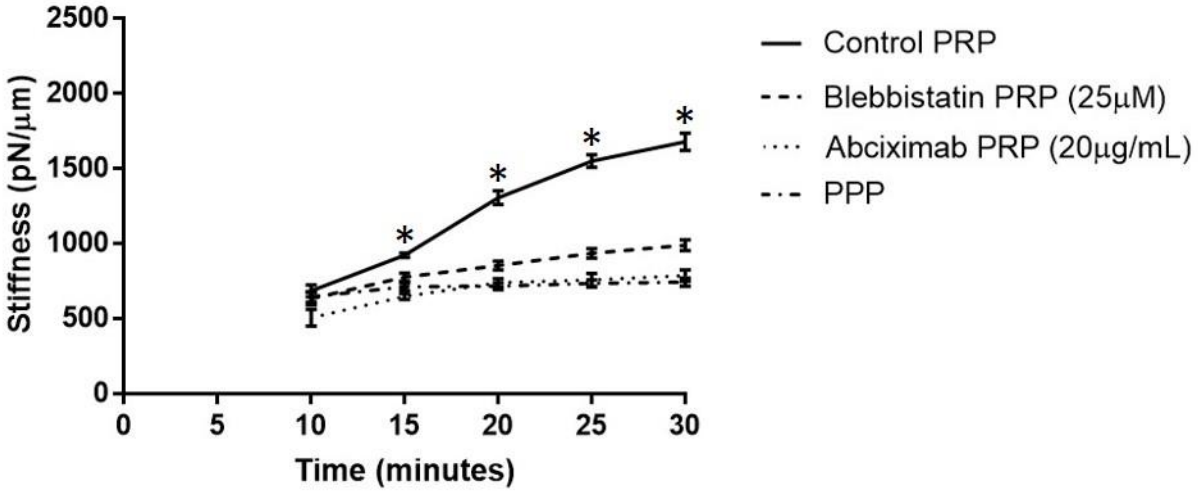

Figure 3-3: Plasma clot stiffness measured by electromagnetic force. Stiffness of control PRP, abciximab-treated PRP, blebbistatin-treated PRP and PPP clots was measured by electromagnetic force every 5 minutes from 10-30 minutes post clot initiation. Abciximab-treated (20μg/mL) PRP, blebbistatin-treated (25μM) PRP, and PPP clots were significantly less stiff than control PRP clots (*$p < 0.05$ for $t \geq 15$ minutes using paired student t-tests). Data are plotted as mean ± standard error of the mean; n = 5 subjects, 5 beads per subject.

3.4: Discussion

The electromagnetic force study was conducted to estimate the contribution of the platelet $\alpha_{IIb}\beta_3$ integrin and platelet myosin II ATPase to plasma clot stiffness. The study aimed to build on existing knowledge, and provide additional insight regarding the effect of abciximab-mediated inhibition of the platelet $\alpha_{IIb}\beta_3$ integrin and blebbistatin-mediated inhibition of platelet myosin II ATPase on the stiffness of plasma clots. The following discussion offers interpretation of the

electromagnetic force stiffness results, and compares the electromagnetic force results with those of the sonorheometry study. Finally, the limitations of the study and relevant future experiments are highlighted.

3.4.1: Plasma Clot Stiffness Measured by Electromagnetic Force

The electromagnetic force results for plasma clot stiffness suggest that the platelet $\alpha_{IIb}\beta_3$ integrin and platelet myosin II ATPase are critical regulators of clot stiffness during coagulation. A previous study using the TEG found that abciximab-mediated inhibition of platelet $\alpha_{IIb}\beta_3$ integrin function reduced PRP clot stiffness by approximately 55% compared to control (57). Our electromagnetic force study found that abciximab treatment attenuated PRP clot stiffness by 53%, which agrees well with the previous study using the TEG (**Table 3-2**).

Similarly, our electromagnetic force study found that blebbistatin-mediated inhibition of platelet myosin II ATPase function reduced PRP clot stiffness by 41% (**Table 3-2**). As mentioned previously, to our knowledge there have been no prior studies of the contribution of platelet myosin II ATPase to global clot stiffness. Our electromagnetic force results suggest that inhibition of platelet myosin II ATPase significantly attenuates global clot stiffness, which may be due to blebbistatin-mediated inhibition of local platelet contractile stress, as previously observed (51). Overall, our electromagnetic force results for plasma clot stiffness generally agree with those of our sonorheometry stiffness study, and suggest that the platelet $\alpha_{IIb}\beta_3$ integrin and platelet myosin II ATPase enhance clot stiffness during coagulation.

Table 3-2: Plasma clot stiffness summary

	Electromagnetic Force	Sonorheometry	Previous Study*
Abciximab in PRP	Clot Stiffness 53%	Clot Stiffness 65%	Clot Stiffness 55%
Blebbistatin in PRP	Clot Stiffness 41%	Clot Stiffness 44%	—
PPP	Clot Stiffness 56%	Clot Stiffness 80%	Clot Stiffness 55%

(*Previous Study: Lang et al. 2004 (TEG))

3.4.2: Plasma Clot Stiffness Measured by Electromagnetic Force vs. Sonorheometry

The plasma clot stiffness results obtained by electromagnetic force agree well with the plasma stiffness results previously measured with the TEG (57), and are generally consistent with the findings of the sonorheometry plasma stiffness study discussed in Chapter 2 (**Table 3-2**). Interestingly, the electromagnetic force results for reduced clot stiffness due to abciximab treatment or removal of a majority of the platelets (PPP) are nearly identical to the TEG plasma clot stiffness findings. When comparing the electromagnetic force and sonorheometry stiffness results, the attenuating effect of blebbistatin treatment on PRP clot stiffness is comparable between the two measurement techniques. By contrast, the comparison of our two plasma stiffness studies suggests that the effect of abciximab treatment or platelet removal on plasma clot stiffness may be greatly underestimated (approximately 12-24%) by our electromagnetic force assay.

The discrepancy between the electromagnetic force and sonorheometry stiffness results may be due to biological or assay-specific differences. Chapter 2 highlighted the role of the plasma sonorheometry study as a means to compare the whole blood sonorheometry results with the plasma electromagnetic force results, and to subsequently evaluate if discrepancies between the

whole blood sonorheometry data and the plasma electromagnetic force data could be attributed to assay-specific differences or biological differences. The whole blood and plasma sonorheometry results of Chapter 2 indicated that there were measurable differences between whole blood and plasma clot stiffness (**Table 2-3, Section 2.4.2**), suggesting that a biological difference (i.e. red blood cells) may partly account for the discrepancy between whole blood and plasma clot stiffness.

The remaining discrepancy between the electromagnetic force data and the sonorheometry stiffness results is likely due assay-specific differences. Similar to the TEG, the large force applied to the beads by the electromagnet may result in the application of large strains on the plasma sample, which may ultimately interfere with clot formation. Additionally, the large force applied to the plasma samples in the electromagnetic force assay caused a number of beads to dislodge from soft plasma clots. Soft clots with a mean stiffness of roughly 500 pN/μm or less were particularly susceptible to bead dislodgement, suggesting that clot stiffness magnitude for soft clots (i.e. abciximab-treated PRP or PPP clots) may have been greatly overestimated in the electromagnetic force assay. This would suggest that the attenuating effect of abciximab treatment or platelet removal (PPP) would ultimately be underestimated by electromagnetic force measurement compared to sonorheometry (**Table 3-2**). Despite the measurable discrepancy in clot stiffness magnitude, the general findings of the electromagnetic force study of plasma clot stiffness agree strongly with the sonorheometry plasma clot stiffness study (R=0.85).

3.4.3: Electromagnetic Force Study Limitations and Future Directions

The primary limitation of the electromagnetic force study was the narrow dynamic range for estimating plasma clot stiffness. The maximum clot stiffness that could be measured by the electromagnetic force assay was approximately 2000 pN/μm due to the microscopy resolution

limit (60X oil immersion objective, 1.4NA). This upper bound of resolvable clot stiffness may have skewed the control PRP clot stiffness results of the electromagnetic force study, since some of the control clots approached a stiffness of 2000 pN/μm by 30 minutes post clot initiation.

Similarly, the minimum clot stiffness that could be measured by the electromagnetic force assay was approximately 500 pN/μm due to the large force applied by the electromagnet. Soft clots (i.e. clots 0-10 minutes post clot formation, or abciximab-treated PRP or PPP clots) were particularly susceptible to the lower bound of resolvable clot stiffness, as the application of electromagnetic force fully dislodged many of the beads from the clotting plasma samples. As a result, the abciximab-treated PRP and PPP clot stiffness results of the electromagnetic force study may have been skewed by the lower bound of clot stiffness, since some of the abciximab-treated PRP and PPP clots approached a stiffness of 500 pN/μm. The limited dynamic range of the electromagnetic force assay prevented the assessment of clot stiffness from 0-10 minutes post clot initiation, and likely contributed to the discrepancy observed between the electromagnetic force and sonorheometry stiffness results for abciximab-treated PRP and PPP clots.

In contrast to the limited dynamic range for clot stiffness assessment inherent to the electromagnetic force assay, sonorheometry has a dynamic range of approximately five orders of magnitude for stiffness measurements (46). This wide dynamic range exhibited by sonorheometry is due to the application of an adaptive force rather than a fixed force, as applied by the electromagnetic force assay and the TEG. In future experiments, it would be valuable to expand the dynamic range of the electromagnetic force assay by applying an adaptive force technique. This could be especially valuable for reducing the lower bound of the dynamic range of the electromagnetic force assay, which would enable the measurement of clot stiffness from 0-10

minutes post clot initiation, and would likely improve clot stiffness measurements for soft abciximab-treated PRP and PPP clots.

Another potential limitation of the electromagnetic force clot stiffness assay is the possibility that the force applied to the plasma clot by the electromagnet may disrupt clot formation, similar to the effect of high shear strains applied by the TEG and ROTEM (41,42). In order to evaluate if the force applied by the electromagnet disrupts clot formation, a valuable future experiment would be to measure the stiffness of a plasma clot at t = 30 minutes by electromagnetic force, and compare this to the results of the electromagnetic force study where stiffness was measured intermittently (i.e. clot stiffness assessed by electromagnetic force every 5 minutes from 10 to 30 minutes post clot initiation). If the force applied by the electromagnet disrupts clot formation, I predict that the stiffness of the plasma clot measured at t= 30 minutes would be significantly greater than the stiffness of the plasma clot measured intermittently. Overall, this study could provide additional insight regarding the capabilities or limitations of the electromagnetic force assay as a means of quantifying clot stiffness.

Finally, in contrast to existing point of care clot stiffness measurement tools such as the TEG, ROTEM, or Quantra, the electromagnetic force study was limited to the application of plasma clots versus whole blood, and therefore did not measure the combined effects of all components of hemostasis. Although the electromagnetic force study exhibited a number of limitations, the assay served as a novel means for quantifying plasma clot stiffness, and offers the potential for simultaneous assessment of plasma clot structure and stiffness, unlike any of the existing point of care coagulation technologies.

Chapter 4: Evaluating the Contribution of the Platelet $\alpha_{IIb}\beta_3$ Integrin or Platelet Myosin II ATPase to Fibrin Network Structure by Confocal Microscopy and Image Analysis

4.1: Introduction

Previous studies have used features of abnormal clot structure to identify patients at risk of thrombotic events and to evaluate the efficacy of anti-thrombotic drugs (48,49), highlighting the value of clot structure as a metric of vascular disease. To evaluate if changes in clot stiffness can be linked to platelet-driven changes in clot structure, we used confocal microscopy and image analysis to measure the contribution of the platelet $\alpha_{IIb}\beta_3$ integrin and platelet myosin II ATPase to fibrin network structure.

4.1.1: The Platelet $\alpha_{IIb}\beta_3$ Integrin and Platelet Myosin II ATPase in Clot Structure

Previous studies have used confocal microscopy, scanning electron microscopy, and subsequent image analysis techniques to investigate the platelet contribution to blood clot structure. Collet et al. found that abciximab-mediated platelet $\alpha_{IIb}\beta_3$ integrin inhibition significantly impaired platelet aggregation during coagulation, which ultimately reduced clot resistance to degradation by fibrinolysis (72,73). The group observed that dense platelet aggregates found in control PRP clots were significantly attenuated following abciximab treatment, and suggested that inhibition of the platelet $\alpha_{IIb}\beta_3$ integrin by abciximab ultimately facilitated the rate and degree of clot lysis by promoting the accessibility of tissue plasminogen activator (tPA) to the clot fibrin network (5).

Similarly, a recent study found that inhibition of myosin II ATPase by blebbistatin significantly reduced fibrin compaction in local regions of platelets (51). The group observed that

blebbistatin-mediated inhibition of platelet myosin II ATPase significantly attenuated the rate and extent of fibrin densification in PRP clots during clot contraction, suggesting that myosin II ATPase is a critical component of clot structural maturation during the clot contraction phase of coagulation (51).

Although the previous studies investigated the effect of platelet $\alpha_{IIb}\beta_3$ integrin or platelet myosin II ATPase inhibition on clot structure, they focused primarily on platelet-specific changes, such as platelet aggregation and fibrin densification on platelets. By contrast, our study is a comprehensive investigation of the contribution of the platelet $\alpha_{IIb}\beta_3$ integrin or platelet myosin II ATPase to specific features of fibrin network structure (including fiber segment length, fiber junction density, clot porosity, and clot structural heterogeneity) during clot formation.

4.1.2: Clot Structure Study Goals

The goal of the confocal microscopy structure study was to build on existing knowledge regarding the contribution of the platelet $\alpha_{IIb}\beta_3$ integrin or platelet myosin II ATPase to clot structure. The study aimed to measure the effect of abciximab-mediated inhibition of the platelet $\alpha_{IIb}\beta_3$ integrin or blebbistatin-mediated inhibition of platelet myosin II ATPase on specific structural features of the clot fibrin network including fibrin fiber segment length, fiber junction density, and clot porosity. In addition, the confocal microscopy study of clot structure aimed to evaluate perturbations to fibrin network structural heterogeneity following inhibition of platelet $\alpha_{IIb}\beta_3$ integrin-mediated adhesion to the clot fibrin network, or inhibition of platelet myosin II ATPase-mediated tensioning of the clot fibrin network. Finally, to evaluate if the platelet-mediated changes in fibrin network structure could be used to predict changes in clot stiffness, we applied an existing network model to the clot structure results to estimate clot stiffness (74). We

hypothesized that inhibition of $\alpha_{IIb}\beta_3$ integrin-mediated platelet binding to the fibrin network or inhibition of platelet myosin II ATPase-mediated tensioning of the clot network would disrupt fibrin network structure, resulting in reduced clot stiffness as predicted by the model.

To our knowledge, our confocal microscopy study of clot structure is the first comprehensive investigation of the contribution of the platelet $\alpha_{IIb}\beta_3$ integrin and platelet myosin II ATPase to specific structural features of the clot fibrin network during clot formation. Overall, the confocal microscopy structure study aimed to contribute to the field by measuring the effect of abciximab dependent inhibition of platelet-fibrin binding and blebbistatin dependent inhibition of platelet-fibrin tensioning on fibrin fiber length, junction density, clot porosity, and clot structural heterogeneity during coagulation. By further understanding the platelet contribution to global clot structure, this work could be valuable in identifying platelet-driven clot structural features that may serve as a novel means to detect or target thrombosis.

4.2: Methods

4.2.1: Ethics Statement

The objective of the confocal microscopy portion of the study was to evaluate the structural properties of human blood in response to various biochemical stimuli. As a result, the study required the use of primary human cells. Blood was collected from healthy, consenting adults by venipuncture in accordance with a protocol (IRB-HSR 12600) approved by the University of Virginia Institutional Review Board. All contaminated materials, biohazardous waste, and reagents were handled and disposed of properly, in accordance with the University of Virginia and OSHA regulations.

4.2.2: Blood Collection and Plasma Separation

Blood was drawn by venipuncture from healthy volunteers into 3.2% sodium citrate (0.109M) 2.7mL Vacutainer® tubes. Whole blood samples were placed on a rocker prior to experimentation to maintain adequate blood mixing. Blood samples were used for experimentation within 6 hours post blood draw. To obtain PRP, the citrated whole blood was centrifuged at 100 x g at 25°C for 20 minutes, and the PRP supernatant of the centrifuged sample was collected by pipette. To obtain PPP, the blood was centrifuged two additional times at 3000 x g at 25°C for 15 minutes, and the PPP supernatant was subsequently collected by pipette.

4.2.3: Reagents

The inhibitor abciximab (Reopro®) was used to block platelet $\alpha_{IIb}\beta_3$ integrin-mediated adhesion to the fibrin fiber network. PRP samples were incubated with 20µg/mL abciximab to ensure saturation of the platelet $\alpha_{IIb}\beta_3$ integrin (14,26,57). The inhibitor blebbistatin was used to block platelet myosin II ATPase. PRP samples were incubated with 25µM blebbistatin to achieve adequate inhibition of platelet myosin II ATPase (22). To image the clot fibrin network by confocal microscopy, the plasma samples were incubated with 30µg/mL Alexa-Fluor 488-labeled human fibrinogen (Thermo Fisher, Waltham, MA, USA). To image the platelets by confocal microscopy, the plasma samples were incubated with 10µg/mL WGA rhodamine (Vector Labs, Burlingame, CA, USA). $CaCl_2$ was used to re-calcify the citrated plasma samples (12mM final concentration), and contact with the glass coverslip initiated clotting within the plasma sample through the intrinsic activation pathway (**Figure 1-2, Section 1.1.2**).

4.2.4: Plasma Clot Structure Evaluated by Confocal Microscopy

Confocal microscopy and subsequent image processing and image analysis techniques were used to evaluate plasma clot structural perturbations following inhibition of $\alpha_{IIb}\beta_3$ integrin-mediated platelet binding to the fibrin network or inhibition of myosin II ATPase-mediated platelet tensioning of the fibrin network. Whole blood was centrifuged at 100 x g for 20 minutes to obtain PRP, and two additional times at 3000 x g for 15 minutes to obtain PPP. Plasma samples were loaded with fluorescent dyes, inhibitors, and $CaCl_2$, and pipetted into a sealed glass chamber for imaging by confocal microscopy (**Figure 4-1**). The glass chamber consisted of a microscope slide base, and a glass coverslip affixed to the microscope slide using double-sided tape. The interior dimensions of the glass chamber were 22mm X 6mm X 0.09mm, which accommodated a plasma sample volume of approximately 12µL. After the plasma sample was pipetted into the glass chamber, the chamber ends were sealed with a wax-based sealant.

The plasma samples were imaged by spinning disk confocal microscopy using a 60X oil immersion objective with 1.4NA (Nikon Eclipse Ti, Nikon, Melville, NY, USA) and NIS Elements imaging software (Nikon, Melville, NY, USA). A series of 3µm-thick z-stack images were acquired every two minutes from 0-30 minutes post clot initiation, with a distance of 0.8µm between each of the 5 z-stack slices at a resolution of 1024 X 1024 pixels (**Figure 4-1**). The confocal images were subsequently processed to quantify fibrin network structural features, as described below (**Section 4.2.5**).

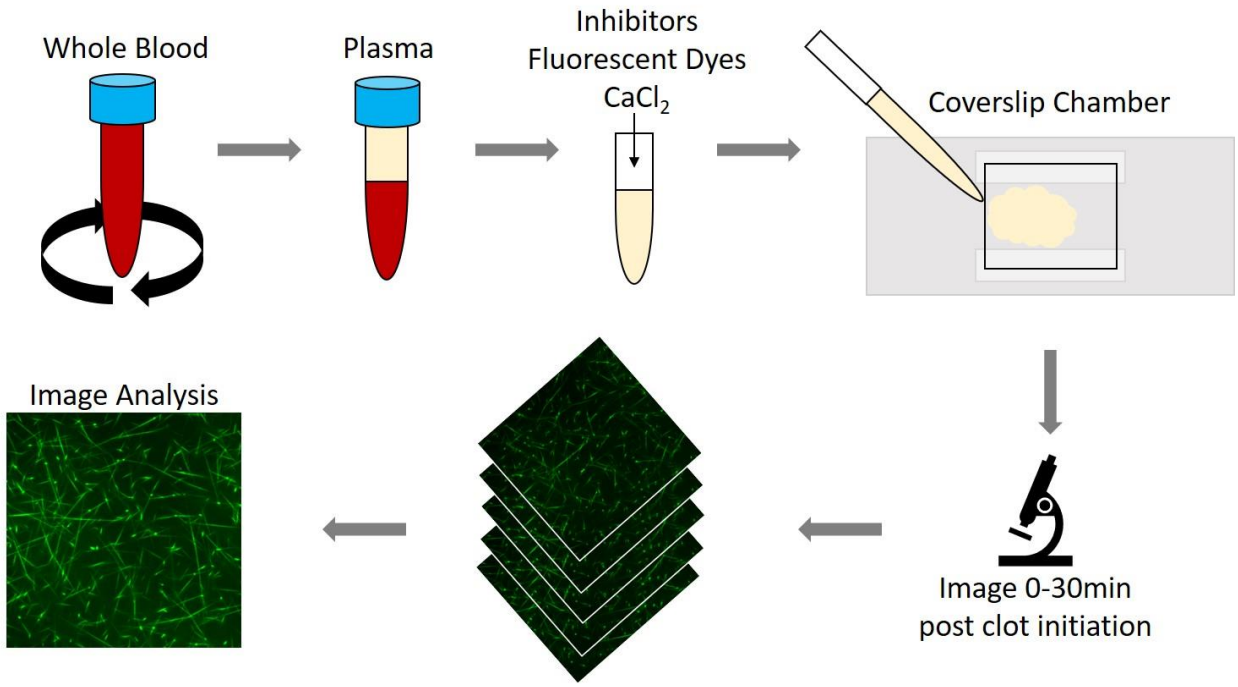

Figure 4-1: Plasma clot structure evaluated by confocal microscopy. Citrated whole blood was centrifuged to obtain plasma. The plasma was incubated with inhibitors (20µg/mL abciximab or 25µM blebbistatin), fluorescent dyes (30µg/mL Alexa-Fluor 488-labeled fibrinogen and 10µg/mL WGA rhodamine) and $CaCl_2$ (12mM), and pipetted into a glass coverslip chamber. The plasma sample was imaged by confocal microscopy from 0-30 minutes post clot initiation, and the resulting images were processed and analyzed to measure fibrin network structural perturbations.

4.2.5: Image Processing and Data Analysis

The confocal microscopy images were processed using a two-step technique to quantify clot structure perturbations due to abciximab-mediated inhibition of the platelet $\alpha_{IIb}\beta_3$ integrin and blebbistatin-mediated inhibition of platelet myosin II ATPase. First, the images were run through a MATLAB-based filament detection algorithm developed by the Rohde Lab (University of Virginia, Charlottesville, VA, USA) (75,76). The algorithm applied a filament orientation map to improve image resolution between the fibrin network and image background, and to subsequently estimate the location of filaments (**Figure 4-2**) (75). Next, the resulting images from the filament

detection algorithm were analyzed in FIJI using the Ridge Detection plugin (70,77). The plugin measured fiber segment length and fiber junction density of the clot fibrin networks, and the binary image output by the Ridge Detection plugin was used to estimate clot porosity via the FIJI Measure tool (**Figure 4-2**). Mean fiber segment length, junction density, and clot porosity were quantified for control PRP, abciximab-treated PRP, blebbistatin-treated PRP, and PPP clots from 0-30 minutes post clot initiation. The fiber segment length data was subsequently used to estimate clot stiffness by a simple network model, as described below (**Section 4.2.6**).

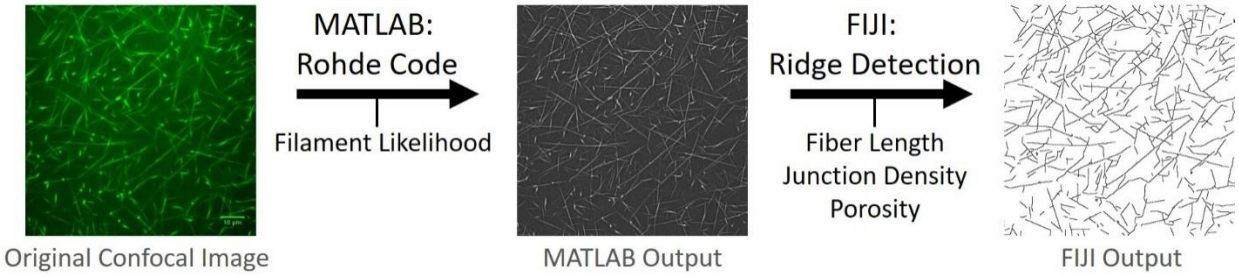

Figure 4-2: Image processing and data analysis. The confocal clot structure images were processed using a two-step technique: 1. Filament likelihood was evaluated using the Rohde code in MATLAB, and 2. The FIJI Ridge Detection plugin was implemented to quantify fiber segment length, junction density, and porosity of the plasma clots.

To evaluate the heterogeneity of the plasma clots, the image processing and data analysis techniques were applied to platelet-rich and platelet-free regions of the clot structure images. Mean fiber segment length, junction density, and clot porosity were measured in 100 X 100 pixels localized platelet regions and platelet-free regions, and the ratio between regions of platelets and no platelets was calculated to estimate clot heterogeneity (**Figure 4-3**). The measurement was repeated using 50 X 50 and 200 X 200 pixels regions to determine if the heterogeneity estimate was dependent on the size of the selected regions.

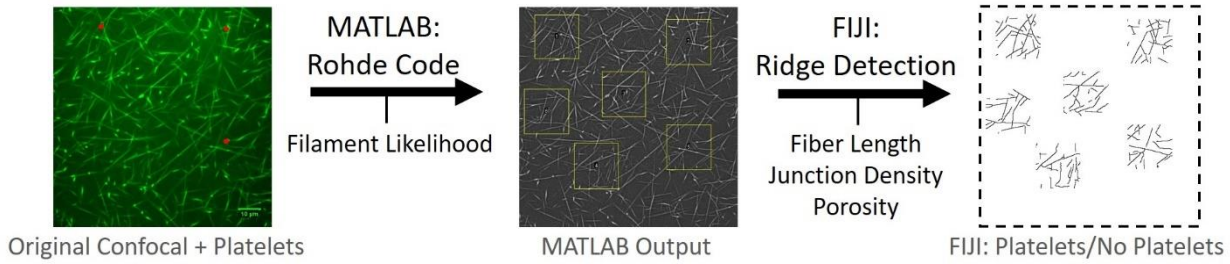

Figure 4-3: Image processing and data analysis for clot heterogeneity estimate. Regions of platelets and no platelets were identified in the confocal clot structure images. The original confocal images were processed using the Rohde code in MATLAB, and the FIJI Ridge Detection plugin was implemented to quantify fiber segment length, junction density, and clot porosity in 100 X 100 pixels regions of platelets and no platelets. The ratio of platelets/no platelets was calculated to estimate clot heterogeneity.

4.2.6: Clot Stiffness Estimate from Structure Data

To quantitatively compare the plasma clot structure data with the stiffness portion of the study, a simple network model was implemented to calculate the elastic modulus of the fibrin networks and ultimately the stiffness of the plasma clots. Shin et al. described a model to theoretically relate the elastic modulus of a network of filaments to the bending modulus of a single filament given (74):

$$E_0 \sim \kappa_0^2/(k_B T \xi^2 l_c^3) \qquad \text{(Equation 3)}$$

Where E_0 is the network elastic modulus, κ_0 is the bending modulus of a single filament, k_B is Boltzmann's constant, T is temperature, ξ is the network pore size, and l_c is the distance between crosslinks. The FIJI Ridge Detection plugin evaluated fiber length as the distance between junctions, therefore mean fiber segment length was used for l_c. Network pore size was estimated as l_c assuming a lattice network structure, and the bending modulus of a fibrin fiber was assumed to be 4.5×10^{-24} Nm^2 (78). Next, the network elastic modulus was used to estimate plasma clot stiffness (shear modulus) given:

$$G_0 = E_0/(2\ x\ (1 + \ p)) \quad \text{(Equation 4)}$$

Where G_0 is the shear modulus of the clot, E_0 is the network elastic modulus, and p is Poisson's ratio for the plasma clot, which was assumed to be 0.5 (78). Mean clot stiffness was estimated for control PRP, abciximab-treated PRP, blebbistatin-treated PRP, and PPP clots, and reduced clot stiffness (%) due to abciximab-mediated inhibition of platelet integrin $\alpha_{IIb}\beta_3$, blebbistatin-mediated inhibition of platelet myosin II ATPase, or platelet depletion (i.e. PPP clots) was calculated.

4.2.7: Statistical Analysis

A power analysis was completed to calculate the appropriate sample size for the fibrin network structure measurements given a 5% level of significance and 80% power. A two-way ANOVA and paired student t-tests were used to calculate statistical significance (defined as $p < 0.05$).

4.3: Results

4.3.1: Platelet $\alpha_{IIb}\beta_3$ Integrin and Platelet Myosin II ATPase Direct Fibrin Network Structure

Confocal microscopy and image analysis were used to evaluate the contribution of the platelet $\alpha_{IIb}\beta_3$ integrin and platelet myosin II ATPase to the fibrin network structure of plasma clots. Control PRP clots demonstrated substantial fibrin network structural evolution during coagulation, including a visible increase in fibrin fiber density and regional structural heterogeneity from 4-30 minutes post clot initiation **(Figure 4-4**). By contrast, abciximab-treated PRP, blebbistatin-treated PRP, and PPP clots exhibited remarkably static fibrin network structures that lacked any notable visible differences between the time of clot formation and t = 30 minutes (**Figure 4-4)**. Structural features of the clot fibrin network including fiber segment length, junction

density, and clot porosity were measured to evaluate the effects of platelet $\alpha_{IIb}\beta_3$ integrin inhibition and platelet myosin II ATPase inhibition on global clot structure.

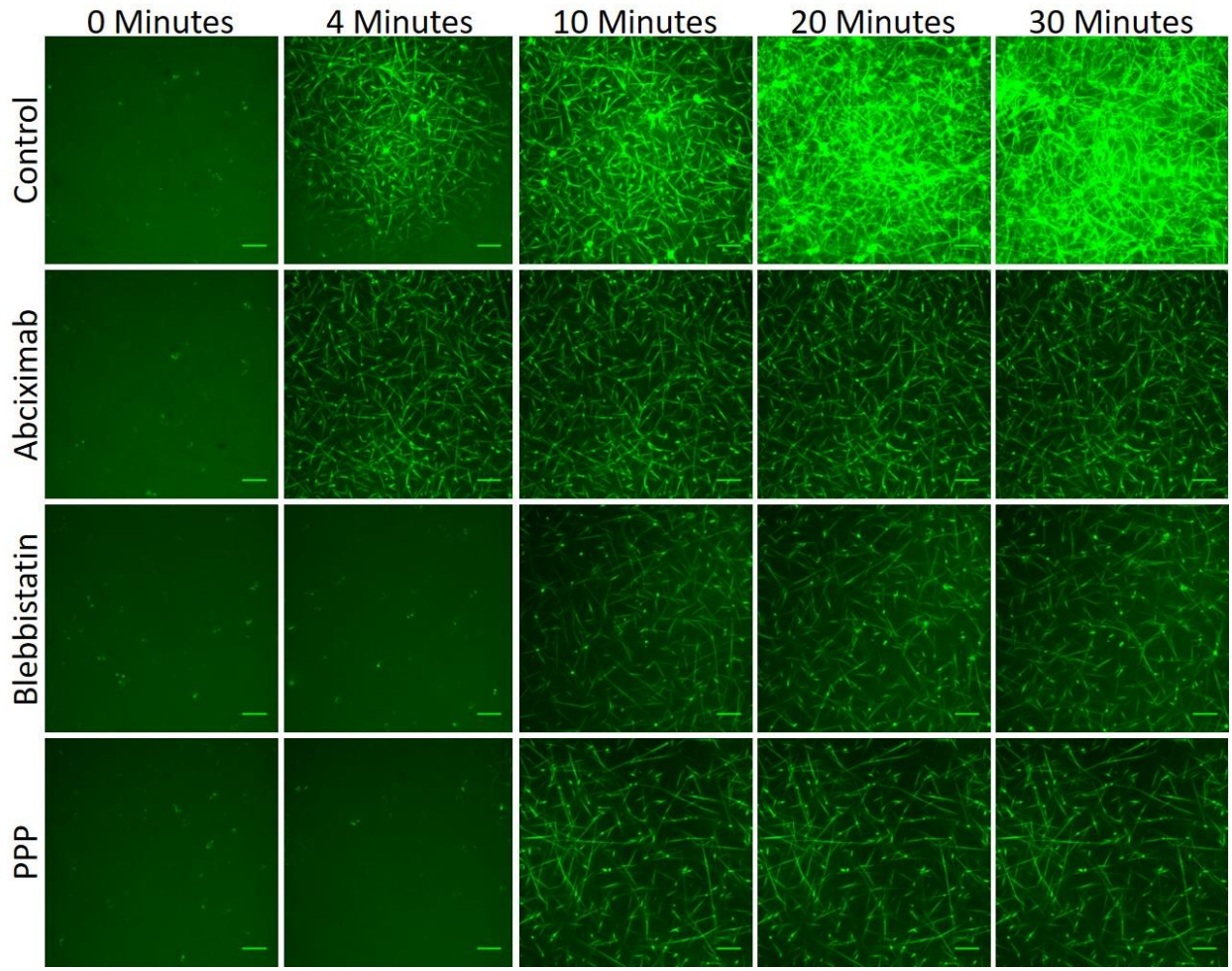

Figure 4-4: Confocal microscopy images of plasma clot structure. Control PRP, abciximab-treated (20μg/mL) PRP, blebbistatin-treated (25μM) PRP, and PPP clots were imaged by confocal microscopy every 2 minutes from 0-30 minutes post clot initiation. Alexa 488-labelled fibrin fibers are shown in green. Images were taken at 60X; contrast was enhanced by 0.8% for all images to distinguish fibrin network from background. Scale bar = 10μm

The length of fibrin fiber segments between fiber junctions was quantified for control PRP, abciximab-treated PRP, blebbistatin-treated PRP, and PPP clots. Control PRP clots exhibited a decrease in fiber segment length from 4 to 30 minutes post clot initiation, and reached a mean fiber segment length of 1.65 ± 0.06μm by t = 30 minutes (**Figure 4-5A**). Inhibition of the platelet $\alpha_{IIb}\beta_3$ integrin by abciximab or inhibition of platelet myosin II ATPase by blebbistatin produced clots with significantly ($p < 0.05$) greater mean fiber segment lengths compared to control PRP clots (**Figure 4-5A**). Fiber length for drug-treated and PPP clots remained relatively constant between the time of initial clot formation and 30 minutes post clot initiation. By t = 30 minutes, abciximab-treated PRP, blebbistatin-treated PRP, and PPP clots exhibited mean fiber segment lengths of 2.37 ± 0.10μm, 2.49 ± 0.14μm, and 2.66 ± 0.16μm, respectively. Overall, the fiber segment length results suggest that $\alpha_{IIb}\beta_3$ integrin-mediated platelet binding to the fibrin network and myosin II ATPase-mediated platelet tensioning of the fibrin network are significant components of clot structure progression during coagulation.

Fiber junction density, defined as the number of fiber branch points and regions of fiber overlap per field of view (FOV), was quantified for control PRP, drug-treated PRP, and PPP clots. The junction density results for control PRP clots were complementary to the control fiber length data, demonstrating an increase in fiber junction density during coagulation (**Figure 4-5B**). By t = 30 minutes, mean fiber junction density for control PRP clots was 4440 ± 429 junctions/FOV. Inhibition of the platelet $\alpha_{IIb}\beta_3$ integrin by abciximab or inhibition of platelet myosin II ATPase by blebbistatin significantly ($p < 0.05$) attenuated mean fiber junction density compared to control PRP clots (**Figure 4-5B**). By 30 minutes post clot initiation, abciximab-treated PRP, blebbistatin-treated PRP, and PPP clots exhibited mean junction densities of 1821 ± 181 junctions/FOV, 1555 ± 295 junctions/FOV, and 1361 ± 215 junctions/FOV, respectively. Similar to the fiber segment

length data, the junction density results suggest that the platelet $\alpha_{IIb}\beta_3$ and platelet myosin II ATPase are critical regulators of fibrin network structure during coagulation.

Finally, clot porosity was quantified for control PRP, abciximab-treated PRP, blebbistatin-treated PRP, and PPP clots from the binarized confocal images of fibrin network structure. Control PRP clots exhibited a notable decrease in clot porosity from 2 to 20 minutes post clot initiation, and reached a mean clot porosity of 83.2 ± 0.7% by t = 30 minutes (**Figure 4-5C**). Inhibition of the platelet $\alpha_{IIb}\beta_3$ integrin by abciximab or inhibition of platelet myosin II ATPase by blebbistatin produced clots with significantly ($p < 0.05$) greater mean clot porosities compared to control PRP (**Figure 4-5C**). At t = 30 minutes, abciximab-treated PRP, blebbistatin-treated PRP, and PPP clots exhibited mean clot porosities of 89.6 ± 0.5%, 90.6 ± 1.0%, and 91.2 ± 0.6%, respectively. The clot porosity data agree well with the fiber segment length and junction density results, and support the suggestion that the platelet $\alpha_{IIb}\beta_3$ integrin and platelet myosin II ATPase are critical modulators of fibrin network structure during clot formation.

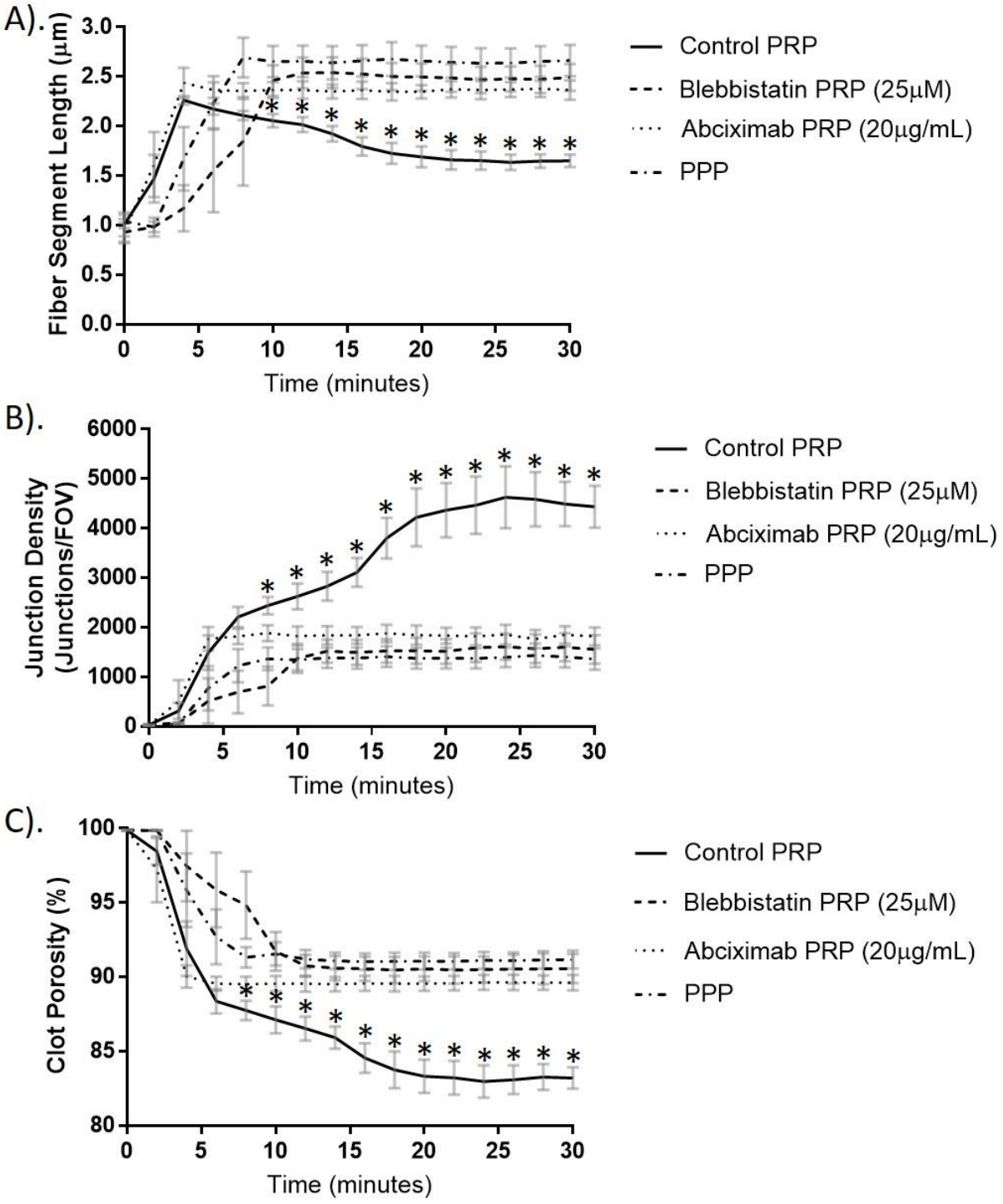

Figure 4-5: Fibrin network structure measured by confocal image analysis. Abciximab-treated PRP, blebbistatin-treated PRP, and PPP clots exhibited significantly (*$p < 0.05$ using paired t-tests) longer fiber segments (A), fewer fiber junctions (B), and greater clot porosity (C) compared to control PRP clots. Data are plotted as mean ± SEM; n = 5 subjects.

4.3.2: Platelet $\alpha_{IIb}\beta_3$ Integrin and Platelet Myosin II ATPase Enhance Fibrin Network Spatial Heterogeneity

To evaluate the spatial heterogeneity of the plasma clots, the fibrin network structure analysis was replicated in 100 X 100 pixels (9.3μm X 9.3μm) localized platelet regions and platelet-free regions, and the ratio between regions of platelets and no platelets was calculated to estimate clot structural heterogeneity for each experimental condition. The goal of the structural heterogeneity portion of the confocal image analysis study was to determine if abciximab-mediated inhibition of the platelet $\alpha_{IIb}\beta_3$ integrin or blebbistatin-mediated inhibition of platelet myosin II ATPase produced a less heterogeneous clot structure compared to control clots, due to the inability of the platelet to bind or exert tension on the fibrin network, respectively.

At t = 30 minutes, platelet-rich regions of control PRP clots exhibited 25% shorter fiber segments compared to platelet-free regions (**Figure 4-6A**). Inhibition of the platelet $\alpha_{IIb}\beta_3$ integrin by abciximab or inhibition of platelet myosin II ATPase by blebbistatin significantly ($p < 0.05$) reduced fiber segment length heterogeneity between regions of platelets and no platelets compared to control PRP clots (**Figure 4-6A**). Removal of a majority of the platelets (PPP) also significantly ($p < 0.05$) reduced fiber segment length heterogeneity compared to control PRP (**Figure 4-6A**). By 30 minutes post clot initiation, abciximab-treated PRP, blebbistatin-treated PRP, and PPP clots exhibited nearly equal mean fiber segment lengths in regions of platelets and no platelets. Overall, the results suggest that inhibition of $\alpha_{IIb}\beta_3$ integrin-mediated platelet binding to the fibrin network and myosin II ATPase-mediated platelet tensioning of the fibrin network significantly attenuates fibrin network structural heterogeneity inherent to control clots.

Similarly, by t = 30 minutes platelet-rich regions of control PRP clots were comprised of nearly twice as many fiber junctions than platelet-free regions **(Figure 4-6B)**. Inhibition of the

platelet $\alpha_{IIb}\beta_3$ integrin by abciximab or inhibition of platelet myosin II ATPase by blebbistatin significantly ($p < 0.05$) reduced fiber junction density heterogeneity between regions of platelets and no platelets compared to control PRP clots (**Figure 4-6B**). Additionally, PPP clots exhibited significantly ($p < 0.05$) reduced heterogeneity in fiber junction density compared to control PRP (**Figure 4-6B**). At 30 minutes post clot initiation, abciximab-treated PRP, blebbistatin-treated PRP, and PPP clots exhibited no notable difference in mean junction density between regions of platelets and no platelets. Similar to the fiber length heterogeneity study, the complementary junction density results suggest that the platelet $\alpha_{IIb}\beta_3$ integrin and platelet myosin II ATPase are significant modulators of clot structure progression, and particularly clot spatial heterogeneity, during coagulation.

Finally, clot porosity was measured in regions of platelets and no platelets for control PRP, abciximab-treated PRP, blebbistatin-treated PRP, and PPP clots. At t = 30 minutes, platelet-rich regions of control PRP clots exhibited 5% less clot porosity compared to platelet-free regions (**Figure 4-6C**). Platelet $\alpha_{IIb}\beta_3$ integrin inhibition by abciximab and platelet myosin II ATPase inhibition by blebbistatin significantly ($p < 0.05$) reduced clot porosity heterogeneity between regions of platelets versus no platelets compared to control PRP clots (**Figure 4-6C**). Similarly, PPP clots exhibited significantly ($p < 0.05$) reduced clot porosity heterogeneity compared to control (**Figure 4-6C**). By 30 minutes post clot initiation, drug-treated PRP and PPP clots exhibited no notable difference in clot porosity between regions of platelets and no platelets. The clot porosity data agrees well with the fiber length and junction density results of the structural heterogeneity study, and support the suggestion that the platelet $\alpha_{IIb}\beta_3$ integrin and platelet myosin II ATPase are critical modulators of fibrin network structure.

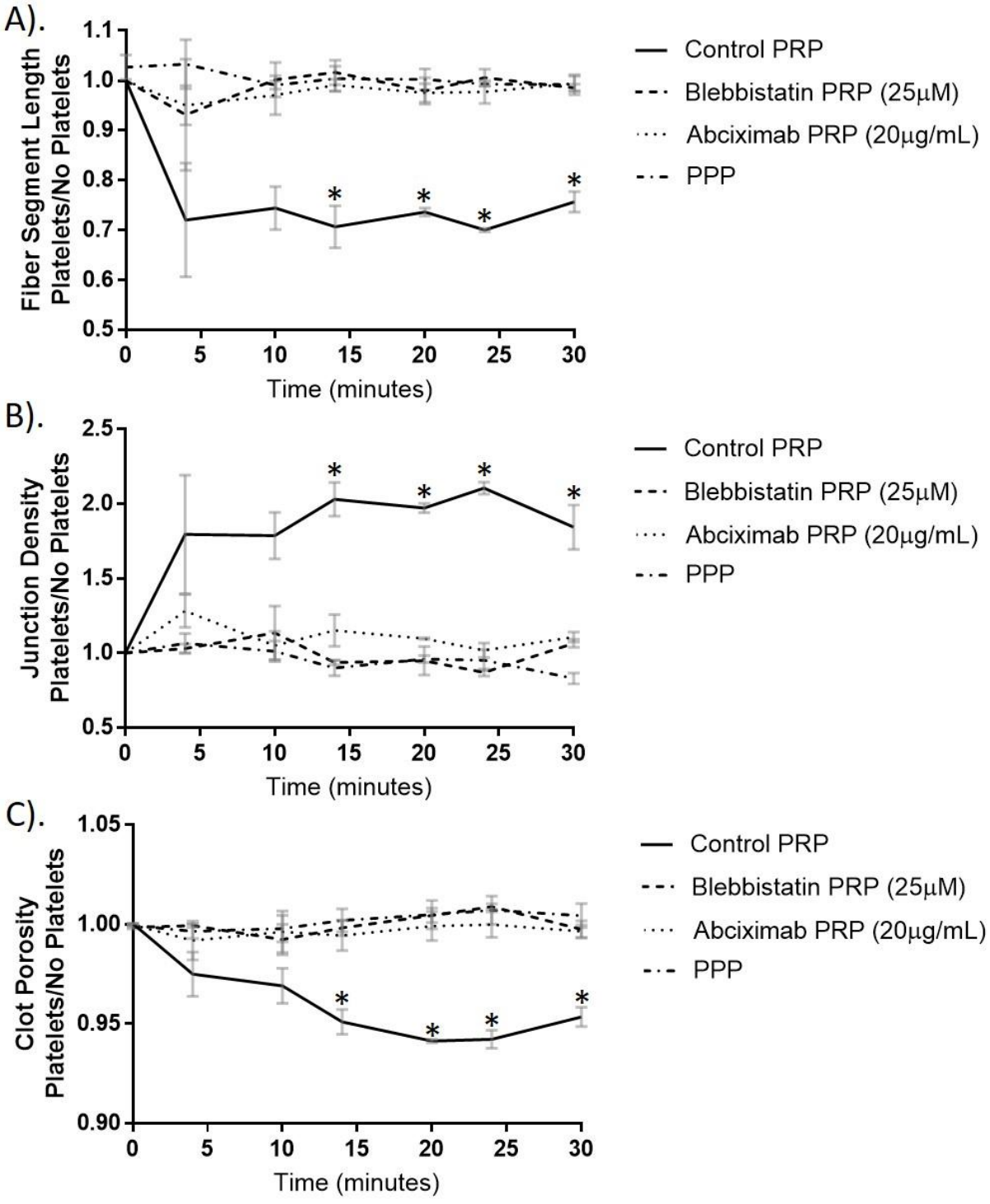

Figure 4-6: Fibrin network spatial heterogeneity evaluated by confocal image analysis. Control PRP clots exhibited significant (*$p < 0.05$ using paired t-tests) spatial heterogeneity in fiber segment length (A), junction density (B), and clot porosity (C) between regions of platelets versus no platelets. Data are plotted as mean ± SEM; n = 3 subjects.

To determine if the structural heterogeneity data was dependent on the selected size (100 X 100 pixels) of the regions of platelets and no platelets, the measurement was repeated using 50 X 50 and 200 X 200 pixels regions. The results of the 50 X 50 pixels region analysis were consistent with the findings of the original 100 X 100 pixels heterogeneity study, and found that control clots exhibited significant heterogeneity ($p < 0.05$) between regions of platelets and no platelets, while abciximab-treated PRP, blebbistatin-treated PRP, and PPP clots were effectively homogenous (**Figure 4-7**). One notable difference of the 50 X 50 region analysis compared to the original heterogeneity study was the increase in measurement variability (depicted by the larger error bars) due to the reduced number of measurements that could be acquired per field of view.

Interestingly, when the region size was extended to 200 X 200 pixels, the results found that control PRP, abciximab-treated PRP, blebbistatin-treated PRP, and PPP clots exhibited no measurable difference between regions of platelets versus no platelets for mean fiber length, junction density, or clot porosity (**Figure 4-8**). The data for abciximab-treated PRP, blebbistatin-treated PRP, and PPP clots agree well with the findings of the original (100 X 100 pixels) heterogeneity study, which suggests that the attenuated clot structural heterogeneity observed for the drug-treated and PPP clots is not dependent on region size. By contrast, the significant spatial heterogeneity observed in control PRP clots in the original 100 X 100 pixels heterogeneity study was effectively abolished when the selected region size was expanded to 200 X 200 pixels. The discrepancy between the 100 X 100 and 200 X 200 pixels region analyses indicates that control PRP clot structural heterogeneity is dependent on the selected size of the regions of platelets and no platelets.

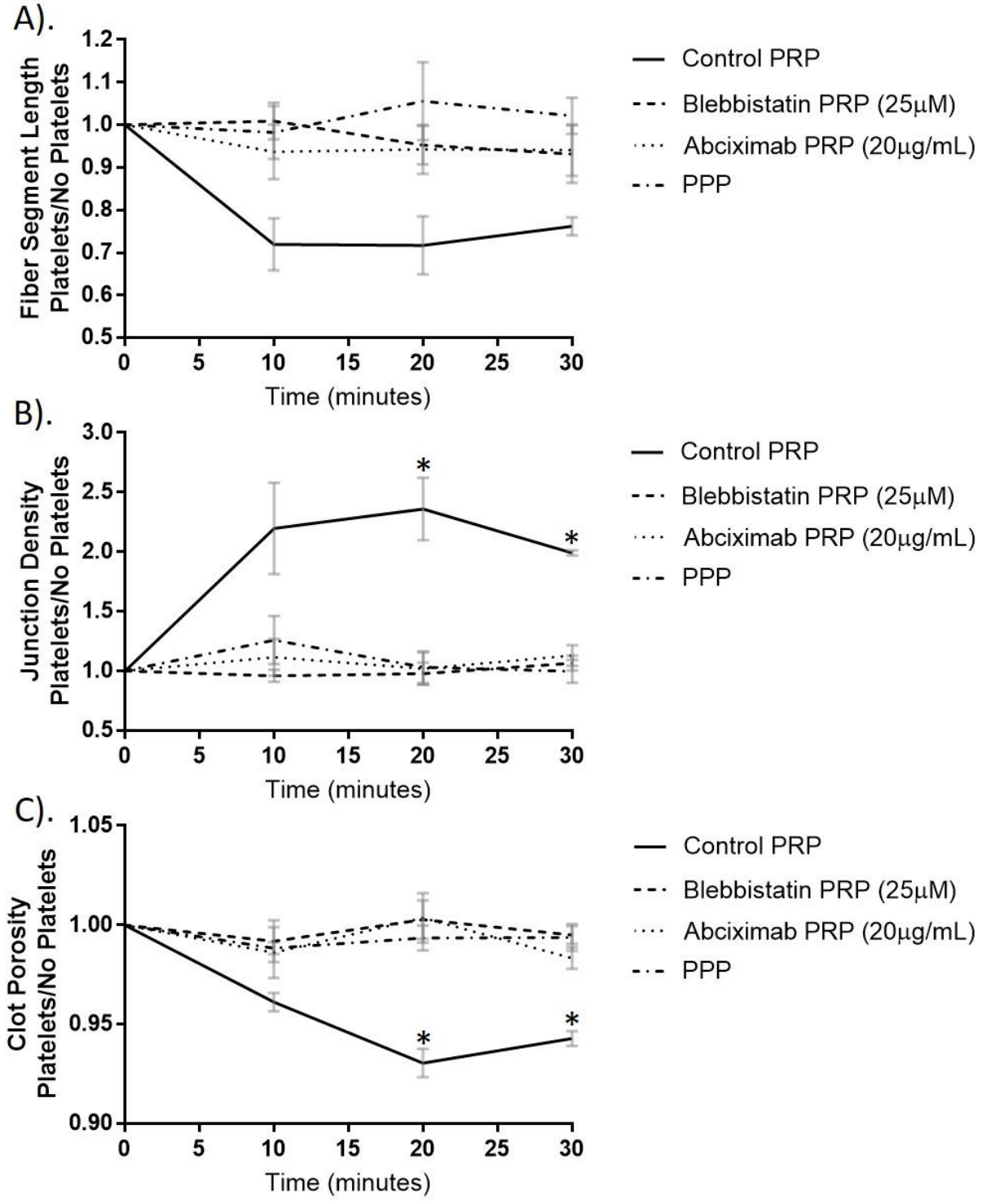

Figure 4-7: Fibrin network spatial heterogeneity evaluated in 50 X 50 pixels regions. Control PRP clots exhibited substantial (*$p < 0.05$ using paired t-tests) spatial heterogeneity in fiber segment length (A), junction density (B), and clot porosity (C) between regions of platelets versus no platelets. Data are plotted as mean ± SEM; n = 3 subjects.

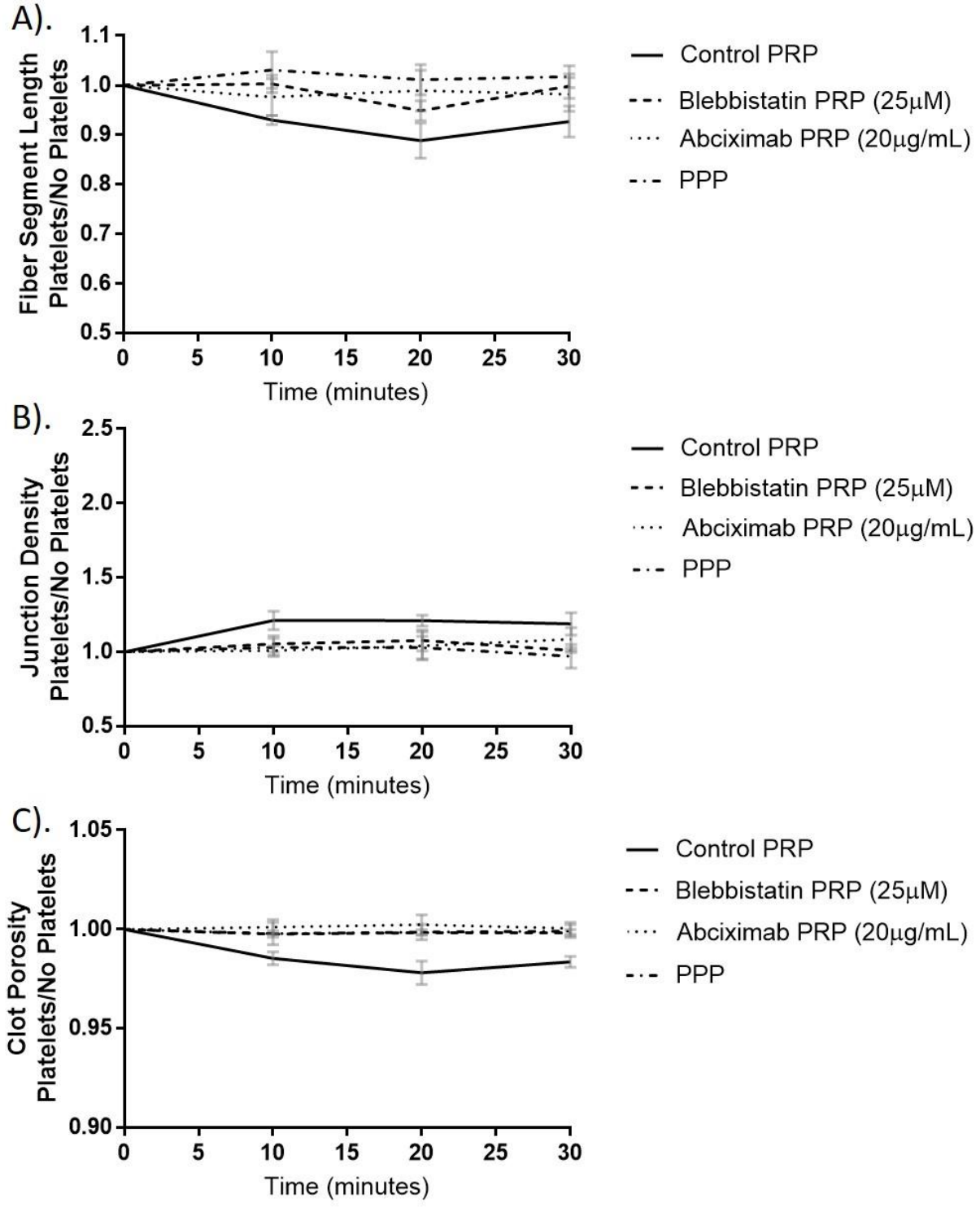

Figure 4-8: Fibrin network spatial heterogeneity evaluated in 200 X 200 pixels regions. Control PRP, abciximab-treated PRP, blebbistatin-treated PRP, and PPP clots exhibited no measurable spatial heterogeneity in fiber segment length (A), junction density (B), or clot porosity (C) between regions of platelets versus no platelets. Data are plotted as mean ± SEM; n=3 subjects.

4.3.3: Fibrin Network Structure Can Predict Relative Changes in Clot Stiffness

A simple network model (**Equation 3, Section 4.2.6**) was implemented to evaluate if platelet-driven changes in fibrin network structural features could be used to predict changes in clot stiffness (**Equation 4, Section 4.2.6**). Mean clot stiffness (shear modulus) was estimated for control PRP, abciximab-treated PRP, blebbistatin-treated PRP, and PPP clots, and reduced clot stiffness (%) due to abciximab-mediated inhibition of platelet integrin $\alpha_{IIb}\beta_3$, blebbistatin-mediated inhibition of platelet myosin II ATPase, or platelet depletion (i.e. PPP clots) was calculated.

The model predicted that control PRP samples would clot within 2 minutes and reach a clot stiffness of 147 ± 31 Pa by t = 30 minutes (**Figure 4-9**). Inhibition of the platelet $\alpha_{IIb}\beta_3$ integrin by abciximab was predicted to significantly ($p < 0.05$) reduce PRP clot stiffness (**Figure 4-9**). By 30 minutes post clot initiation, abciximab-treated PRP clots reached an estimated clot stiffness of 24 ± 4 Pa, indicating that abciximab-mediated inhibition of platelet $\alpha_{IIb}\beta_3$ integrin function would reduce PRP clot stiffness by 84%.

Similarly, the network model predicted that inhibition of platelet myosin II ATPase by blebbistatin would significantly ($p < 0.05$) reduce PRP clot stiffness (**Figure 4-9**). At 30 minutes post clot initiation, blebbistatin-treated PRP samples reached an estimated clot stiffness of 21 ± 6 Pa, suggesting that blebbistatin-mediated inhibition of platelet myosin II ATPase would attenuate PRP clot stiffness by 86%. Finally, PPP clots were predicted to be significantly ($p < 0.05$) less stiff than control PRP clots (**Figure 4-9**), where PPP clot stiffness (15 ± 4 Pa) was estimated to be 93% softer than control PRP clot stiffness by t = 30 minutes.

The calculated stiffness predictions generally support the results of the sonorheometry and electromagnetic force studies, and suggest that the platelet $\alpha_{IIb}\beta_3$ integrin and platelet myosin II ATPase are significant components of plasma clot stiffening. Additionally, the model predictions suggest that changes in fibrin network structural features due to abciximab-mediated platelet $\alpha_{IIb}\beta_3$

integrin inhibition or blebbistatin-mediated myosin II ATPase inhibition could be used to approximate changes in plasma clot stiffness. A more thorough comparison of the sonorheometry stiffness results, electromagnetic force stiffness results, and model stiffness predictions is provided in the discussion section, below (**Section 4.4.3**).

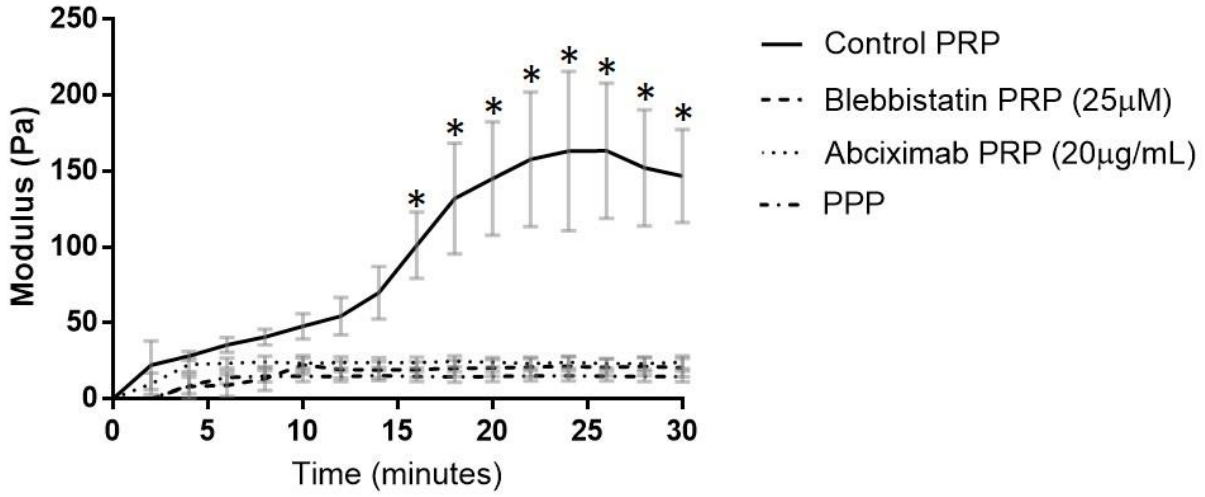

Figure 4-9: Plasma clot stiffness predicted from fibrin network structure. Shear modulus (stiffness) of control PRP, abciximab-treated PRP, blebbistatin-treated PRP and PPP clots was calculated from clot structure data for 0-30 minutes post clot initiation. Control PRP clots were predicted to be significantly (*$p < 0.05$ using paired t-tests) stiffer than abciximab-treated (20μg/mL) PRP, blebbistatin-treated (25μM) PRP, and PPP clots. Data are plotted as mean ± standard error of the mean; n = 5 subjects.

4.4: Discussion

Confocal microscopy and image analysis were used to evaluate the contribution of the platelet $\alpha_{IIb}\beta_3$ integrin and platelet myosin II ATPase to the fibrin network structure of plasma clots. The study aimed to build on existing knowledge, and provide further detail regarding the effect of abciximab-mediated inhibition of the platelet $\alpha_{IIb}\beta_3$ integrin and blebbistatin-mediated

inhibition of platelet myosin II ATPase on specific structural features of plasma clots including mean fiber segment length, fiber junction density, clot porosity, and overall clot structural heterogeneity. To quantitatively compare the plasma clot structure data with the stiffness results of our study, a simple network model was applied to the fibrin network structure data to predict plasma clot stiffness. The following discussion offers interpretation of the confocal image analysis results for fibrin network structure, and compares our structure findings with those of previous studies. In addition, the discussion compares the model predictions of clot stiffness with the results of the sonorheometry and electromagnetic force portions of the study. Finally, the limitations of the clot structure study and relevant future experiments are discussed.

4.4.1: Fibrin Network Structure Evaluated by Confocal Microscopy and Image Analysis

The fibrin network structure analysis found that inhibition of the platelet $\alpha_{IIb}\beta_3$ integrin by abciximab or inhibition of platelet myosin II ATPase by blebbistatin produced clots with significantly ($p < 0.05$) longer fiber segment lengths, fewer fiber junctions, and greater clot porosity compared to control PRP clots. The complementary fiber segment length, junction density, and clot porosity data indicate that the platelet $\alpha_{IIb}\beta_3$ integrin and platelet myosin II ATPase are critical modulators of fibrin network structure during clot formation.

To our knowledge, there have been no previous studies of the effect of abciximab-mediated inhibition of the platelet $\alpha_{IIb}\beta_3$ integrin or blebbistatin-mediated inhibition of platelet myosin II ATPase on fiber length, fiber junction density, or clot porosity. However, Alber et al. calculated fibrin fiber branch point density and mean fiber length of PPP clots from 3D images to develop a confocal image-based 3D computational model to estimate elastic properties of fibrin networks (52). The Alber study found that unstimulated PPP clots (i.e. clotting initiated through contact with

the glass slide versus the addition of thrombin) exhibited a mean branch point density of 1855 branches/sample (1024 X 1024 pixels), and a mean fiber length of 4.1 ± 3.6μm (52). By comparison, our 2D analysis of plasma clots found a mean junction density of 1361 ± 215 junctions/FOV (1024 X 1024 pixels), and a mean fiber segment length of 2.66 ± 0.16μm for PPP clots. Overall, our junction density and fiber segment length results are comparable to those of the Alber study, which suggests that our 2D analysis of the 3D clot network can be used to sufficiently quantify features of clot structure. In our structure study, mean fiber length was estimated as the average fiber segment length between junctions (i.e. no fiber overlap), which likely accounts for the slight discrepancy in mean fiber length estimates between the two studies (given that the Alber study allowed fiber overlap in their fiber length calculation).

Previous research has found that plasma clots exhibit an overall porosity of > 99%, while platelet-retracted clots exhibit 90-99% porosity (79). Our fibrin network structure analysis found clot porosities that ranged from 83-91% by 30 minutes post clot initiation. Our underestimation of clot porosity is potentially due to our 2D estimate of porosity from a 3D clot. Although our structure analysis may underestimate clot porosity magnitude, the relative differences in clot porosity between control and drug-treated PRP clots provide valuable insight regarding the contribution of the platelet $\alpha_{IIb}\beta_3$ integrin or platelet myosin II ATPase to clot porosity.

Unlike our sonorheometry or electromagnetic force stiffness results, the fibrin network structure analysis found no difference in efficacy between abciximab or blebbistatin treatment. Additionally, the structure analysis found no significant difference between drug-treated PRP and PPP clots, suggesting that inhibition of the platelet $\alpha_{IIb}\beta_3$ integrin or inhibition of platelet myosin II ATPase effectively eliminated the platelet contribution to fiber length, junction density, and clot porosity during coagulation.

4.4.2: Fibrin Network Spatial Heterogeneity Evaluated by Confocal Image Analysis

The goal of the structural heterogeneity analysis was to determine if abciximab-mediated inhibition of the platelet $\alpha_{IIb}\beta_3$ integrin or blebbistatin-mediated inhibition of platelet myosin II ATPase produced a less heterogeneous clot structure compared to control PRP. The study results found that by t = 30 minutes, platelet-rich regions of control PRP clots exhibited 25% shorter fiber segments, nearly twice as many fiber junctions, and 5% less clot porosity compared to platelet-free regions. By contrast, inhibition of the platelet $\alpha_{IIb}\beta_3$ integrin by abciximab or inhibition of platelet myosin II ATPase by blebbistatin significantly ($p < 0.05$) attenuated fiber segment length heterogeneity, junction density heterogeneity, and clot porosity heterogeneity compared to control PRP clots.

Overall, the heterogeneity study results indicate that the platelet $\alpha_{IIb}\beta_3$ integrin and platelet myosin II ATPase are critical modulators of fibrin network structural heterogeneity during coagulation. To our knowledge, no previous study has quantified the effect of abciximab-mediated inhibition of platelet $\alpha_{IIb}\beta_3$ integrin or blebbistatin-mediated inhibition of platelet myosin II ATPase on clot structure heterogeneity. Collet et al. observed a qualitative attenuation in fibrin network structural heterogeneity following the addition of abciximab, and suggested that abciximab-mediated reduced clot structural heterogeneity contributed to enhanced susceptibility to clot lysis (73). Overall, the results of our structure heterogeneity study support this observation.

To evaluate if the structural heterogeneity data was dependent on the selected size (100 X 100 pixels) of the regions of platelets and no platelets, the measurement was repeated using 50 X 50 and 200 X 200 pixels regions. The results of the 50 X 50 pixels region analysis were consistent with the findings of the original 100 X 100 pixels heterogeneity study, and found that control clots exhibited significant heterogeneity ($p < 0.05$) between regions of platelets and no platelets, while

abciximab-treated PRP, blebbistatin-treated PRP, and PPP clots were effectively homogenous. By contrast, the 200 X 200 pixels region analysis found that control PRP, abciximab-treated PRP, blebbistatin-treated PRP, and PPP clots exhibited no measurable difference between regions of platelets versus no platelets for mean fiber length, junction density, or clot porosity. The significant spatial heterogeneity observed in control PRP clots in the original 100 X 100 pixels heterogeneity study was effectively abolished when the selected region size was extended to 200 X 200 pixels.

The results indicate that control PRP clot structural heterogeneity depends on the selected size of the regions of platelets and no platelets, suggesting that there is a spatial limit to platelet-mediated modulation of clot structure (i.e. a platelet effect size). Our heterogeneity study suggests that the platelet effect size in control PRP clots extends at least 9.3μm (100 pixels) from the center of the platelet. By contrast, the homogenous fibrin network structures of abciximab-treated PRP, blebbistatin-treated PRP, and PPP clots did not vary with the selected region size, suggesting that inhibition of the platelet $\alpha_{IIb}\beta_3$ integrin or inhibition of platelet myosin II ATPase severely attenuates the effect size of platelet-mediated clot structure modulation.

4.4.3: Plasma Clot Stiffness Estimated from Fibrin Network Structure

A simple network model was implemented to evaluate if changes in fibrin network structure could be used to predict changes in clot stiffness. The model predicted that by 30 minutes post clot initiation, abciximab-mediated inhibition of the platelet $\alpha_{IIb}\beta_3$ integrin or blebbistatin-mediated inhibition of platelet myosin II ATPase would attenuate PRP clot stiffness by 84% and 86%, respectively (**Table 4-1**). By contrast, our sonorheometry and electromagnetic force studies found that abciximab-mediated inhibition of platelet $\alpha_{IIb}\beta_3$ integrin function reduced PRP clot stiffness by 65% and 53%, respectively (**Table 4-1**). Similarly, our sonorheometry and

electromagnetic force results found that blebbistatin-mediated inhibition of platelet myosin II ATPase reduced PRP clot stiffness by 44% and 41%, respectively (**Table 4-1**).

Additionally, the model severely underestimated clot stiffness (shear modulus) magnitude compared to shear modulus measured for plasma clots using sonorheometry (**Table 4-2**). The discrepancy between the measured stiffness results (sonorheometry and electromagnetic force) and the calculated stiffness predictions (network model) suggests that fiber segment length and subsequently network pore size are not sufficient to accurately calculate clot stiffness magnitude. The structure analysis found that blebbistatin had a greater attenuating effect on clot structural features compared to abciximab, while the stiffness studies found that abciximab treatment was a more effective inhibitor. This discrepancy suggests that other features of fibrin network structure beyond fiber segment length, junction density, and clot porosity may play a more significant role in modulating clot stiffness.

Although the model stiffness estimates agree with the relative findings of the sonorheometry and electromagnetic force results, the model severely underestimated clot stiffness magnitude. To more accurately predict the plasma clot stiffness measured by sonorheometry, the model would require mean fiber segment lengths that are approximately 50-60% shorter than those measured by image analysis to achieve stiffness estimates that are 25-90X greater than the original stiffness predictions. Additionally, the model prediction of stiffness dynamics differed from the sonorheometry stiffness results, where the model estimated that clot stiffness would increase gradually from 0-15 minutes post clot initiation, while the sonorheometry results found that clot stiffness increased rapidly from 0-15 minutes and plateaued around t = 20 minutes.

The model prediction of clot stiffness may have been limited by the assumptions of a single fiber bending modulus and equivalent mean fiber widths between the various experimental

conditions. In the future, it would be valuable to measure fiber width or fiber fibrin content to determine if fiber bending modulus varies between control PRP and drug-treated PRP clots.

Although the structure-based stiffness predictions found that fiber length and network pore size were inadequate for the accurate calculation of clot stiffness, the results qualitatively support the sonorheometry and electromagnetic force study results, and suggest that $\alpha_{IIb}\beta_3$ integrin-mediated platelet binding to the fibrin network and myosin II ATPase-mediated platelet tensioning of the fibrin network are significant components of plasma clot stiffening. Additionally, the model predictions suggest that platelet-driven changes in fibrin network structural features can be used to approximate changes in plasma clot stiffness, but additional investigation of relevant clot structural features is needed.

Table 4-1: Plasma clot stiffness summary: Predicted vs. measured stiffness

	Network Model	Sonorheometry	Electromagnetic Force
Abciximab in PRP	Clot Stiffness 84%	Clot Stiffness 65%	Clot Stiffness 53%
Blebbistatin in PRP	Clot Stiffness 86%	Clot Stiffness 44%	Clot Stiffness 41%
PPP	Clot Stiffness 90%	Clot Stiffness 80%	Clot Stiffness 56%

Table 4-2: Plasma clot stiffness magnitude: Predict vs. measured stiffness, t = 30 minutes

	Network Model	Sonorheometry
Control	147 ± 31 Pa	3455 ± 518 Pa
Abciximab	24 ± 4 Pa	1192 ± 202 Pa
Blebbistatin	21 ± 6 Pa	1918 ± 79 Pa
PPP	15 ± 4 Pa	667 ± 159 Pa

4.4.4: Clot Structure Study Limitations and Future Directions

At the onset of the confocal microscopy-based clot structure study, we anticipated that one of the primary limitations of the study would be the use of 2D image analysis techniques to estimate structural features of a 3D clot. However, comparing our fiber length and junction density results with the 3D image analysis results of a previous study, the findings suggest that a 2D image analysis approach may sufficiently recapitulate the 3D clot structure. By contrast, our clot structure image analysis approach significantly underestimated clot porosity magnitude, likely due to our 2D estimate of porosity from a 3D clot. However, valuable insight was gained from the relative difference in clot porosity between control and drug-treated clots. Overall, the results found that our 2D analysis of the 3D clot structure was not a predominant limitation of the study, but suggest that certain clot structure features (i.e. clot porosity) may be more sensitive to a 2D versus 3D analysis than other structure parameters (i.e. fiber segment length or junction density). As a result, future studies of fibrin network structure may need to adopt a 3D analysis approach, depending on what clot structural features are investigated.

The primary limitation of the structure portion of the study was the estimate of clot stiffness using an analytical model of fiber length and network pore size. The model did not accurately

predict clot stiffness magnitude for control PRP, abciximab-treated PRP, blebbistatin-treated PRP, or PPP clots, suggesting that alternative features of fibrin network structure may play a more significant role in modulating clot stiffness. In the future, it would be valuable to develop an expanded analytical model that accounts for additional clot structure parameters to more accurately predict clot stiffness. Further investigation of the mechanistic relationship between fibrin network structure and clot strength could improve our understanding of platelet function in vascular disease, and could be valuable for identifying platelet-driven features of clot structure or stiffness that may serve as a novel means to detect or target thrombosis.

Finally, it would be valuable to expand the clot structure analysis to more thoroughly capture the dynamic rearrangement of the fibrin network due to the platelets during clot formation. This could potentially be achieved by tracking the motion of the platelets and fiber junctions during coagulation, and could provide novel insight regarding the platelet-mediated spatial rearrangement of the clot fibrin network. Similarly, it would be valuable to conduct a fiber brightness analysis to estimate the relative fiber fibrin content, and to ultimately estimate fiber width. The fiber brightness analysis would be especially useful for the model prediction of clot stiffness, as it would indicate if the previous assumptions of a single fiber bending modulus and uniform fiber thickness for each experimental condition are reasonable.

Chapter 5: Discussion and Future Directions

The overall goal of the study was to investigate features of fibrin network structure or clot stiffness that could ultimately be used to better assess hemorrhagic or thrombotic risk in patients, and to potentially assist in monitoring and managing hemostasis. Cardiovascular disease is a leading cause of death worldwide, and thrombosis is a prominent underlying pathology of numerous cardiovascular disorders including ischemic heart disease, stroke, and VTE (80). Previous research suggests that clot structure and stiffness could serve as useful metrics to guide the detection of vascular disease, and subsequently aid in the development and assessment of novel anticoagulant therapies. This discussion aims to highlight the novelty of the study results, and provides insight regarding the clinical implications of the findings and the contribution of the study to coagulation research. Finally, future directions of clot structure and stiffness assessment in thrombosis and hemostasis research are discussed.

5.1: Significance and Clinical Implications of the Study

This study aimed to investigate the platelet contribution to blood clot structure and strength, and to elucidate potential novel means of targeting platelets in vascular disorder therapies. More specifically, the study served as a thorough investigation of the contribution of platelet $\alpha_{IIb}\beta_3$ integrin-mediated fibrin binding and platelet myosin II ATPase-mediated fibrin tensioning to fibrin network structure and clot stiffness. The study elucidated novel findings regarding the contributions of the platelet $\alpha_{IIb}\beta_3$ integrin and platelet myosin II ATPase to clot structure and strength, which could help guide the detection and treatment of thrombosis. In addition, the study highlighted a variety of diagnostic techniques that could be used to improve our understanding of vascular disease and the hemostatic process.

5.1.1: Significance and Clinical Implications of the Sonorheometry Stiffness Study

The sonorheometry study results suggest that $\alpha_{IIb}\beta_3$ integrin-mediated platelet binding to the fibrin network and myosin II ATPase-mediated platelet tensioning of the fibrin network are significant components of clot stiffening during coagulation. Previous studies using TEG and SEER sonorheometry found that abciximab-mediated inhibition of platelet $\alpha_{IIb}\beta_3$ integrin significantly attenuated clot stiffness (14,57), and our whole blood and plasma sonorheometry results for abciximab-mediated platelet $\alpha_{IIb}\beta_3$ integrin inhibition agree well with the previous studies.

To our knowledge, there has been no previous study of the contribution of platelet myosin II ATPase to global clot stiffness. A recent study found that inhibition of platelet myosin II ATPase by blebbistatin significantly reduced local platelet contractile stress in regions near platelets (51). Our observation of significantly attenuated global clot stiffness following blebbistatin-mediated inhibition of platelet myosin II ATPase may be due, in part, to reduced local platelet contractility. Our sonorheometry study recapitulated existing knowledge regarding the effect of abciximab-mediated inhibition of the platelet $\alpha_{IIb}\beta_3$ integrin on clot stiffness, but elucidated the novel finding that platelet myosin II ATPase is a critical modulator of clot stiffening during coagulation.

Both the whole blood and plasma sonorheometry studies found that abciximab treatment attenuated clot stiffness more effectively than blebbistatin treatment, which we predict is likely due to the more complete inhibition of platelet-fibrin binding by abciximab versus inhibition of platelet-fibrin tensioning by blebbistatin. However, the PPP clot stiffness data indicate that neither inhibition of the platelet $\alpha_{IIb}\beta_3$ integrin nor inhibition of platelet myosin II ATPase fully eliminated the platelet contribution to clot stiffness. Additionally, when comparing the whole blood and plasma clot stiffness results, we observed a prominent decrease in stiffness magnitude for whole

blood clots. We hypothesize that the decreased stiffness in whole blood versus plasma clots is due to a buffering effect of the red blood cells, with the red blood cells in whole blood clots serving as physical barriers that limit the clot fibrin network density and therefore limit clot stiffness (81).

Overall, the sonorheometry study of clot stiffness elucidated the novel finding of reduced whole blood clot stiffness due to blebbistatin-mediated inhibition of platelet myosin II ATPase, suggesting that platelet myosin II ATPase is a critical modulator of whole blood clot stiffening during coagulation. Additionally, the sonorheometry study highlighted biological differences (i.e. red blood cell buffering effects) that may affect clot stiffness measurements obtained by clinical, point of care technologies.

5.1.2: Significance and Clinical Implications of the Electromagnetic Force Stiffness Study

The electromagnetic force results for plasma clot stiffness suggest that the platelet $\alpha_{IIb}\beta_3$ integrin and platelet myosin II ATPase are critical regulators of clot stiffness during coagulation. Our electromagnetic force study found that abciximab-mediated inhibition of platelet $\alpha_{IIb}\beta_3$ integrin function significantly attenuated plasma clot stiffness, which agrees with our sonorheometry study results and previous study results using the TEG (57).

Similar to our sonorheometry study, the electromagnetic force data found that blebbistatin-mediated inhibition of platelet myosin II ATPase function significantly reduced plasma clot stiffness. As mentioned above, to our knowledge there have been no prior studies of the contribution of platelet myosin II ATPase to global clot stiffness. Our electromagnetic force results suggest that inhibition of platelet myosin II ATPase significantly attenuates global clot stiffness, which may be due to blebbistatin-mediated inhibition of local platelet contractile stress, as previously observed (51). Overall, our electromagnetic force results for plasma clot stiffness

generally agree with those of our sonorheometry stiffness study, and suggest that the platelet $\alpha_{IIb}\beta_3$ integrin and platelet myosin II ATPase enhance clot stiffness during coagulation.

The electromagnetic force clot stiffness assay presented in this study serves as a novel means of quantifying plasma clot stiffness. Additionally, the electromagnetic force assay offers the potential for simultaneous assessment of fibrin network structure and global clot stiffness, unlike any of the existing point of care coagulation technologies. By combining clot stiffness assessment by electromagnetic force with clot structure assessment by microscopy, the assay could be used to more directly probe the mechanistic relationship between clot structure and strength, and could potentially elucidate novel means of detecting and treating thrombosis.

5.1.3: Significance and Clinical Implications of the Fibrin Network Structure Study

The fibrin network structure analysis found that inhibition of the platelet $\alpha_{IIb}\beta_3$ integrin by abciximab or inhibition of platelet myosin II ATPase by blebbistatin produced clots with significantly greater fiber segment lengths, fewer fiber junctions, and increased clot porosity compared to control PRP. Additionally, the spatial heterogeneity study found that inhibition of the platelet $\alpha_{IIb}\beta_3$ integrin or inhibition of platelet myosin II ATPase significantly attenuated fibrin network structural heterogeneity inherent to control clots. Finally, the structure-based model prediction of clot stiffness found that increased fiber segment length and subsequently increased clot porosity due to abciximab or blebbistatin treatment predicted significantly softer clots compared to control. Overall, the findings of the confocal microcopy study suggest that the platelet $\alpha_{IIb}\beta_3$ integrin and platelet myosin II ATPase are critical modulators of clot structure during coagulation, and perturbations in clot structure due to platelet $\alpha_{IIb}\beta_3$ integrin or myosin II ATPase inhibition could be used to predict changes in clot stiffness.

Previous studies of the effect of abciximab-mediated inhibition of platelet $\alpha_{IIb}\beta_3$ integrin function on clot structure found that abciximab treatment significantly impaired platelet aggregation during coagulation (72,73). Alternatively, a previous study of blebbistatin-mediated inhibition of platelet myosin II ATPase function on clot structure found that blebbistatin treatment significantly reduced fibrin compaction in regions of platelets (51). To our knowledge, our confocal microscopy structure study is the first comprehensive investigation of the contribution of the platelet $\alpha_{IIb}\beta_3$ integrin or platelet myosin II ATPase to features of overall fibrin network structure during clot formation.

The structure study elucidated the novel findings of increased mean fiber segment length, reduced fiber junction density, increased clot porosity, and ultimately reduced clot structural heterogeneity due to abciximab-mediated inhibition of the platelet $\alpha_{IIb}\beta_3$ integrin or blebbistatin-mediated inhibition of platelet myosin II ATPase. Previous studies have found that fibrin network structural abnormalities are prevalent in cases of vascular disease (3,48,49), therefore quantifiable features of fibrin network structure may represent a novel means to identify individuals at risk of thrombotic or bleeding events.

5.2: Contribution of the Study to Coagulation Research

Previous research has found that platelet integrin-mediated adhesion to the clot fibrin network and platelet cytoskeleton-mediated tensioning of the clot network are critical components of coagulation (51,55,57,58). This study aimed to provide novel insight regarding the contribution of the platelet $\alpha_{IIb}\beta_3$ integrin and platelet myosin II ATPase to blood clot structure and strength. Previous studies have shown that inhibition of the platelet $\alpha_{IIb}\beta_3$ integrin by abciximab reduces whole blood and plasma clot stiffness (14,57), and inhibition of platelet myosin II ATPase by

blebbistatin reduces local platelet contractile stress (51) (**Table 5-1**). In addition, previous studies have shown that inhibition of the platelet $\alpha_{IIb}\beta_3$ integrin by abciximab reduces platelet aggregation and subsequently enhances clot lysis (72,73), while inhibition of platelet myosin II ATPase by blebbistatin attenuates fibrin densification around platelets (51) (**Table 5-1**).

Table 5-1: Known vs. unknown: The platelet $\alpha_{IIb}\beta_3$ integrin & myosin II ATPase in coagulation

Previous Studies:	Unknown:
Inhibition of platelet $\alpha_{IIb}\beta_3$ integrin reduces whole blood and plasma clot stiffness	Does inhibition of the platelet $\alpha_{IIb}\beta_3$ integrin affect fibrin network structure?
Inhibition of platelet $\alpha_{IIb}\beta_3$ integrin reduces platelet aggregation, making clots more susceptible to lysis	Does inhibition of platelet myosin II ATPase affect global clot stiffness?
Inhibition of platelet myosin II ATPase reduces local platelet contractile stress in regions of platelets	Does inhibition of platelet myosin II ATPase affect fibrin network structure?
Inhibition of platelet myosin II ATPase reduces fibrin densification on platelets	Can platelet-mediated changes in clot structure predict changes in clot stiffness?

Although the previous studies provided critical insight regarding the contribution of the platelet $\alpha_{IIb}\beta_3$ integrin and platelet myosin II ATPase to coagulation, a number of questions remain (**Table 5-1**). For example, given the suggestion from recent studies that clot structural features could be used to guide the detection and treatment of thrombotic disorders (3,48,49), what effect does inhibition of platelet $\alpha_{IIb}\beta_3$ integrin or platelet myosin II ATPase have on the structure of the clot fibrin network? Similarly, considering the significant effect of platelet $\alpha_{IIb}\beta_3$ integrin inhibition

on the stiffness of whole blood and plasma clots during clot formation (14,57), what effect does inhibition of downstream signaling targets such as platelet myosin II ATPase have on global clot stiffness during clot formation? And finally, given the value of clot structure and stiffness as metrics of vascular disease, can changes in clot structure predict changes in clot stiffness?

This study aimed to tackle the questions listed above, and to ultimately provide additional insight regarding the contribution of the platelet $\alpha_{IIb}\beta_3$ integrin and platelet myosin II ATPase to clot structure and strength (**Table 5-2**). The sonorheometry and electromagnetic force studies of clot stiffness elucidated the novel finding that inhibition of platelet myosin II ATPase by blebbistatin significantly reduced global clot stiffness, which may be due to blebbistatin-mediated inhibition of local platelet contractile stress (51) or blebbistatin-mediated attenuation of fibrin network structural integrity. Our clot structure study found that inhibition of $\alpha_{IIb}\beta_3$ integrin dependent platelet-fibrin binding or inhibition of myosin II ATPase dependent platelet-fibrin tensioning produced clots with longer fibers, fewer junctions, increased porosity, and reduced heterogeneity compared to control. Taken together, our data indicate that the platelet $\alpha_{IIb}\beta_3$ integrin and myosin II ATPase significantly enhance clot stiffness, which may be due to platelet integrin- and cytoskeleton-mediated regulation of the clot fibrin network. Finally, the study highlighted the utility of existing technologies for measuring clot structure and strength (confocal microscopy and sonorheometry), and presented a novel technique that offers the potential for simultaneous assessment of clot structure and stiffness (electromagnetic force).

The platelet $\alpha_{IIb}\beta_3$ integrin continues to be a primary target of anti-platelet and subsequently anti-thrombotic therapies (17,26). Since the development of abciximab in 1994, anti-$\alpha_{IIb}\beta_3$ drugs have proven effective in the treatment of acute coronary syndromes due largely to their ability to significantly attenuate platelet aggregation compared to other anti-platelet drugs such as aspirin or

clopidogrel (17). Unfortunately, due to increased bleeding risks, anti-$\alpha_{IIb}\beta_3$ therapies are often reserved for patients with the highest risk of developing thrombosis. The platelet $\alpha_{IIb}\beta_3$ integrin is an invaluable target of anti-thrombotic therapies, but there is still room for improvement. By further understanding the underlying mechanism of platelet $\alpha_{IIb}\beta_3$ integrin function, novel targets of anti-platelet drugs may be discovered, and subsequently safer and more effective anti-thrombotic therapies may be developed.

Table 5-2: Achievements of the study

Unknown:	Study Results:
Does inhibition of the platelet $\alpha_{IIb}\beta_3$ integrin affect fibrin network structure? ✓	Confocal microscopy: $\alpha_{IIb}\beta_3$ integrin inhibition increased mean fiber length and clot porosity, and reduced fiber junction density and clot structural heterogeneity.
Does inhibition of platelet myosin II ATPase affect global clot stiffness? ✓	Sonorheometry, electromagnetic force: Myosin II ATPase inhibition reduced whole blood and plasma clot stiffness during clot formation.
Does inhibition of platelet myosin II ATPase affect fibrin network structure? ✓	Confocal microscopy: Platelet myosin II ATPase inhibition increased mean fiber length and clot porosity, and reduced fiber junction density and clot structural heterogeneity.
Can changes in clot structure predict changes in clot stiffness? ✓	Confocal microscopy: Clot structure may be used to estimate clot stiffness using a simple analytical model. Additional studies required.

5.3: Future Directions

5.3.1: Future Experiments to Improve Study Clarity

A number of additional studies should be performed to further clarify the sonorheometry stiffness results as well as offer potentially novel insight regarding the findings of the

sonorheometry study. First, it would be valuable to expand the bead titration analysis of the plasma sonorheometry study to optimize the bead concentration in PRP samples and to subsequently optimize the PRP clot stiffness results. A more thorough study of optimal bead concentration could significantly improve the plasma sonorheometry data, and could be applied to render the Quantra device capable of assessing clot stiffness in both whole blood and plasma clots, unlike existing clinical clot stiffness technologies. Next, a more in-depth study of the discrepancy between reduced whole blood and PRP clot stiffness depending on anti-platelet drug treatment could elucidate novel means through which the various blood components interact to modulate hemostasis.

For the electromagnetic force study, it would be valuable to expand the dynamic range of the electromagnetic force by potentially applying an adaptive force technique. A wider dynamic range of the electromagnetic force would enable the measurement of clot stiffness from 0-10 minutes post clot initiation, and would likely improve clot stiffness measurements for soft abciximab-treated PRP and PPP clots. Additionally, the electromagnetic force assay should be combined with high resolution microscopy to simultaneously measure perturbations in blood clot structure and stiffness, and potentially probe the mechanistic relationship between clot structure and strength. Finally, a study should be conducted to evaluate if the force applied to the clot by the electromagnet disrupts clot formation. Given the potential for the electromagnetic force assay to serve as the first tool to simultaneously measure clot stiffness and structure, the applied force study could provide additional insight regarding the capabilities or limitations of the electromagnetic force assay as a means of quantifying clot stiffness.

Finally, for the confocal microscopy structure study, it would be valuable to develop an expanded analytical model of structure-based clot stiffness that accounts for additional clot

structure parameters to more accurately predict clot stiffness. Additionally, it would be valuable to conduct a fiber brightness analysis to estimate fiber fibrin content and fiber width, which could be used to evaluate the validity of the network model assumptions of a single fiber bending modulus and uniform fiber thickness for all experimental conditions. Similarly, it would be valuable to expand the clot structure analysis to more thoroughly capture the dynamic rearrangement of the fibrin network due to the platelets during clot formation. Finally, due to the potential sensitivity of certain features of clot structure to a 2D versus 3D analysis, future clot structure studies may need to implement a 3D analysis approach to accurately recapitulate the fibrin network, depending on what clot structural features are investigated.

5.3.2: Future Directions in the Study of the Platelet Contribution to Coagulation

The platelet $\alpha_{IIb}\beta_3$ integrin is a prominent target of anti-thrombotic therapies, but additional research to further understand the underlying mechanism of platelet $\alpha_{IIb}\beta_3$ integrin function could elucidate safer, more effective anti-thrombotic targets. At the onset of this study, a primary goal was to evaluate the anti-clotting capabilities of downstream signaling molecules of the platelet $\alpha_{IIb}\beta_3$ integrin to infer mechanism. Unfortunately, the inhibition of a number of presumably significant downstream targets produced negligible results (**Figure 5-1**). In our preliminary studies of the mechanism underlying platelet $\alpha_{IIb}\beta_3$ integrin function, a single downstream signaling target was inhibited at once. This suggests that other intracellular signaling targets may play a more prominent role in modulating platelet $\alpha_{IIb}\beta_3$ integrin function, or that there may be redundancy in the signaling pathway that ultimately compensates for the inhibition of a single target. In the future, to more efficiently investigate the underlying mechanism of platelet $\alpha_{IIb}\beta_3$ integrin function, it would be useful to incorporate a computational model of the platelet $\alpha_{IIb}\beta_3$ integrin signaling

pathway to guide the detection of critical downstream targets. By further understanding the underlying mechanism of platelet $\alpha_{IIb}\beta_3$ integrin function, novel targets of anti-platelet drugs may be discovered and the safety limitations associated with platelet $\alpha_{IIb}\beta_3$ integrin anti-thrombotic therapies may be overcome.

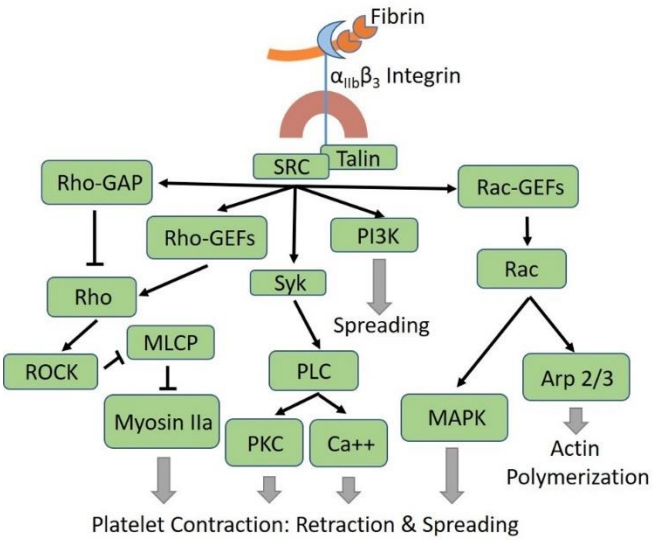

Target:	Drug:
✓ $\alpha_{IIb}\beta_3$ Integrin	Abciximab, Eptifibatide
⊘ SRC	PP2, Dasatinib
⊘ ROCK	Y-27632
⊘ MAPK	SB203580
✓ Myosin II ATPase	Blebbistatin
⊘ PI3K	Wortmannin

Figure 5-1: The platelet $\alpha_{IIb}\beta_3$ integrin signaling pathway and the targets probed to infer mechanism. The platelet $\alpha_{IIb}\beta_3$ integrin signaling pathway consists of many downstream targets (left). A number of downstream targets were inhibited in our preliminary studies to investigate the mechanism underlying platelet $\alpha_{IIb}\beta_3$ integrin function, but most of the studies produced negligible results (right). Signaling pathway adapted from Shen et al. 2012.

The platelet $\alpha_{IIb}\beta_3$ integrin is a prominent target of anti-platelet and subsequently anti-thrombotic therapies (17,26), however due to increased bleeding risks, anti-$\alpha_{IIb}\beta_3$ drugs are generally limited to patients at high risk of developing thrombosis. Additional limitations of current anti-$\alpha_{IIb}\beta_3$ therapies include their required intravenous administration, and their association with the development of thrombocytopenia (82). Although the platelet $\alpha_{IIb}\beta_3$ integrin is a critical component of coagulation, I predict that clinical anti-thrombotic therapies will continue to shift in the direction of direct oral anti-coagulants such as rivaroxaban (Xarelto®) or apixaban (Eliquis®). Rivaroxaban and apixaban directly inhibit factor Xa in the coagulation cascade, and they offer

distinct advantages over other classes of anti-coagulants, including an enhanced safety profile (i.e. reduced bleeding risk), a wide therapeutic window, quick drug clearance, and oral administration (83). While clinical anti-thrombotic therapies may move away from anti-$\alpha_{IIb}\beta_3$ drugs, the efficacy of anti-$\alpha_{IIb}\beta_3$ therapies will likely continue to be an invaluable asset for *in vitro* diagnostic tests of coagulation function.

Literature Cited

1. Weisel JW. Enigmas of Blood Clot Elasticity. Science. 2008 Apr 25;320(5875):456–7.
2. Furie B, Furie BC. The molecular basis of blood coagulation. Cell. 1988 May 20;53(4):505–18.
3. Undas A, Ariëns RAS. Fibrin Clot Structure and Function: A Role in the Pathophysiology of Arterial and Venous Thromboembolic Diseases. Arterioscler Thromb Vasc Biol. 2011 Dec 1;31(12):e88–99.
4. Wolberg AS. Thrombin generation and fibrin clot structure. Blood Rev. 2007 May 1;21(3):131–42.
5. Weisel JW. Structure of fibrin: impact on clot stability. J Thromb Haemost. 2007 Jul 1;5:116–24.
6. Weisel JW, Nagaswami C. Computer modeling of fibrin polymerization kinetics correlated with electron microscope and turbidity observations: clot structure and assembly are kinetically controlled. Biophys J. 1992 Jul;63(1):111–28.
7. Piechocka IK, Bacabac RG, Potters M, MacKintosh FC, Koenderink GH. Structural Hierarchy Governs Fibrin Gel Mechanics. Biophys J. 2010 May 19;98(10):2281–9.
8. Dahlbäck Björn. Blood coagulation and its regulation by anticoagulant pathways: genetic pathogenesis of bleeding and thrombotic diseases. J Intern Med. 2005 Feb 16;257(3):209–23.
9. Mackman N, Tilley RE, Key NS. Role of the Extrinsic Pathway of Blood Coagulation in Hemostasis and Thrombosis. Arterioscler Thromb Vasc Biol. 2007 Aug 1;27(8):1687–93.
10. Davie EW, Fujikawa K, Kisiel W. The coagulation cascade: initiation, maintenance, and regulation. Biochemistry (Mosc). 1991 Oct 1;30(43):10363–70.
11. Gailani D, Renné T. Intrinsic Pathway of Coagulation and Arterial Thrombosis. Arterioscler Thromb Vasc Biol. 2007 Dec 1;27(12):2507–13.
12. Capoor MN, Stonemetz JL, Baird JC, Ahmed FS, Awan A, Birkenmaier C, et al. Prothrombin Time and Activated Partial Thromboplastin Time Testing: A Comparative Effectiveness Study in a Million-Patient Sample. PLoS ONE. 2015 Aug 11;10(8).
13. Lancé MD. A general review of major global coagulation assays: thrombelastography, thrombin generation test and clot waveform analysis. Thromb J. 2015 Jan 12;13.
14. Ferrante EA, Blasier KR, Givens TB, Lloyd CA, Fischer TJ, Viola F. A Novel Device for the Evaluation of Hemostatic Function in Critical Care Settings. Anesth Analg. 2016 Dec;123(6):1372–9.
15. Geddis AE, Kaushansky K. The Root of Platelet Production. Science. 2007 Sep 21;317(5845):1689–91.
16. Junt T, Schulze H, Chen Z, Massberg S, Goerge T, Krueger A, et al. Dynamic Visualization of Thrombopoiesis Within Bone Marrow. Science. 2007 Sep 21;317(5845):1767–70.

17. Coller BS. Historical Perspective and Future Directions in Platelet Research. J Thromb Haemost JTH. 2011 Jul;9(Suppl 1):374–95.

18. Heemskerk JWM, Bevers EM, Lindhout T. Platelet activation and blood coagulation. Thromb Haemost. 2002 Aug;88(2):186–93.

19. Whiteheart SW. Platelet granules: surprise packages. Blood. 2011 Aug 4;118(5):1190–1.

20. Watson SP, Auger JM, McCarty OJT, Pearce AC. GPVI and integrin alphaIIb beta3 signaling in platelets. J Thromb Haemost JTH. 2005 Aug;3(8):1752–62.

21. Kroll MH, Harris TS, Moake JL, Handin RI, Schafer AI. von Willebrand factor binding to platelet GpIb initiates signals for platelet activation. J Clin Invest. 1991 Nov;88(5):1568–73.

22. Kovács M, Tóth J, Hetényi C, Málnási-Csizmadia A, Sellers JR. Mechanism of Blebbistatin Inhibition of Myosin II. J Biol Chem. 2004 Aug 20;279(34):35557–63.

23. Shinton NK. Desk Reference for Hematology, Second Edition. Second. CRC Press; 2007.

24. Shen B, Delaney MK, Du X. Inside-out, outside-in, and inside-outside-in: G protein signaling in integrin-mediated cell adhesion, spreading, and retraction. Curr Opin Cell Biol. 2012 Oct;24(5):600–6.

25. Li Z, Delaney MK, O'Brien KA, Du X. Signaling during platelet adhesion and activation. Arterioscler Thromb Vasc Biol. 2010 Dec;30(12):2341–9.

26. Hashemzadeh M, Furukawa M, Goldsberry S, Movahed MR. Chemical structures and mode of action of intravenous glycoprotein IIb/IIIa receptor blockers: A review. Exp Clin Cardiol. 2008;13(4):192–7.

27. Schwarz M, Katagiri Y, Kotani M, Bassler N, Loeffler C, Bode C, et al. Reversibility versus Persistence of GPIIb/IIIa Blocker-Induced Conformational Change of GPIIb/IIIa (αIIbβ3, CD41/CD61). J Pharmacol Exp Ther. 2004 Mar 1;308(3):1002–11.

28. Jenkins AL, Nannizzi-Alaimo L, Silver D, Sellers JR, Ginsberg MH, Law DA, et al. Tyrosine Phosphorylation of the β3 Cytoplasmic Domain Mediates Integrin-Cytoskeletal Interactions. J Biol Chem. 1998 May 29;273(22):13878–85.

29. Suzuki-Inoue K, Hughes CE, Inoue O, Kaneko M, Cuyun-Lira O, Takafuta T, et al. Involvement of Src kinases and PLCγ2 in clot retraction. Thromb Res. 2007;120(2):251–8.

30. Ono A, Westein E, Hsiao S, Nesbitt WS, Hamilton JR, Schoenwaelder SM, et al. Identification of a fibrin-independent platelet contractile mechanism regulating primary hemostasis and thrombus growth. Blood. 2008 Jul 1;112(1):90–9.

31. Hayward CPM, Rao AK, Cattaneo M. Congenital platelet disorders: overview of their mechanisms, diagnostic evaluation and treatment. Haemophilia. 2006 Jul 1;12:128–36.

32. Solh T, Botsford A, Solh M. Glanzmann's thrombasthenia: pathogenesis, diagnosis, and current and emerging treatment options. J Blood Med. 2015 Jul 8;6:219–27.

33. Izak M, Bussel JB. Management of thrombocytopenia. F1000Prime Rep. 2014 Jun 2;6.

34. Bleeker JS, Hogan WJ. Thrombocytosis: Diagnostic Evaluation, Thrombotic Risk Stratification, and Risk-Based Management Strategies. Thrombosis. 2011;2011.

35. Billett HH. Antiplatelet agents and arterial thrombosis. Cardiol Clin. 2008 May;26(2):189–201, vi.

36. Paniccia R, Priora R, Alessandrello Liotta A, Abbate R. Platelet function tests: a comparative review. Vasc Health Risk Manag. 2015 Feb 18;11:133–48.

37. Tran R, Myers DR, Ciciliano J, Trybus Hardy EL, Sakurai Y, Ahn B, et al. Biomechanics of haemostasis and thrombosis in health and disease: from the macro- to molecular scale. J Cell Mol Med. 2013 May;17(5):579–96.

38. Elliott A, Wetzel J, Roper T, Pivalizza E, McCarthy J, Wallace C, et al. Thromboelastography in Patients with Acute Ischemic Stroke. Int J Stroke. 2015 Feb 1;10(2):194–201.

39. Collet JP, Allali Y, Lesty C, Tanguy ML, Silvain J, Ankri A, et al. Altered fibrin architecture is associated with hypofibrinolysis and premature coronary atherothrombosis. Arterioscler Thromb Vasc Biol. 2006 Nov;26(11):2567–73.

40. Feuring M, Wehling M, Burkhardt H, Schultz A. Coagulation status in coronary artery disease patients with type II diabetes mellitus compared with non-diabetic coronary artery disease patients using the PFA-100® and ROTEM®. Platelets. 2010;21(8):616–22.

41. Evans PA, Hawkins K, Lawrence M, Williams RL, Barrow MS, Thirumalai N, et al. Rheometry and associated techniques for blood coagulation studies. Med Eng Phys. 2008 Jul 1;30(6):671–9.

42. Burghardt WR, Goldstick TK, Leneschmidt J, Kempka K. Nonlinear viscoelasticity and the thrombelastograph: 1. Studies on bovine plasma clots. Biorheology. 1995 Dec;32(6):621–30.

43. Wang CW, Perez MJ, Helmke BP, Viola F, Lawrence MB. Integration of Acoustic Radiation Force and Optical Imaging for Blood Plasma Clot Stiffness Measurement. PLOS ONE. 2015 Jun 4;10(6):e0128799.

44. Xu X, Zhu J, Chen Z. Dynamic and quantitative assessment of blood coagulation using optical coherence elastography. Sci Rep. 2016 Apr 19;6:24294.

45. Corey FS, Walker WF. Sonic Estimation of Elasticity via Resonance: A New Method of Assessing Hemostasis. Ann Biomed Eng. 2016 May 1;44(5):1405–24.

46. Mauldin FW, Viola F, Hamer TC, Ahmed EM, Crawford SB, Haverstick DM, et al. Adaptive force sonorheometry for assessment of whole blood coagulation. Clin Chim Acta. 2010 May 2;411(9):638–44.

47. Viola F, Mauldin FW, Lin-Schmidt X, Haverstick DM, Lawrence MB, Walker WF. A novel ultrasound-based method to evaluate hemostatic function of whole blood. Clin Chim Acta. 2010 Jan 4;411(1):106–13.

48. Lawrence MJ, Sabra A, Mills G, Pillai SG, Abdullah W, Hawkins K, et al. A new biomarker quantifies differences in clot microstructure in patients with venous thromboembolism. Br J Haematol. 2015 Feb 1;168(4):571–5.

49. Undas A, Celinska-Löwenhoff M, Löwenhoff T, Szczeklik A. Statins, fenofibrate, and quinapril increase clot permeability and enhance fibrinolysis in patients with coronary artery disease. J Thromb Haemost. 2006 May 1;4(5):1029–36.

50. Chernysh IN, Weisel JW. Dynamic imaging of fibrin network formation correlated with other measures of polymerization. Blood. 2008 May 15;111(10):4854–61.

51. Kim OV, Litvinov RI, Alber MS, Weisel JW. Quantitative structural mechanobiology of platelet-driven blood clot contraction. Nat Commun. 2017 Nov 2;8(1):1274.

52. Kim E, Kim OV, Machlus KR, Liu X, Kupaev T, Lioi J, et al. Correlation between fibrin network structure and mechanical properties: an experimental and computational analysis. Soft Matter. 2011 May 3;7(10):4983–92.

53. Braaten JV, Jerome WG, Hantgan RR. Uncoupling fibrin from integrin receptors hastens fibrinolysis at the platelet-fibrin interface. Blood. 1994 Feb 15;83(4):982–93.

54. Whiting D, DiNardo JA. TEG and ROTEM: Technology and clinical applications. Am J Hematol. 2014 Feb 1;89(2):228–32.

55. Tutwiler V, Litvinov RI, Lozhkin AP, Peshkova AD, Lebedeva T, Ataullakhanov FI, et al. Kinetics and mechanics of clot contraction are governed by the molecular and cellular composition of the blood. Blood. 2016 Jan 7;127(1):149–59.

56. Jen CJ, McIntire LV. The structural properties and contractile force of a clot. Cell Motil. 1982 Jan 1;2(5):445–55.

57. Lang T, Toller W, Gütl M, Mahla E, Metzler H, Rehak P, et al. Different effects of abciximab and cytochalasin D on clot strength in thrombelastography. J Thromb Haemost. 2004 Jan 1;2(1):147–53.

58. Qiu Y, Ciciliano J, Myers DR, Tran R, Lam WA. Platelets and physics: How platelets “feel” and respond to their mechanical microenvironment. Blood Rev. 2015 Nov 1;29(6):377–86.

59. Muthard RW, Diamond SL. Blood Clots Are Rapidly Assembled Hemodynamic Sensors: Flow Arrest Triggers Intraluminal Thrombus Contraction. Blood. 2012 Nov 16;120(21):2164–2164.

60. Limouze J, Straight AF, Mitchison T, Sellers JR. Specificity of blebbistatin, an inhibitor of myosin II. J Muscle Res Cell Motil. 2004 Aug 1;25(4–5):337–41.

61. Mikulich A, Kavaliauskiene S, Juzenas P. Blebbistatin, a myosin inhibitor, is phototoxic to human cancer cells under exposure to blue light. Biochim Biophys Acta. 2012 Jul;1820(7):870–7.

62. Smith AS, Nowak RB, Zhou S, Giannetto M, Gokhin DS, Papoin J, et al. Myosin IIA interacts with the spectrin-actin membrane skeleton to control red blood cell membrane curvature and deformability. Proc Natl Acad Sci. 2018 Apr 2;201718285.

63. Huffmyer JL, Fernandez LG, Haghighian C, Terkawi AS, Groves DS. Comparison of Seer Sonorheometry With Rotational Thromboelastometry and Laboratory Parameters in Cardiac Surgery. Anesth Analg. 2016 Dec 1;123(6):1390–9.

64. Reynolds PS, Middleton P, McCarthy H, Spiess BD. A Comparison of a New Ultrasound-Based Whole Blood Viscoelastic Test (SEER Sonorheometry) Versus Thromboelastography in Cardiac Surgery. Anesth Analg. 2016 Dec;123(6):1400.

65. Khurshid H, Friedman B, Berwin B, Shi Y, Ness DB, Weaver JB. Blood clot detection using magnetic nanoparticles. AIP Adv. 2017 Feb 16;7(5).

66. Voros E, Cho M, Ramirez M, Palange AL, De Rosa E, Key J, et al. TPA Immobilization on Iron Oxide Nanocubes and Localized Magnetic Hyperthermia Accelerate Blood Clot Lysis. Adv Funct Mater. 2015 Mar 1;25(11):1709–18.

67. Drozdov AS, Vinogradov VV, Dudanov IP, Vinogradov VV. Leach-proof magnetic thrombolytic nanoparticles and coatings of enhanced activity. Sci Rep. 2016 Jun 20;6:28119.

68. Oldenburg AL, Wu G, Spivak D, Tsui F, Wolberg AS, Fischer TH. Imaging and Elastometry of Blood Clots Using Magnetomotive Optical Coherence Tomography and Labeled Platelets. IEEE J Sel Top Quantum Electron Publ IEEE Lasers Electro-Opt Soc. 2011 Jul 21;18(3):1100–9.

69. Judith RM, Fisher JK, Spero RC, Fiser BL, Turner A, Oberhardt B, et al. Micro-elastometry on whole blood clots using actuated surface-attached posts (ASAPs). Lab Chip. 2015 Mar 7;15(5):1385–93.

70. Schindelin J, Arganda-Carreras I, Frise E, Kaynig V, Longair M, Pietzsch T, et al. Fiji: an open-source platform for biological-image analysis. Nat Methods. 2012 Jul;9(7):676–82.

71. Merrill EW. Rheology of blood. Physiol Rev. 1969 Oct 1;49(4):863–88.

72. Collet JP, Montalescot G, Lesty C, Soria J, Mishal Z, Thomas D, et al. Disaggregation of In Vitro Preformed Platelet-Rich Clots by Abciximab Increases Fibrin Exposure and Promotes Fibrinolysis. Arterioscler Thromb Vasc Biol. 2001 Jan 1;21(1):142–8.

73. Collet JP, Montalescot G, Lesty C, Weisel JW. A Structural and Dynamic Investigation of the Facilitating Effect of Glycoprotein IIb/IIIa Inhibitors in Dissolving Platelet-Rich Clots. Circ Res. 2002 Mar 8;90(4):428–34.

74. Shin JH, Gardel ML, Mahadevan L, Matsudaira P, Weitz DA. Relating microstructure to rheology of a bundled and cross-linked F-actin network in vitro. Proc Natl Acad Sci. 2004 Jun 29;101(26):9636–41.

75. Basu S, Liu C, Rohde GK. Localizing and extracting filament distributions from microscopy images. J Microsc. 2015 Apr 1;258(1):13–23.

76. Basu S, Liu C, Rohde GK. Extraction of Individual Filaments from 2D Confocal Microscopy Images of Flat Cells. IEEE/ACM Trans Comput Biol Bioinform. 2015 May;12(3):632–43.

77. Steger C. An unbiased detector of curvilinear structures. IEEE Trans Pattern Anal Mach Intell. 1998 Feb;20(2):113–25.

78. Wufsus AR, Rana K, Brown A, Dorgan JR, Liberatore MW, Neeves KB. Elastic Behavior and Platelet Retraction in Low- and High-Density Fibrin Gels. Biophys J. 2015 Jan 6;108(1):173–83.

79. Diamond SL. Engineering Design of Optimal Strategies for Blood Clot Dissolution. Annu Rev Biomed Eng. 1999;1(1):427–61.

80. ISTH Steering Committee for World Thrombosis Day. Thrombosis: a major contributor to the global disease burden. J Thromb Haemost. 2014 Oct 1;12(10):1580–90.

81. Gersh KC, Nagaswami C, Weisel JW. Fibrin network structure and clot mechanical properties are altered by incorporation of erythrocytes. Thromb Haemost. 2009 Dec;102(6):1169–75.

82. Aster R. H., Curtis B. R., Bougie D. W., Dunkley S., Greinacher A., Warkentin T. E., et al. Thrombocytopenia associated with the use of GPIIb/IIIa inhibitors: position paper of the ISTH working group on thrombocytopenia and GPIIb/IIIa inhibitors. J Thromb Haemost. 2006 Feb 6;4(3):678–9.

83. Mekaj YH, Mekaj AY, Duci SB, Miftari EI. New oral anticoagulants: their advantages and disadvantages compared with vitamin K antagonists in the prevention and treatment of patients with thromboembolic events. Ther Clin Risk Manag. 2015 Jun 24;11:967–77.